AD-A144 598 AN INVESTIGATION INTO THE QUASI-SSATIC PHASE OF THE SURFACE BURST SOURCE..(U) AIR FORCE INST OF TECH WRIGHT-PATTERSON AFB OH SCHOOL OF ENGI.. K M HODGDON 1/2

UNCLASSIFIED MAR 84 AFIT/GNE/ENP/84M-7 F/G 20/14 NL

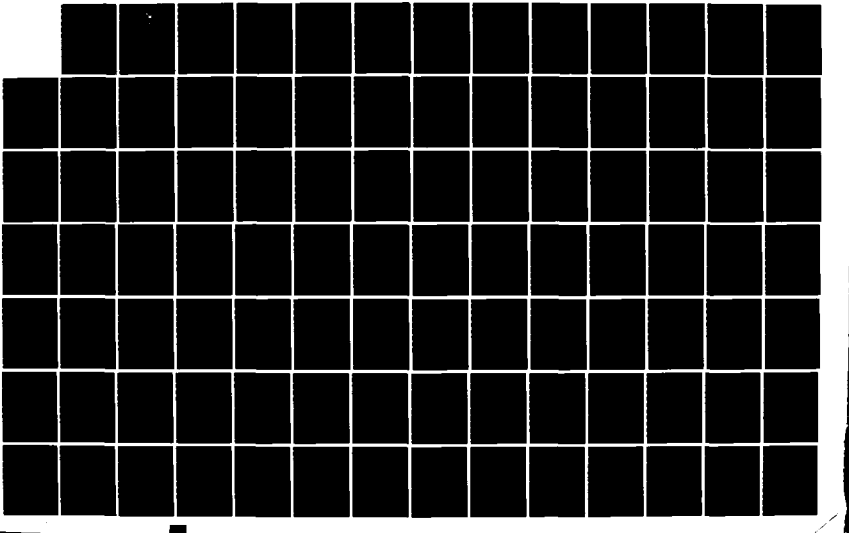

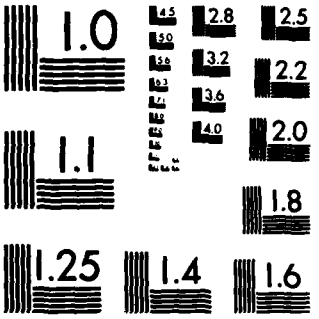


# AN INVESTIGATION INTO THE QUASI-STATIC PHASE OF THE SURFACE BURST SOURCE REGION EMP

THESIS

Kenneth M. Hodgdon
First Lieutenant, USAF



DEPARTMENT OF THE AIR FORCE
AIR UNIVERSITY
AIR FORCE INSTITUTE OF TECHNOLOGY

Wright-Patterson Air Force Base, Ohio

AFIT/GNE/ENP/84M-7

# AN INVESTIGATION INTO THE QUASI-STATIC PHASE OF THE SURFACE BURST SOURCE REGION EMP

THESIS

Kenneth M. Hodgdon
First Lieutenant, USAF

AFIT/GNE/ENP/84M-7

AFIT/GNE/ENP/84M-7

# AN INVESTIGATION INTO THE QUASI-STATIC PHASE OF THE SURFACE BURST SOURCE REGION EMP.

THESIS

Presented to the Faculty of the School of Engineering

of the Air Force Institute of Technology

Air University

In Partial Fulfillment of the

Requirements for the Degree of

Master of Science in Nuclear Engineering

Kenneth M. Hodgdon, M.S.

First Lieutenant, USAF

A-1

March 1984

## Preface

This work is really a small part of a potential series of studies intended to determine the effects of late-time source region EMP on vulnerable systems. Lt. Jim Downey (Ref 4) developed the time-independent numerical code which enabled the above ground electric fields to be calculated. This work added the capability of calculating the above ground magnetic fields as well as investigated the limitations of the boundary condition at the earth's surface and the quasi-static approximations. From here, the below ground electric and magnetic fields should be calculated, and the interaction of the late-time source region EMP with operational systems determined.

I would first like to thank Lt. Jim Downey of the Nuclear Criteria Group Secretariat for his invaluable help in getting me started on this project.

Dave Richardson of the Aeronautical Systems Division Computer Center also deserves special appreciation for his tireless help in developing the contour plots presented in this work.

Finally, I would like to express my gratitude to my faculty advisor, Lt. Col. John Erkkila, without whom, quite frankly, I would not have made it.

Kenneth M. Hodgdon

## Table of Contents

## List of Figures

## Abstract

A numerical solution was developed to find the above ground late-time magnetic fields resulting from a surface nuclear burst. The time derivative in Maxwell's magnetic curl equation was ignored and the result was expressed in integral form using Stokes' law. This expression is expanded in spherical coordinates, the radial Compton current and the radial conduction current source terms were calculated, using the time-independent code developed by Downey (Ref 4), and the polar integrals were calculated, using Simpson's Composite Rule. Magnetic field values were calculated and compared with Longmire's (Ref 20) analytic expression for the magnetic field. For ranges less than 2 Km, the results differed by less than 2%; however, for ranges greater than 2 Km, the numerical values were as much as an order of magnitude larger than the analytic values.

The results of the electric and magnetic field calculations were then used to test the spatial and temporal regions of validity of the simplified boundary condition and the quasi-static approximations. The assumption that the ground conductivity greatly exceeds the air conductivity leads to a simplified boundary condition at the earth's surface ($E_r = 0$), and, in turn, to an inner radial limit to the validity of the results. The quasi-static approximation that the conduction current greatly exceeds the displacement current leads to an outer radial limit, and, finally, the quasi-static approximation that the electric fields be derivable from a scalar potential determines the time regime over which

the results are valid. The quasi-static phase was found to be valid for times greater than 60 microseconds and for ranges between one and three kilometers. The spatial region of validity was shown to be a strong function of yield and time, and the temporal region was shown to be a function of air and ground conductivities.

The computer program included in this report should be useful for late-time EMP calculation because of the short execution time and its wide range of applicability. In addition, these results should be a useful starting point for calculating the below ground fields.

# AN INVESTIGATION INTO THE QUASI-STATIC PHASE OF THE SURFACE BURST SOURCE REGION EMP.

## I. Introduction

This chapter provides a brief background to the source region electromagnetic pulse (SREMP) generated from a surface nuclear burst. The basic theory, the assumptions used, the scope and the general approach to the problem are presented.

### Background

Surface nuclear bursts create an electromagnetic pulse (EMP) prin cipally through the interaction of gamma rays and air. The gamma rays in traveling through the air produce a flux of Compton electrons that constitute the source current that generates the EMP. Within this "source region", the electromagnetic environment contains both static and propagating electric and magnetic field components as well as source currents and ionizing radiation (Ref 23:118-119).

Longmire (Ref 16:6) began the investigation into the theory of source region electromagnetic pulse from a surface nuclear burst in the early 1960's. More recently, since the late 1970's, there has been a great deal of interest in calculations of the late-time regime (~1ms) of the source region EMP. Substantial late-time electric and magnetic fields can couple considerable amounts of energy (currents or voltage surges) into hardened underground structures directly exposed to an enemy attack (Ref 11:4441 and 12:1874). Conductors such as antennas,

power lines, telephone lines, pipelines, fences, buried cables and conduits collect this energy over large areas and direct or guide the pulse into sensitive electronic equipment. The net effect ranges from merely tripping circuit breakers to burning out system components.

SREMP is mainly a concern to systems which can survive quite close to a ground burst. The intense fields of the source region EMP decrease rapidly from the burst center over a few kilometers, while other nuclear weapon effects (blast, shock, debris, thermal and nuclear radiation) have ranges extending up to tens of kilometers (Ref 7;17). As a result, the main threat is to buried structures such as command posts, survival shelters, missile silos, and launch control centers.

SREMP

Source region EMP results when a nuclear explosion occurs at or near the surface of the earth, so that the thermal fireball formed during the explosion reaches the ground. As stated previously, the principal mechanism in the generation of the SREMP is the interaction of gamma rays with the air.

The gamma radiation source has several components. Initially, prompt gammas and fast neutrons produced in the nuclear explosion travel outward radially and interact with the surrounding air and ground. The prompt gammas produce free electrons and positive ions through Compton and photoelectric processes, while the fast neutrons add to the gamma source through inelastic scattering in the ground and air. These fast neutrons slowed through inelastic collisions continue to contribute to the gamma source at later-times through neutron capture in the ground

and air. Finally, the longest lived gamma source is produced from the lingering decay of weapon debris, which will last for tens of seconds after the burst.

The photoelectric effect is the dominant electron production process at photon energies of a few keV. However, the prompt gamma spectrum consists mainly of MeV energies and the dominant electron production process is Compton scattering. The photons and fast electrons scattered in the Compton process tend to travel in a radial direction away from the burst point, leaving behind the heavier positive ions (Figure 1). This separation of charges creates an outwardly directed radial electric field.

The fast electrons slow down by ionizing the air through which they move, creating numerous secondary electrons and positive ions which contribute to the air conductivity in a manner proportional to the local ionization rate. These low energy secondary electrons will drift along the electric field lines, creating a conduction current which acts to cancel the electric field set up by the primary current density of the Compton electron flux. These spatial current densities, the Compton current and the conduction current, serve as source terms for Maxwell's equations, which, in turn, determine the magnitude and waveform of the EMP.

For surface bursts, the presence of a highly conducting ground introduces an asymmetry. Soil conductivities are of the order of $10^{-2}$ - $10^{-3}$ Mho/m, which are much greater than the air conductivities over most of the EMP space time source region. The ground, therefore, shorts

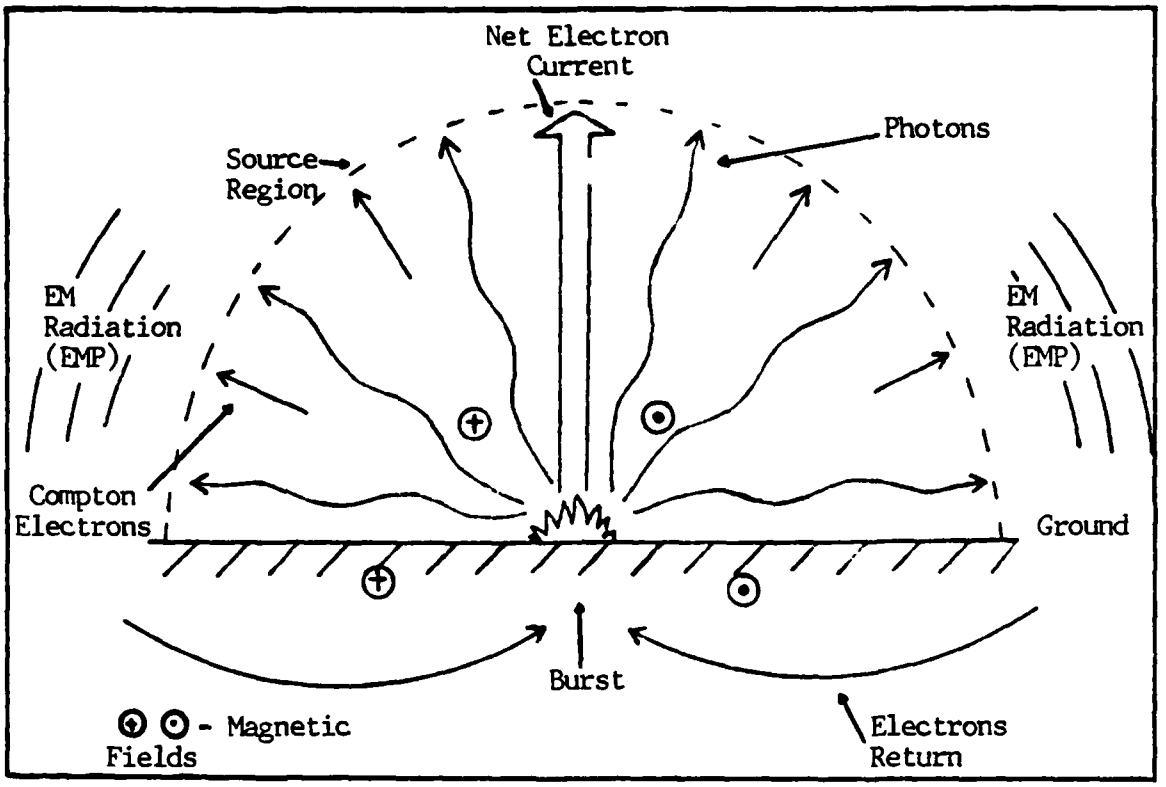


Figure 1. Schematic Representation of the EMP in a Surface Burst (Ref 6:518)

out the radial electric field near the earth's surface and is often approximated by a perfect conductor. Current loops are thus formed, driven by the outward radial Compton current in the air and the return conduction current density in the ground. These "toroidal" current loops (Figure 1), in turn, drive a horizontal magnetic field parallel to the earth's surface. Therefore, the asymmetry introduced by the conducting ground creates transverse electric and magnetic field components which can radiate to distances large compared to the source region. These radiated fields are often approximated by the radiated fields of an electric dipole (Ref 16: Ch 1).

Retarded Time

Radiation created by a surface nuclear burst will not appreciably penetrate the ground. The source region, therefore, is primarily an outwardly expanding hemispherical region centered at the burst point. This hemispherical region advances with the gamma ray front at the speed of light out to several gamma ray mean free paths.

In EMP calculations, it is often useful to reference time to the passing of the gamma pulse at a given location in space. This time, referred to as retarded time, is described by $\tau = t - r/c$ where $\tau$ is the retarded time, t is the real time after the burst, r is the radial distance to the observer location and c is the speed of light in air. The calculations presented in this work are in retarded time.

Geometry of the Problem

The hemispherical nature of the source region lends itself to the use of spherical coordinates. The geometry of the problem is shown in Figure 2:

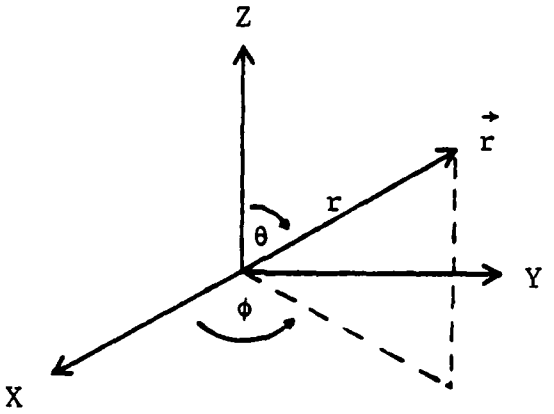


Figure 2. Surface Burst Geometry

$\theta$ is the polar angle measured from the vertical axis, $\phi$ is the azimuthal

angle measured counter clockwise along the surface of the earth, and r is the radial distance and the burst location is the origin.

Quasi-Static Phase

The time regime of interest in this study is retarded times greater than 100 microseconds after the burst. During this late-time phase of the source region EMP, the time derivatives in Maxwell's equations are small relative to the other source terms and can be ignored. The fields are said to be static and the time derivatives are set to zero (the Quasi-Static Approximation). This is known as the quasi-static phase of the source region EMP.

Longmire and Gilbert (Ref 20) calculated the source region EMP in the quasi-static regime using specified functional forms of the radial current density and air conductivity and setting the radial electric field to zero. The source terms were assumed to be independent of the polar angle and constant field-independent air chemistry and air conductivity parameters were used.

Later, Grover (Ref 8) developed a model of the quasi-static SREMP for which the radial electric field was set to zero only at the earth's surface. This approximation is valid when the ground conductivity is infinite; however, when the ground conductivity is much greater than the air conductivity, it is still a reasonable approximation. Using specified functional forms for the Compton current and the air conductivity, Grover expands the scalar potential function in terms of Legendre polynomials and solves the resulting equations to find closed-form expressions for the electric field. Grover also used polar-independent

sources and constant field-independent air chemistry and air conductivity parameters.

More recently, Downey (Ref 4) developed a time-independent numerical method to determine the late-time electric fields of the source region EMP. This model used the quasi-static approximations and set the radial electric field to zero at the earth's surface. However, the source terms were a function of both radius and polar angle, and the solutions incorporated the non-linear dependence of air chemistry and air conductivity parameters on the electric field.

Downey's time-independent numerical code is useful for EMP calculations due to its short execution time.

## Objectives

This study consisted of two parts. The first part added to Downey's code the capability of determining the above ground azimuthal magnetic field. This field was calculated as a function of radius and polar angle during the quasi-static phase of the source region EMP. The addition of this capability of calculating the above ground magnetic field provides a useful starting point for calculating the below ground fields.

The second part of this study used the results of both the electric and magnetic field calculations to test the spatial and temporal regions of validity of the simplified boundary condition and the quasi-static approximations. The assumption that the ground conductivity greatly exceeds the air conductivity leads to a simplified boundary condition at the earth's surface ($E_r = 0$), and, in turn, to an inner radial limit to the validity of the results. The quasi-static approximation that the

conduction current greatly exceeds the displacement current ($\sigma\vec{E} >> \varepsilon\, d\vec{E}/dt$) leads to an outer radial limit, and finally, the quasi-static approximation that the electric fields be derivable from a scalar potential (i.e. $\partial\vec{B}/\partial t = 0$) determines the time regime over which the results are valid. This investigation of the boundary condition and the quasi-static approximations provides a useful test of the space-time regions of validity of the numerical results.

Scope and Assumptions

This study investigates the late-time source region electromagnetic pulse for retarded times greater than 100 microseconds and less than 100 milliseconds. The above ground electric and magnetic fields are considered out to 4500 meters from the burst.

The assumptions used in the development of the time-independent numerical code are:

1) The permittivity $\varepsilon$, and the permeability $\mu$, are constant and are equal to $\varepsilon_o$ and $\mu_o$ (the values for free space).

2) Self-consistent effects between the generated fields and the source currents are ignored. Self-consistent effects become important for electric fields greater than $10^5$ volts/m and for magnetic fields greater than a few gauss (Ref 14:24).

3) The ground conductivity is much greater than the air conductivity. This provides a simplified boundary condition for the solution of Maxwell's equations (i.e. the radial electric field is approximately zero at the earth's surface).

4) Quasi-static approximations:

A) The conduction current is much greater than the displacement

current, and

B) The electric field is derivable from a scalar potential.

These two approximations allow the time derivatives in Maxwell's equations to be set to zero and, hence, the development of time-independent analytic and numerical solutions to the late-time quasi-static electric and magnetic fields.

General Approach

The first step was to determine the above ground late-time magnetic fields. This was done by deriving a numerical expression for the magnetic fields from Maxwell's equations. The input source terms to the expression were determined in solving for the electric field and the polar integrals were calculated numerically, using Simpson's Composite Rule.

Next, the spatial and temporal limits of validity of the boundary condition ($E_r = 0$ at $\theta = 90°$) and of the quasi-static approximations were investigated using the contour plots developed.

Finally, parametric studies of the total electric field were run varying the time, the yield and the water vapor content of the air.

Overview

In Chapter two, an expression for the electric field is derived from Maxwell's equations, using the quasi-static EMP theory. In Chapter three, an expression for the magnetic field is derived from Maxwell's equations, using the quasi-static EMP theory. The magnetic field results are then compared to the results from Longmire's analytic expression. In Chapter four, the simplified boundary condition and the

quasi-static approximations are investigated. In Chapter five, the regions of validity of these approximations are presented. Finally, the parametric studies are run in Chapter six, and the conclusions and recommendations are presented in Chapter seven.

## II. Quasi-Static EMP Theory - Electric Field

In this chapter, an expression for the electric field is derived from Maxwell's equations, using the quasi-static approximation (Ref 4).

### Approach

For retarded times greater than 100 microseconds, the electric and magnetic fields of the source region EMP from a surface nuclear burst vary slowly with time and can be considered to be quasi-static. Consequently, the time derivatives in Maxwell's equations are small and can be set to zero (the quasi-static approximations) (Ref 6:4479; 8:990; and 18:7).

Maxwell's time dependent equations are

$$\vec{\nabla} \times \vec{E} = - \frac{\partial \vec{B}}{\partial t} \tag{2-1}$$

$$\frac{1}{\mu_o} \vec{\nabla} \times \vec{B} = \vec{J} + \frac{\partial \vec{E}}{\partial t} \tag{2-2}$$

where $\vec{E}$ is the electric field (volts/m), $\vec{B}$ is the magnetic field (Webers/$m^2$), $\vec{J}$ is the current density (amps/$m^2$), $\mu_o$ is the magnetic permeability (Henrys/m) and $\epsilon$ is the electric permittivity (Farads/m).

With the quasi-static approximations, Maxwell's equations become

$$\vec{\nabla} \times \vec{E} = 0 \tag{2-3}$$

$$\frac{1}{\mu_o} \vec{\nabla} \times \vec{B} = \vec{J} \tag{2-4}$$

For Eq (2-3) to be valid, the electric fields must be derivable from a scalar potential. From vector analysis

$$\vec{\nabla} \times \vec{\nabla} (\Phi) = 0 \tag{2-5}$$

where $\phi$ is a scalar function. The electric fields can then be defined as

$$\vec{E} = -\vec{\nabla}\phi \tag{2-6}$$

where in spherical coordinates (assuming azimuthal symmetry):

$$E_r = \frac{\partial \phi}{\partial r} \tag{2-7}$$

$$E_\phi = 0 \tag{2-8}$$

$$E_\theta = -\frac{1}{r} \frac{\partial \phi}{\partial \theta} \tag{2-9}$$

In the quasi-static phase, the deposition of charge by the Compton current is balanced by the removal of charge by the conduction current driven by the quasi-static electric field. The conservation of charge equation,

$$\vec{\nabla} \cdot \vec{J} = -\frac{\partial \rho}{\partial t} \tag{2-10}$$

where $\rho$ is the charge density, then becomes

$$\vec{\nabla} \cdot (\vec{J}_c + \sigma\vec{E}) = 0 \tag{2-11}$$

where the current density $\vec{J}$, is described by the Compton current, $\vec{J}_c$ (amps/$m^2$), and the conduction current, $\sigma\vec{E}$ (amps/$m^2$) (Ref 16:38; 20:43; and 22:9).

Substituting Eq (2-6) into Eq (2-11) yields

$$\vec{\nabla} \cdot \vec{J}_c = \vec{\nabla} \cdot (\sigma \vec{\nabla} \phi) \qquad (2\text{-}12)$$

Rearranging Eq (2-12) provides

$$\vec{\nabla} \sigma (\vec{\nabla} \phi) + \sigma \vec{\nabla} \phi = \vec{\nabla} \cdot \vec{J}_c \qquad (2\text{-}13)$$

Again, assuming azimuthal symmetry and expanding Eq (2-13) in spherical coordinates yields

$$\left( \frac{\partial \sigma}{\partial r} a_r + \frac{1}{r} \frac{\partial \sigma}{\partial \theta} a_\theta \right) \left( \frac{\partial \phi}{\partial r} a_r + \frac{1}{r} \frac{\partial \phi}{\partial \theta} a_\theta \right)$$

$$+ \sigma \frac{1}{r^2} \frac{\partial}{\partial r} \left( r^2 \frac{\partial \phi}{\partial r} \right) + \sigma \frac{1}{r^2 \, \mathrm{SIN}\theta} \frac{\partial}{\partial \theta} \left( \mathrm{SIN}\theta \frac{\partial \phi}{\partial \theta} \right)$$

$$= \frac{1}{r^2} \frac{\partial}{\partial r} (r^2 J_r) + \frac{1}{r \, \mathrm{SIN}\theta} \frac{\partial}{\partial \theta} (\mathrm{SIN}\theta \, J_\theta) \qquad (2\text{-}14)$$

Rearranging Eq (2-14) obtains

$$\frac{1}{r^2} \frac{\partial}{\partial r} \left( r^2 \frac{\partial \phi}{\partial r} \right) + \frac{1}{r^2 \, \mathrm{SIN}\theta} \frac{\partial}{\partial \theta} \left( \mathrm{SIN}\theta \frac{\partial \phi}{\partial \theta} \right)$$

$$+ \frac{1}{\sigma} \frac{\partial \sigma}{\partial r} \frac{\partial \phi}{\partial r} + \frac{1}{\sigma r^2} \frac{\partial \sigma}{\partial \theta} \frac{\partial \phi}{\partial \theta}$$

$$= \frac{1}{\sigma r^2} \frac{\partial}{\partial r} (r^2 J_r) + \frac{1}{\sigma r \, \mathrm{SIN}\theta} \frac{\partial}{\partial \theta} (\mathrm{SIN}\theta \, J_\theta) \qquad (2\text{-}15)$$

The scalar potential function is expanded in terms of Legendre

polynomials and Eq (2-15) is solved numerically, using finite difference methods to find $\phi$ (Ref 4:Ch 3). The radial and polar components of the electric fields are then determined from Eqs (2-7) and (2-9).

The source terms are functional curve fits from Monte Carlo calculations and are a function of both radius and polar angle. The non-linear dependence of the air chemistry and air conductivity parameters on the electric field is incorporated by iterating until the electric field values converge (Ref 4:Ch 4; and 25).

Figures 3, 4, and 5 are contour plots of the total, polar and radial electric fields one millisecond after a ten megaton surface nuclear burst. Figure 3 shows peak total electric field values of about 45,000 V/m on the ground between 1000 and 1500 meters from the burst. Figure 3 also shows the combined effect of the radial electric field, whose peak values exist quite close to the burst (less than 1000 meters), and the polar electric field, which persists to much farther distances (several kilometers). Figure 4 shows the "radiating dipole" nature of the polar electric field as well as the strong contribution of the polar electric field at late-times (peak values of 40,000 V/m near the earth's surface). Finally, Figure 5 shows the spherical nature of the radial electric field as well as the shorting effect of the highly conducting ground ($E_r = 0$ at $\theta = 90°$). The radial electric field values are negative above the zero degree contour.

Standard Case

In order to compare results with Downey's and Longmire's work, and to provide a constant reference throughout this work, a standard case was selected (Ref 4:21). This case is one millisecond (retarded time)

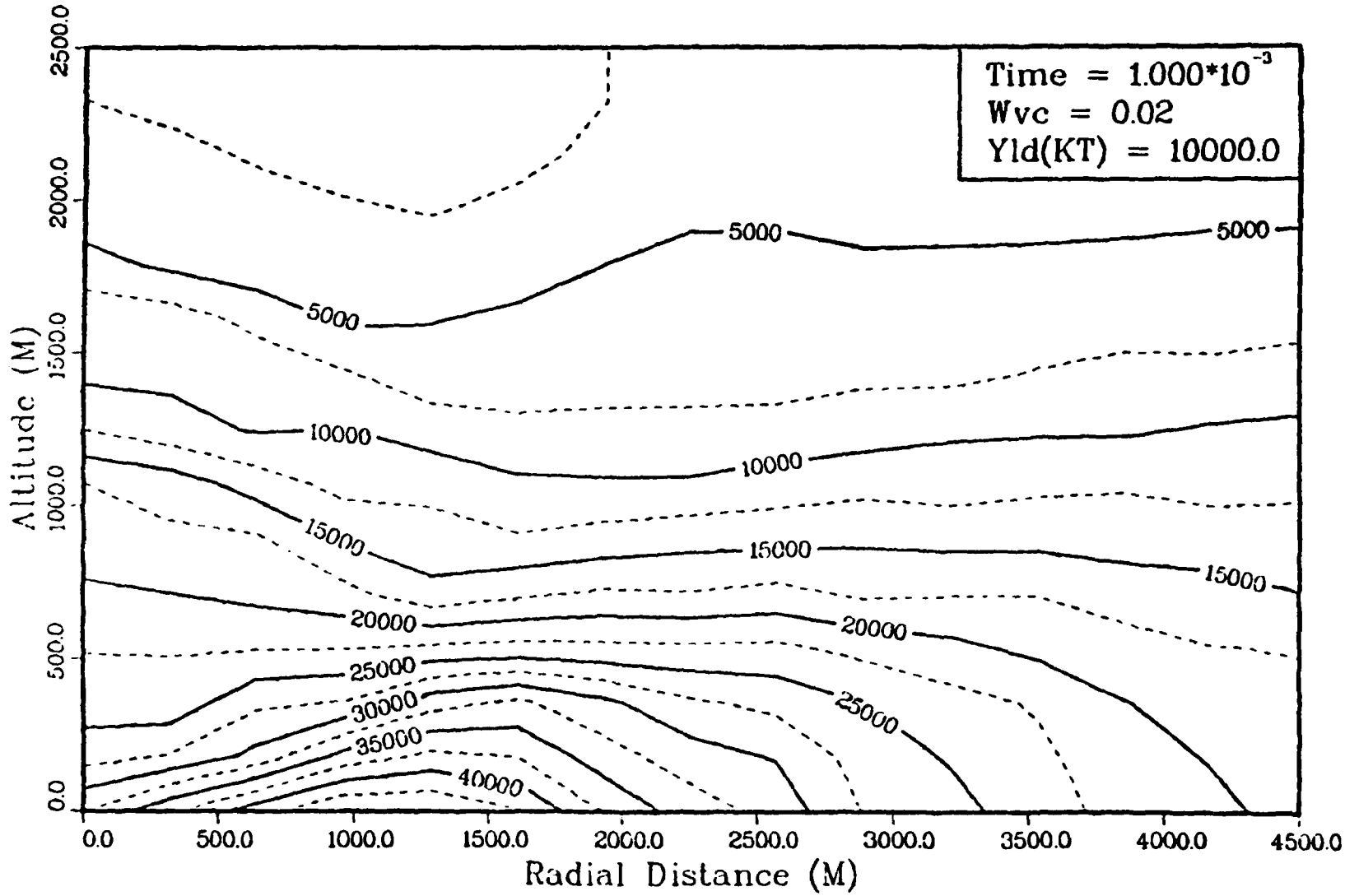


Figure 3. Total Electric Field (V/m)

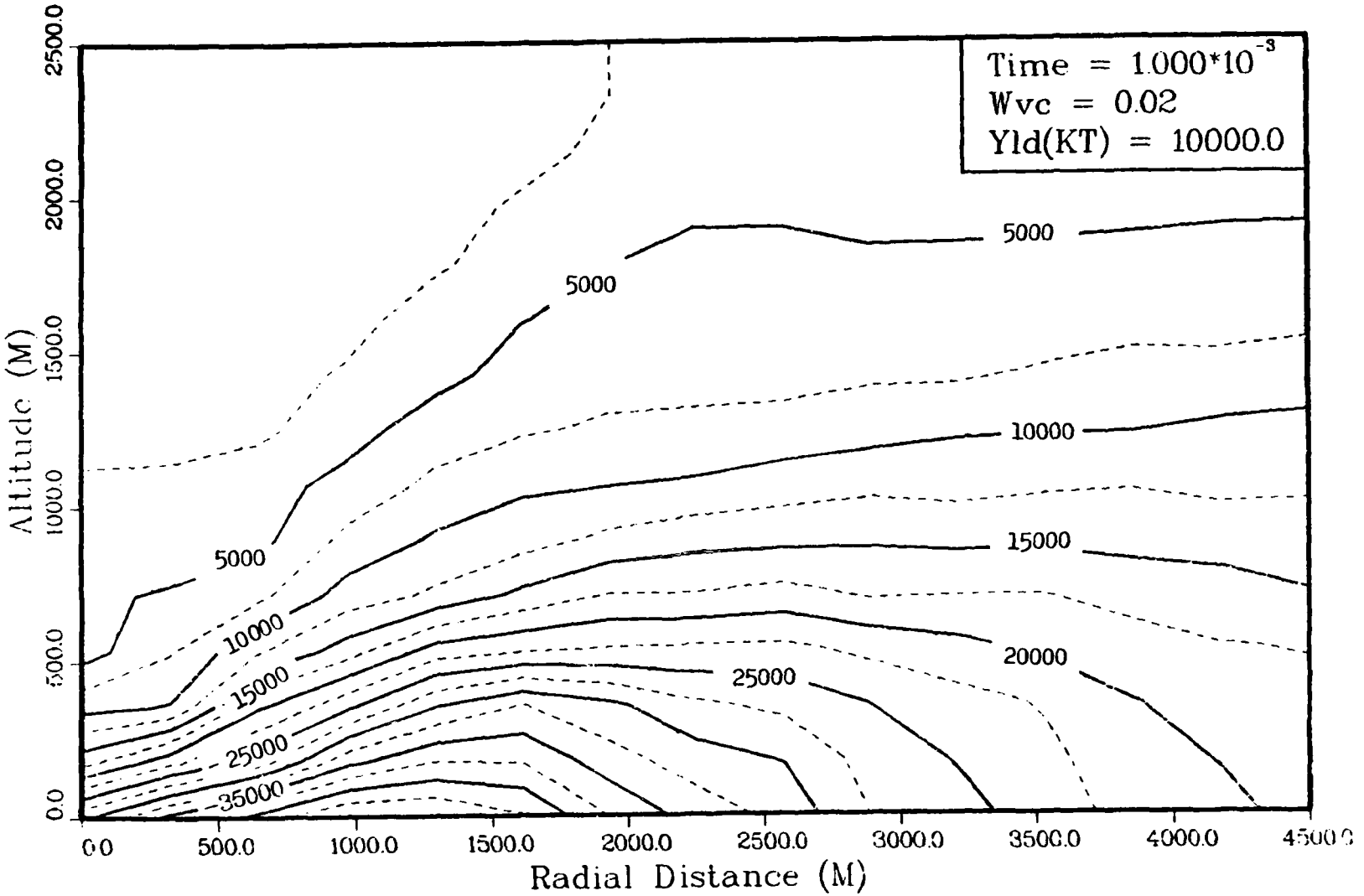


Figure 4. Polar Electric Field (V/m)

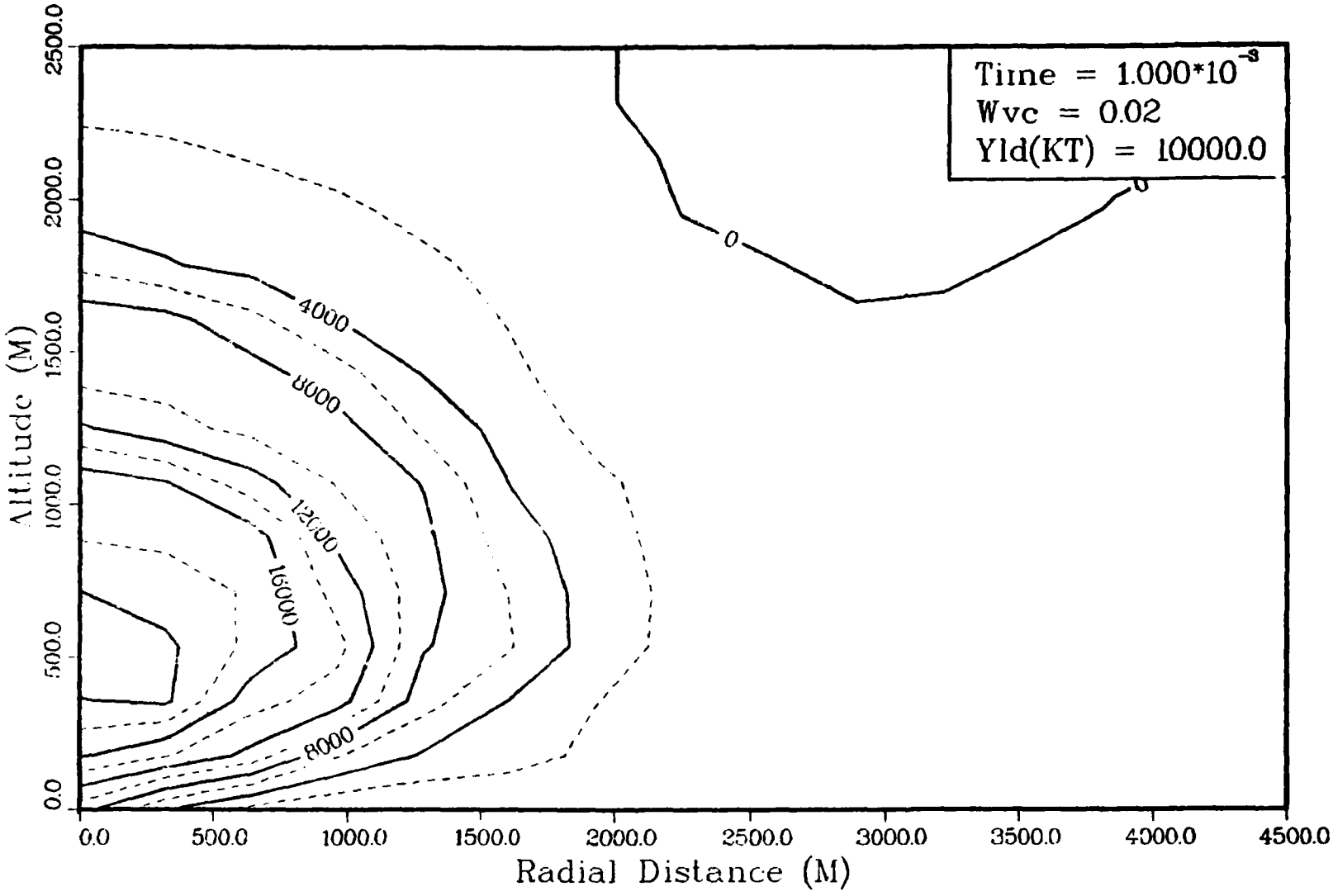


Figure 5. Radial Electric Field (V/m)

after a ten megaton surface nuclear burst with an air water vapor fraction of 0.02. The initial results of Chapters 2, 3, and 4 will be presented, using this case, with additional results presented in Chapters 5 and 6.

Contour Plots

The contour plots are not ideal. The mesh sizes and number of data points are finite due to computer resource limitations, and as a result, the linear interpolation method used is sometimes inadequate in handling rapidly changing data values (i.e. sharp contour gradients give it fits). This problem introduces non-real "zig-zags" in some of the contour plots - particularly in the contour plots of the conductivity where the conductivity values are rapidly increasing near the earth's surface. The "zig-zags" can be eliminated with finer meshes and more data points at the expense of computer resources.

In addition, there are no data points for radii less than 500 meters from the burst and, therefore, all contour lines within this region are questionable.

## III. Quasi-Static EMP Theory - Magnetic Field

In this chapter, a closed form expression for the azimuthal magnetic field is derived from Maxwell's equations, using the quasi-static approximation. Then a numerical expression is derived for the azimuthal magnetic field as a function of radial and polar variations, and finally, the analytical and numerical results are compared.

### Analytical Approach

Longmire derived a closed-form expression for the azimuthal magnetic field starting from Maxwell's time-dependent magnetic curl equation (Ref 20:68):

$$\frac{1}{\mu_o} \vec{\nabla} \times \vec{B} = \varepsilon \frac{\partial \vec{E}}{\partial t} + \vec{J} \tag{3-1}$$

Following Longmire and, as in Chapter 2, the displacement current is assumed to be much less than the conduction current (Ref 22:7) ($\varepsilon \, \partial \vec{E}/\partial t << \sigma \vec{E}$) and the time derivative can be set to zero. With this quasi-static approximation, Eq (3-1) then becomes

$$\vec{\nabla} \times \vec{B} = \mu_o \, (\sigma \vec{E} + \vec{J}_c) \tag{3-2}$$

Expanding Eq (3-2) in spherical coordinates yields

$$\begin{aligned} &\frac{1}{r \, \mathrm{SIN}\theta} \left[ \frac{\partial}{\partial \theta} \left( \mathrm{SIN}\theta \, B_\phi \right) - \frac{\partial}{\partial \phi} B_\theta \right] a_r \\ + \quad &\frac{1}{r} \left[ \frac{1}{\mathrm{SIN}\theta} \frac{\partial}{\partial \phi} B_r - \frac{\partial}{\partial r} \left( r \, B_\phi \right) \right] a_\theta \\ + \quad &\frac{1}{r} \left[ \frac{\partial}{\partial r} \left( r \, B_\theta \right) - \frac{\partial}{\partial \theta} B_r \right] a_\phi \\ = \quad &\mu_o \left[ \sigma E_r \, a_r + \sigma E_\theta \, a_\theta + J_c \, a_\theta + J_{cr} \, a_r \right] \end{aligned} \tag{3-3}$$

However, during the quasi-static phase, the radial electric field is much less than the theta electric field ($E_r << E_\theta$) and can be set to zero (Ref 13:6355; 20:66; and 32:13). The r-component of Eq (3-3) then provides

$$\frac{1}{r\ \mathrm{SIN}\theta}\ \frac{\partial}{\partial\theta}\left(\mathrm{SIN}\theta\ B_\phi\right) = \mu_o\ J_{cr} \tag{3-4}$$

or,

$$\frac{\partial}{\partial\theta}\left(\mathrm{SIN}\theta\ B_\phi\right) = \mu_o\ r\ J_{cr}\ \mathrm{SIN}\theta \tag{3-5}$$

Integrating Eq (3-5) over $\theta$ ($J_{cr}$ is assumed to be independent of $\theta$),

$$\int_0^\theta \frac{\partial}{\partial\theta}\ \left(\mathrm{SIN}\theta\ B_\phi\right) d\theta = \mu_o\ r\ J_{cr} \int_0^\theta \mathrm{SIN}\theta\ d\theta \tag{3-6}$$

results in

$$\mathrm{SIN}\theta\ B_\phi = \mu_o\ r\ J_{cr}\ (1 - \mathrm{COS}\theta) \tag{3-7}$$

Solving for $B_\phi$ yields

$$B_\phi = \mu_o\ r\ J_{cr}\ \mathrm{TAN}\left(\frac{\theta}{2}\right) \tag{3-8}$$

where the radial Compton current, $J_{cr}$, at one millisecond (retarded time) after a ten megaton surface nuclear burst equals

$$J_{cr} = -\ 9.02 \times 10^6\ \frac{e^{-r/\lambda}}{r^2}\ \left(\frac{A}{M}\right) \tag{3-9}$$

and $\lambda$, the effective gamma-ray mean free path at sea level, is 320 meters (Ref 4:21,22). These values of $J_{cr}$ and $\lambda$ were used by Downey to compare results with the work of Grover (Ref 8:13) for the reference case started

in Chapter two. These values are used here in order to compare the numerical results with the work of Longmire (Ref 20:68) for the same case. Substituting Eq (3-9) into Eq (3-8) yields

$$B_\phi = -9.02 \times 10^6 \mu_o \frac{e^{-r/\lambda}}{r} \text{TAN} \left(\frac{\vartheta}{2}\right) \tag{3-10}$$

or, solving for $H_\phi$,

$$H_\phi = -9.02 \times 10^6 \frac{e^{-r/\lambda}}{r} \text{TAN} \left(\frac{\theta}{2}\right) \tag{3-11}$$

Numerical Approach

A numerical expression for the azimuthal magnetic field as a function of radial and polar variations can also be derived from Maxwell's time dependent curl Eq (3-1). Again, in the quasi-static approximation, Eq (3-1) reduced to Eq (3-2)

$$\vec{\nabla} \times \vec{H} = \vec{J}_T \tag{3-12}$$

where $\vec{B} = \mu_o \vec{H}$ and $\vec{J}_T$ is the total current density (includes both the Compton and conduction current). The integral form of Eq (3-12), using Stokes Law, is

$$\oint \vec{H} \cdot \vec{dl} = \int_s \vec{J}_T \cdot \vec{d} \tag{3-13}$$

Figure 6 shows the appropriate geometry for this problem. L is the upper portion of the surface of a sphere centered at the burst location with radius r. P is a circle of radius $\rho$ parallel to the ground, and

$\theta_m$ is the polar angle, measured from the vertical to the radial r.

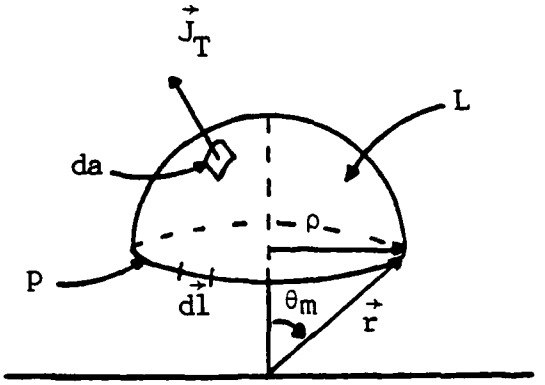


Figure 6. Magnetic Field Geometry

Integrating the magnetic field, H, around P, and the source current, $J_T$, across the surface L (in spherical coordinates), Eq (3-13) becomes

$$\int_0^{2\pi} H(\rho,\theta)\,\rho\,d\phi$$

$$= \int_{\theta=0}^{\theta_m} \int_{\phi=0}^{\phi=2\pi} [J_{cr}(r,\theta) + \sigma(r,\theta)\,E_r(r,\theta)]r^2\,\mathrm{SIN}\theta\,d\phi\,d\theta \qquad (3\text{-}14)$$

where $J_{cr}$ is the radial Compton current and $E_r$ is the radial electric field.

Integrating over $\phi$ yields

$$2\pi\,\rho\,H\,(\rho,\theta)$$

$$= 2\pi\,r^2 \int_0^{\theta_m} [J_{cr}(r,\theta) + \sigma(r,\theta)\,E_r(r,\theta)]\,\mathrm{SIN}\theta\,d\theta \qquad (3\text{-}15)$$

Solving for the azimuthal magnetic field obtains

$$H_\phi(\rho,\theta) = \frac{r^2}{\rho}\int_0^{\theta_m}[J_{cr}(r,\theta) + \sigma(r,\theta)\,E_r(r,\theta)]\,\mathrm{SIN}\theta\,d\theta \qquad (3\text{-}16)$$

Finally, substituting $\rho = r\,\mathrm{SIN}\theta$ leads to

$$H_\phi(r,\theta) = \frac{r}{\mathrm{SIN}\theta_m}\int_0^{\theta_m}[J_{cr}(r,\theta) + \sigma(r,\theta)\,E_r(r,\theta)]\,\mathrm{SIN}\theta\,d\theta \qquad (3\text{-}17)$$

Equation (3-17) was used to numerically determine the azimuthal magnetic field as a function of both radial distance and polar angle. Simpson's Composite Rule (Appendix A) was used to compute the integral over the polar angle and the source terms were determined in solving for the electric field (Appendix B).

Comparison

The numerical results (Eq 3-17) and Longmire's results (Eq 3-11) for the azimuthal magnetic field at one millisecond (retarded time) after a ten megaton surface burst are compared in Figures 7 and 8 for $\theta = 5°$ and $\theta = 90°$.

The results agree quite well (within 2%) for distances less than two kilometers, but the numerical values are as much as an order of magnitude larger for distances greater than two kilometers. Longmire assumed the radial electric field was zero; however, the numerical results set the radial electric field to zero only at the earth's surface. Therefore, the deviation at the larger distances is due to the incorporation

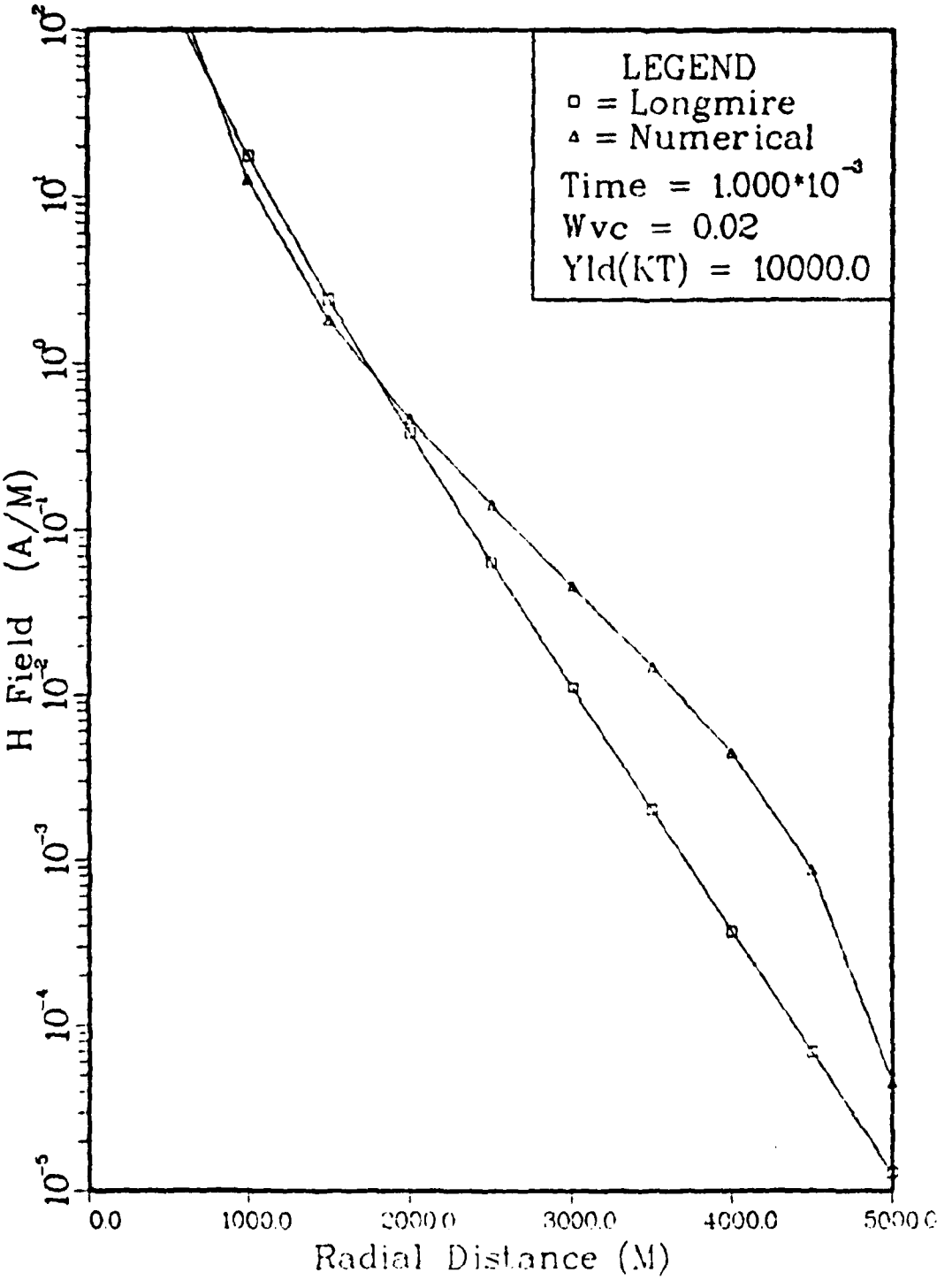


Figure 7. Azimuthal Magnetic Field, $\theta = 5°$

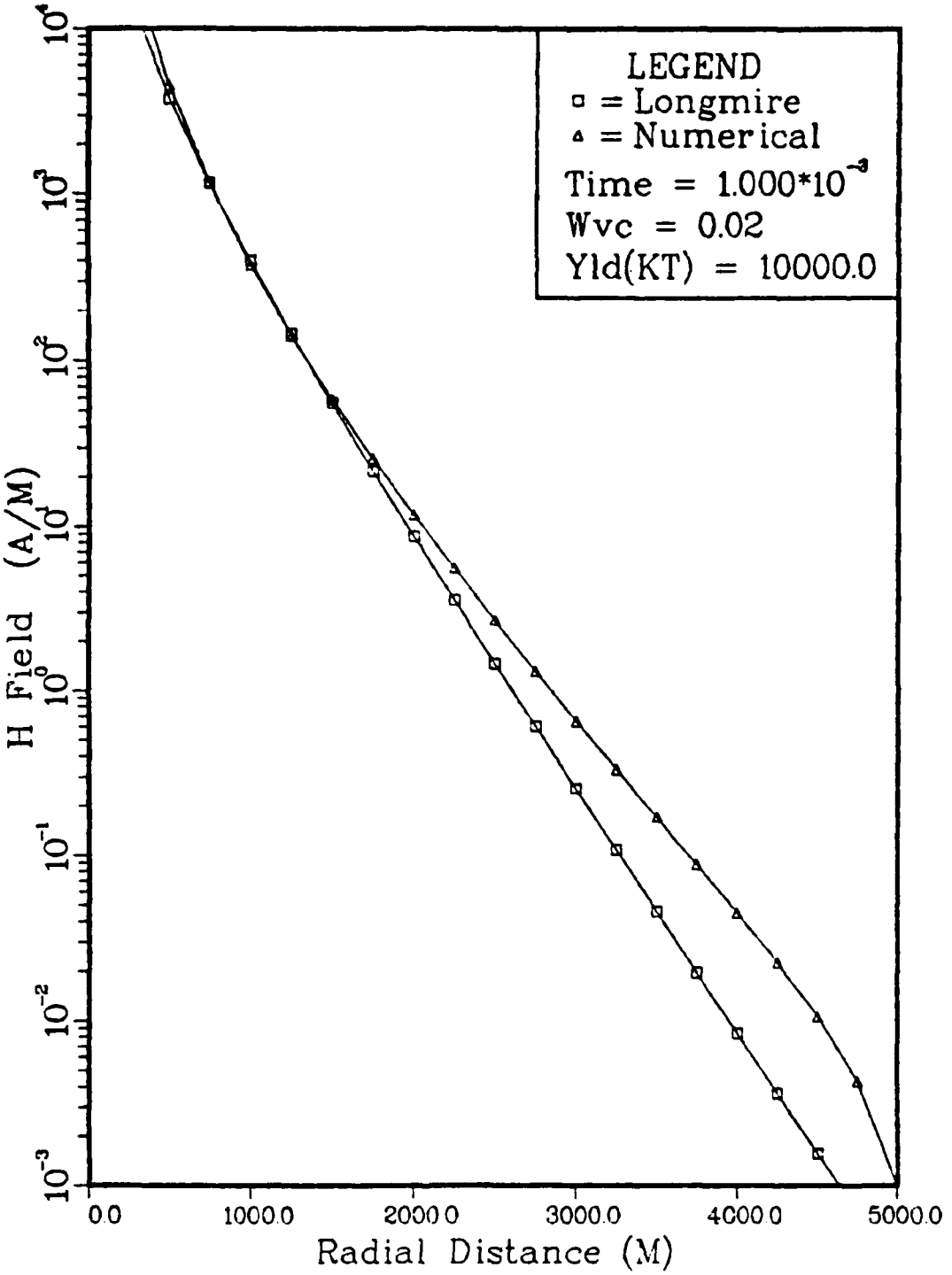


Figure 8. Azimuthal Magnetic Field, $\theta = 90°$

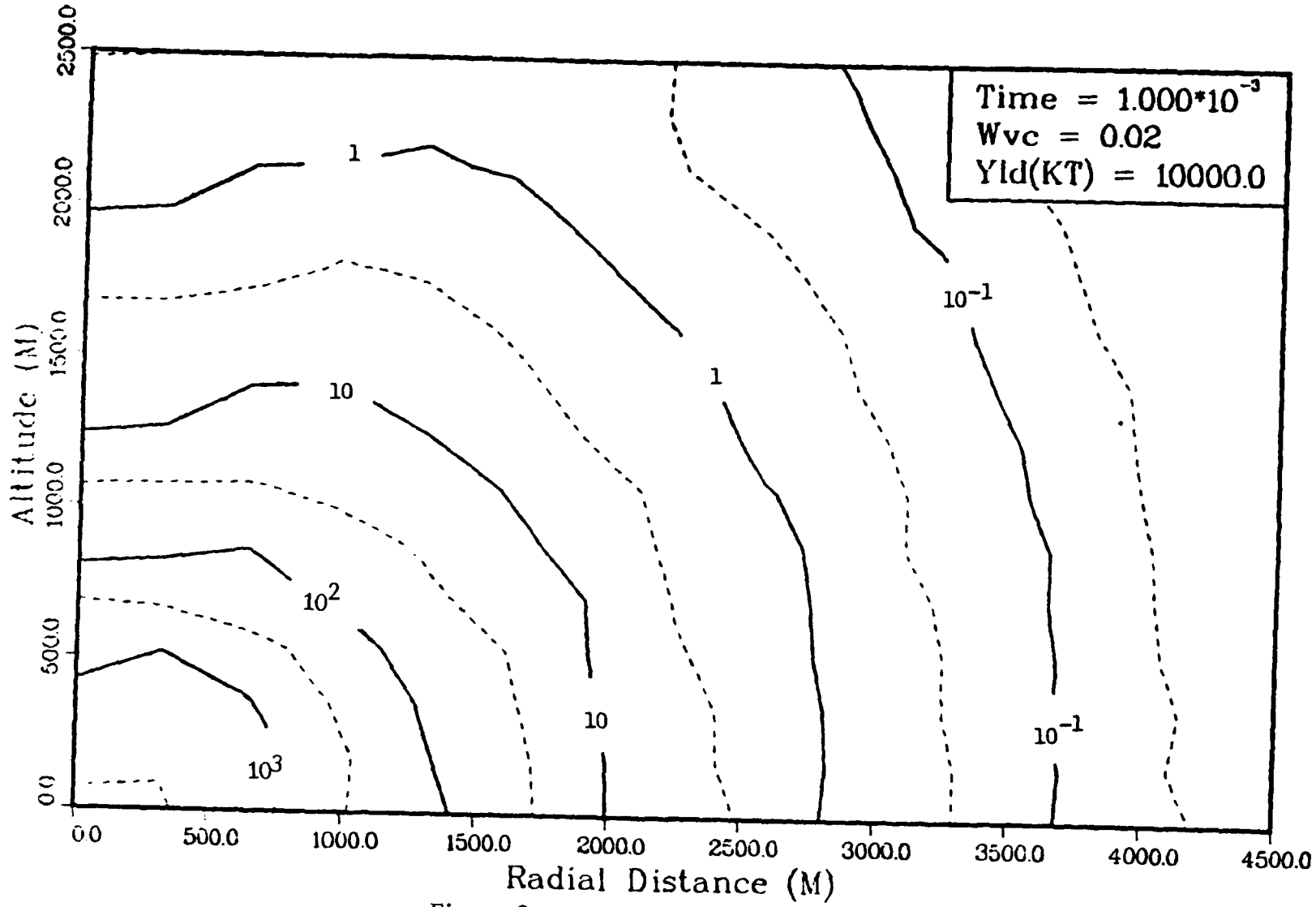


Figure 9. Azimuthal Magnetic Field (A/m)

of the radial conduction current into the numerical calculations and to the improved source term $J_{cr}$ (Ref 4:95).

Figure 9 is a contour plot of the azimuthal magnetic field for the reference case specified above. (NOTE: For graphing convenience, the absolute value of these fields are used; however, the fields are really negative (i.e. point in a clockwise fashion when viewed from above the burst).

## IV. Approximations

In this chapter, three approximations are investigated. First, the simplified boundary condition that the radial electric field goes to zero at the earth's surface provides an inner radial limit to the validity of the results. Second, the approximation that the conduction current is much greater than the displacement current at late times provides an outer radial limit to the validity of the results. Finally, the requirement that the radial electric field be derivable from a scalar potential is examined.

### Boundary Condition

In the development of the time-independent numerical solution of the late time source region EMP, the radial electric field is assumed to be zero at the earth's surface (Ref 4:19; 6:4479; 22:7). This approximation is valid if the ground conductivity is infinite. However, the ground conductivity is on the order of $10^{-2}$ to $10^{-3}$ Mho/m (Ref 6:4479; and 22:7). This approximation is still reasonable if the ground conductivity is much greater than the air conductivity ($\sigma_g >> \sigma_a$).

The air conductivity is determined by free electrons and positive and negative ion contributions. The free electron contribution is described by (Ref 6:990; 16:20-21; and 32:10)

$$\sigma_e = e \mu_e \frac{S}{\alpha_e} \quad (\frac{\text{Mho}}{\text{m}}) \tag{4-1}$$

where e is the electron charge (coulombs), $\mu_e$ is the electron mobility

($m^2$/volt-sec), S is the ionization rate in (ion-pairs/$m^3$ -s), and $\alpha_e$ is the electron attachment rate ($sec^{-1}$). The electron mobility $\mu_e$ and the electron attachment rate $\alpha_e$ are both dependent on the electric field values. This non-linear dependence of the conductivity is incorporated into the code by iterating until the electric field converges (Ref 4:51).

The ion contribution of the air conductivity can be written as

$$\sigma_i = 2e\,\mu_i \left(\frac{S}{K_i}\right)^{\frac{1}{2}} \quad \text{(Mho/m)} \tag{4-2}$$

where $\mu_i$ is the average ion mobility ($m^2$/volt-sec) and $K_i$ is the average ion-ion recombination rate ($m^3$/sec) (Ref 8:990; and 32:10). At late-times, the electrons are predominantly attached and the number of negative ions is approximately equal to the number of positive ions ($N_- = N_+$). Consequently, Eq (4-2) reflects (through the two) the combined positive and negative ion contributions. The ionization rate S, in Eqs (4-1) and (4-2) is described by

$$S = S_o \frac{e^{-r/\lambda}}{r^2} \quad \left(\frac{\text{ion-pairs}}{m^3 - \text{sec}}\right) \tag{4-3}$$

where $S_o$ is constant for a given yield and time (Ref 8:990; and 32:11). Substituting the ionization rate into Eqs (4-1) and (4-2) yields for the total air conductivity (Ref 4:21-22)

$$\sigma_T = e\,\mu_e \frac{S_o e^{-r/\lambda}}{\alpha_e r^2} + 2e\,\mu_i \frac{e}{r}^{-r/2\lambda} \left(\frac{S_o}{K_i}\right)^{\frac{1}{2}} \tag{4-4}$$

where at late-times, because of the radial dependence, the electrons dominate the air conductivity near the burst and the ions dominate the air conductivity farther out (Ref 8:993).

Equation (4-4) was used to determine the air conductivity as an input to the source terms in Maxwell's equations. Figure 10 shows a contour plot of the air conductivity for the reference case.

In close, near the fireball, the air conductivity increases to the point where the ground conductivity is no longer much greater than the air conductivity and the radial electric field can no longer be set to zero at the earth's surface. When the air conductivity at the surface of the earth exceeds one tenth the ground conductivity (i.e. when the ratio $\sigma_g/\sigma_a < 10$) this approximation is no longer justified.

For a ground conductivity of $10^{-3}$ (Mho/m), this occurs when the air conductivity exceeds $10^{-4}$ Mho/m. At one millisecond after a ten megaton surface burst, the air conductivity exceeds $10^{-4}$ Mho/m for ranges less than approximately 750 meters (Figure 10). More results will be presented in Chapter 5.

Quasi-static Approximation - $\partial\vec{E}/\partial t$

In deriving an expression for the azimuthal magnetic field from Maxwell's time-dependent magnetic curl equation, a quasi-static approximation was made that the time derivative was small and could be set to zero ($\partial\vec{E}/\partial t = 0$) (See Chapters 2 and 3). This approximation is valid if the displacement current is much less than the conduction current (i.e. $\epsilon\partial\vec{E}/\partial t << \sigma\vec{E}$); or put differently, when this quasi-static approximation is valid, the ratio of the conduction current to the displacement cur-

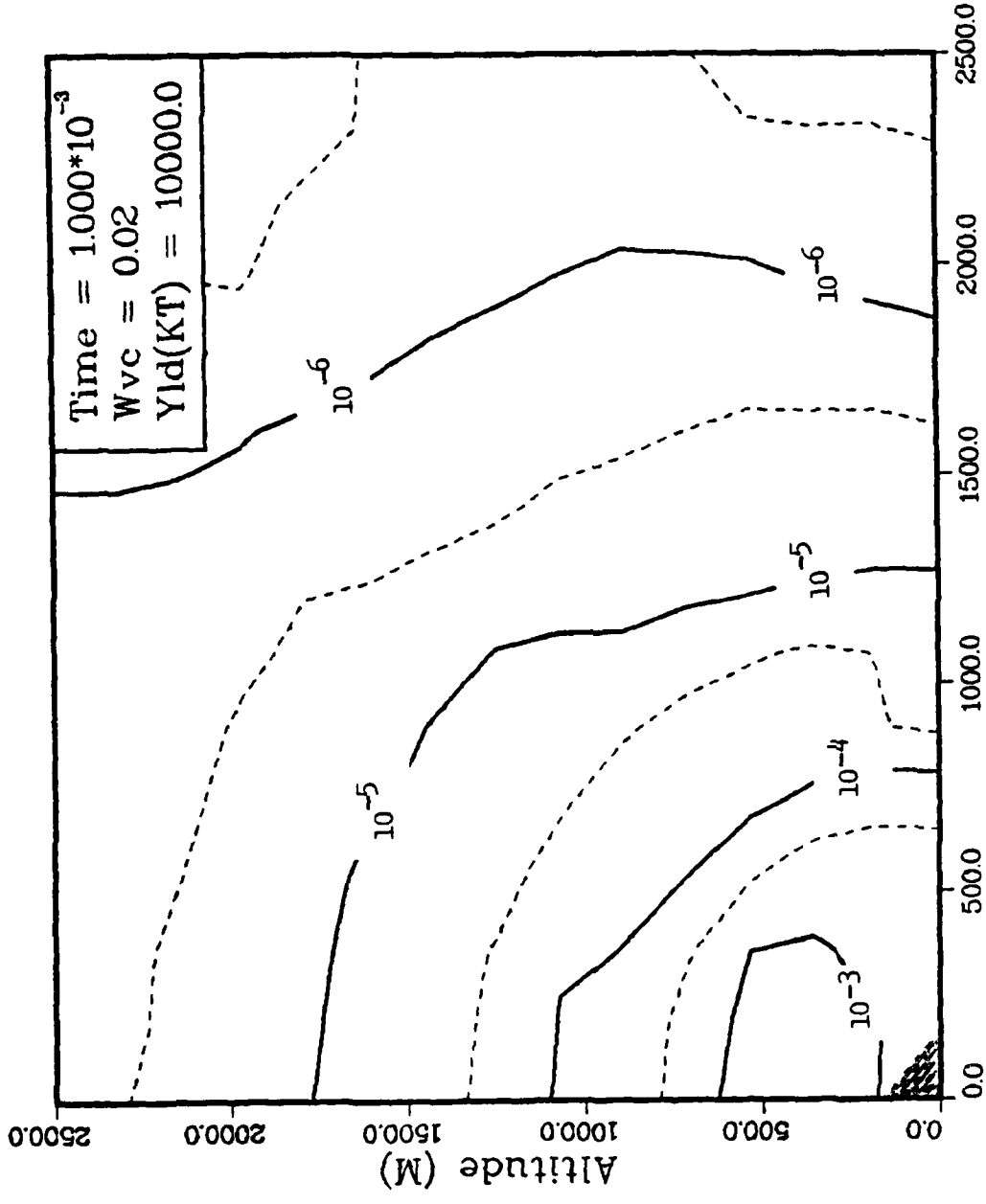


Figure 10. Air Conductivity (Mho/m)

rent is greater than ten (i.e. $\sigma\vec{E}/\varepsilon\partial\vec{E}/\partial t > 10$).

The conduction current is determined by taking average values of the conductivity and the total electric field over a specified time step as a function of radial and polar variations. The displacement current is determined by taking differences in electric field values over the same specified time step as a function of radial and polar variations. The time step is taken as 2 $\tau$, where $\tau$ is the retarded time after the burst. The ratio of the conduction current to the displacement current is computed and is shown in Figure 11 in the form of a contour plot.

At one millisecond after a ten megaton burst, this quasi-static approximation is valid for ranges less than approximately 3250 meters. More results will be presented in Chapter 5.

Quasi-Static Approximation - $\partial\vec{B}/\partial t$

In Chapter 2, an expression for the electric field was derived from Maxwell's time-dependent equations, using the quasi-static approximation that the electric field is derivable from a scalar potential ($\vec{E} = \vec{\nabla}\phi$). This requires that

$$\vec{\nabla} \times \vec{E} = 0 \tag{4-5}$$

and from Eq (2-1), that

$$\frac{\partial \vec{B}}{\partial t} = 0 \tag{4-6}$$

The time rate of change of the magnetic field was calculated by taking the difference in magnetic field values over a specified time step. This time step was taken as 2 $\tau$, where $\tau$ is the retarded time.

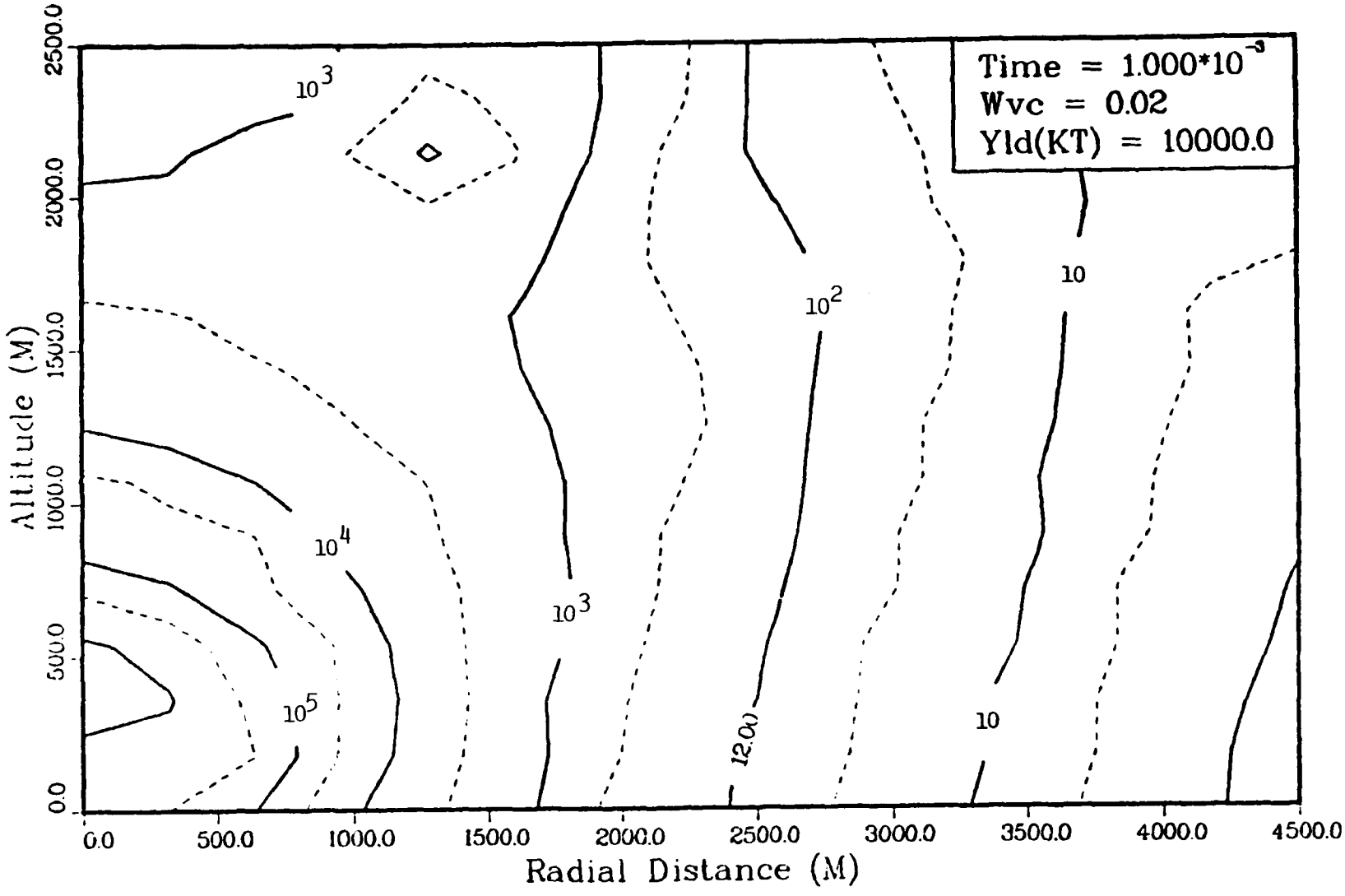


Figure 11. Ratio - Conduction Current/Displacement Current

Figure 12 shows $\partial\vec{B}/\partial t$ as a function of radius along the ground ($\theta = 90°$) for a ten megaton burst. As is evident from Figure 12, $\partial\vec{B}/\partial t$ does not equal zero, and it is thus necessary to determine the conditions when this approximation holds.

Longmire (Ref 20:65) states that the quasi-static phase begins when the skin depth $\delta$ in the air becomes as large as allowed by the spherical geometry (i.e. when $\delta$ exceeds the distance r from the burst point). The quasi-static approximation then requires (Ref 6:4481):

$$\lambda \ll \delta \tag{4-7}$$

where $\delta$ is the time independent skin depth in air and $\lambda$ is the gamma ray attenuation length. The skin depth is defined as (Ref 11:4443; and 12:1876):

$$\delta = \left(\frac{2t}{\mu_o \sigma}\right)^{\frac{1}{2}} \tag{4-8}$$

Equations (4-7) and (4-8) yield

$$\lambda \ll \left(\frac{2t}{\mu_o \sigma}\right)^{\frac{1}{2}} \tag{4-9}$$

or, rearranging (Ref 7:992)

$$\sigma \ll \frac{2t}{\mu_o \lambda^2} \tag{4-10}$$

Alternately,

$$t \gg \frac{\sigma \mu_o \lambda^2}{2} \tag{4-11}$$

This provides a commencement time for the quasi-static phase. For values of $\mu_o = 4\pi \times 10^{-7}$ (Henrys/m), $\lambda$ = 320 meters and a selected

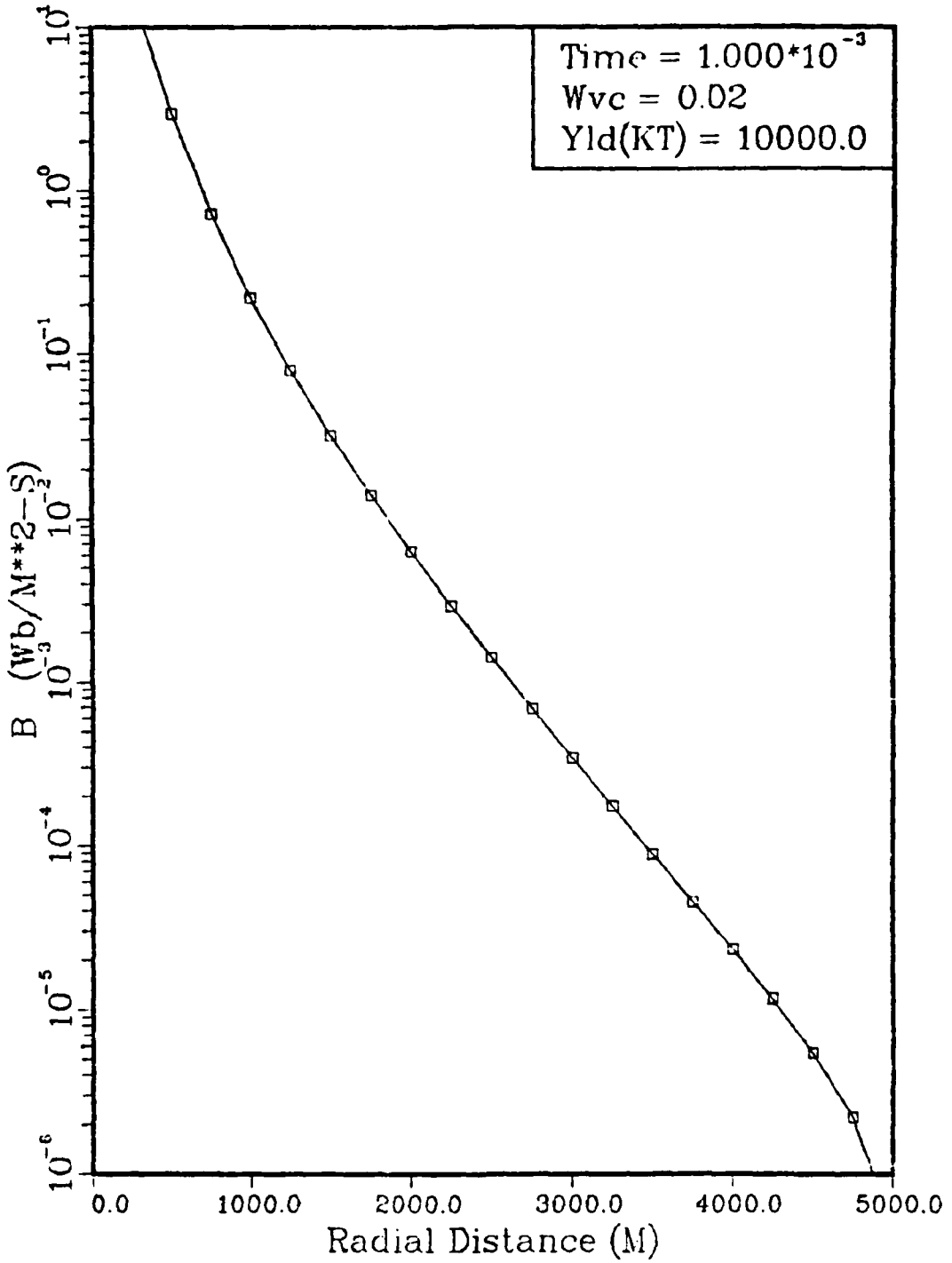


Figure 12. Time Rate of Change of the Magnetic Field for $\Theta = 90°$.

inner radial air conductivity limit of $10^{-4}$ Mho/m, Eq (4-11) provides:

$$t >> 6.4\mu s \qquad (4\text{-}12)$$

The quasi-static phase for a surface nuclear burst over $10^{-3}$ Mho/m conducting soil, is therefore valid for times greater than approximately 60 microseconds.

## V. Results

This chapter presents the results of the investigation of the validity of the boundary condition at the earth's surface ($E_r = 0$) and of the quasi-static approximation that the conduction current is much greater than displacement current ($\sigma\vec{E} >> \varepsilon \partial\vec{E}/\partial t$).

### Yield versus Radius

The requirement that the ratio of the ground conductivity to the air conductivity be greater than ten specifies an inner radius of validity for the boundary condition and hence, the validity of the late-time time-independent numerical code. Conversely, the quasi-static approximation that the displacement current can be ignored specifies an outer radius of validity for the time-independent numerical code.

Figure 13 shows the region of validity of the late-time SREMP code as a function of yield. The data is for various yields at one millisecond retarded time and an air water vapor fraction of 0.02. Additionally, the ground conductivity was selected as $10^{-3}$ Mho/m. For higher conducting ground, the inner radius would be smaller, and, likewise, for lower conducting ground, the inner radius would be larger. The outer radius would not be affected by changes in the ground conductivity. This region of validity is a fairly well behaved function of yield and ranges from 400 meters to 2700 meters for a one megaton burst and from 730 meters to 3220 meters for a ten megaton burst. For low yields, the inner radius is limited by the radius of the highly conducting thermal fireball and does not reach zero.

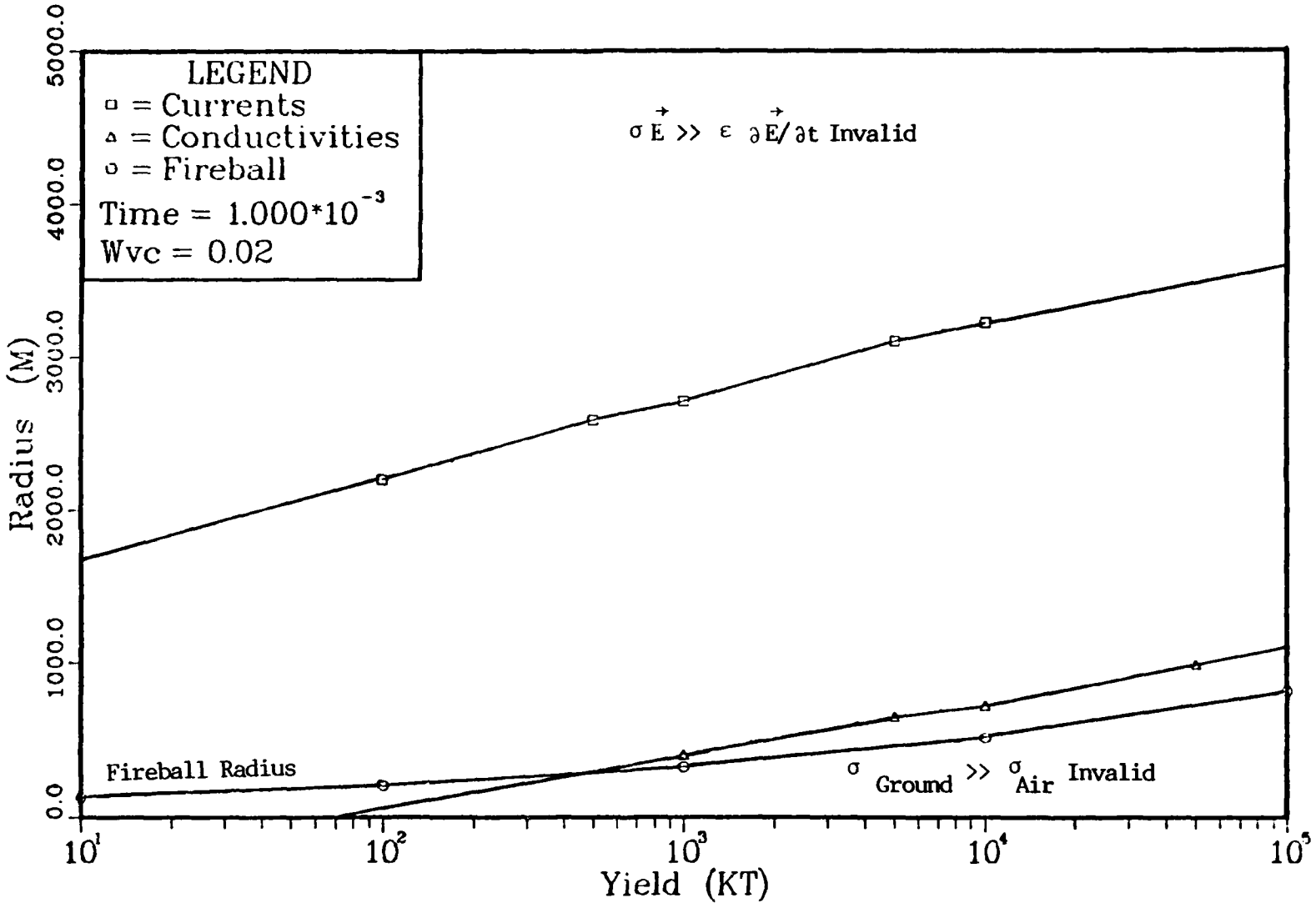


Figure 13. Region of Validity (Yield vs Radius)

Time versus Radius

Figure 14 shows the region of validity of the late-time SREMP code as a function of time. The data is for various times of a ten megaton burst with an air water vapor fraction of 0.02. The inner radius is a fairly well behaved function of time and depicts the decreasing air conductivity with time. Again, the inner radius will be limited (at later times) by the expanding highly conducting thermal fireball. The outer radius reflects the time rate of change of the electric field and is, therefore, not a well behaved function of time (Figure 15). The magnitude of the total electric field changes very little from 100 microseconds to one millisecond, and changes even less after 10 milliseconds. However, between one and ten milliseconds, there is a significant change in the electric field as the dominant gamma source switches from ground capture to air capture neutrons (Ref 4:70).

Figures 17 - 22 are contour plots of the ratio of the conduction current to the displacement current for yields of 0.1, 1.0, and 10 megatons and for times of $10^{-4}$, $10^{-3}$, and $10^{-2}$ seconds. Figures 23 - 28 are contour plots of the air conductivity for the same range of yields and times. The ratio contour plots are a strong function of the electric field values and the conductivity plots are strictly hemispherical in nature.

NOTE: Fireball

The fireball has the following effects on the EMP fields:

1) The fireball thermal ionization conductivity shorts out the radial electric field.

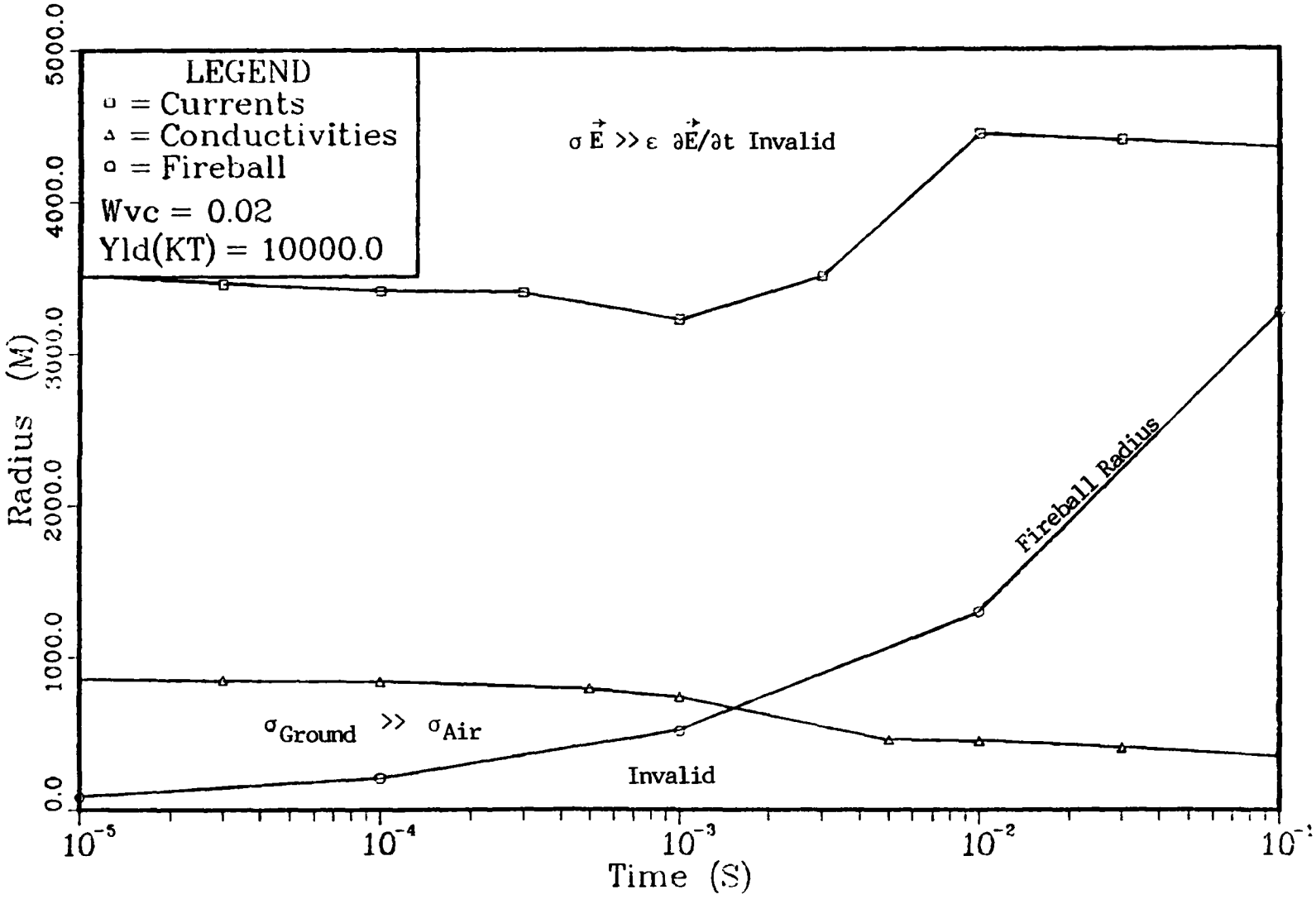


Figure 14. Region of Validity (Time vs Radius)

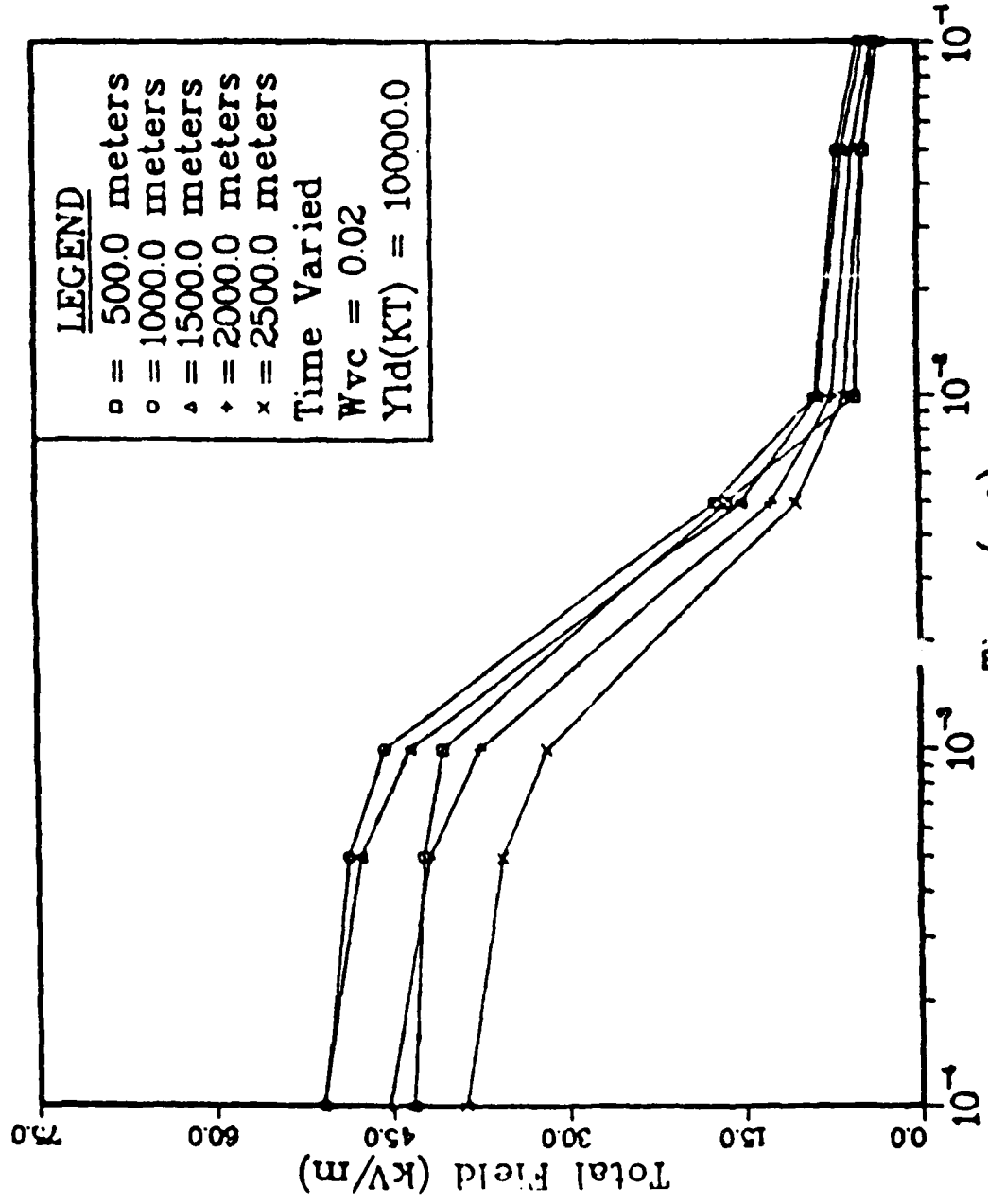


Figure 15. Total Field vs Time, $\theta = 90°$ (Ref 4:69)

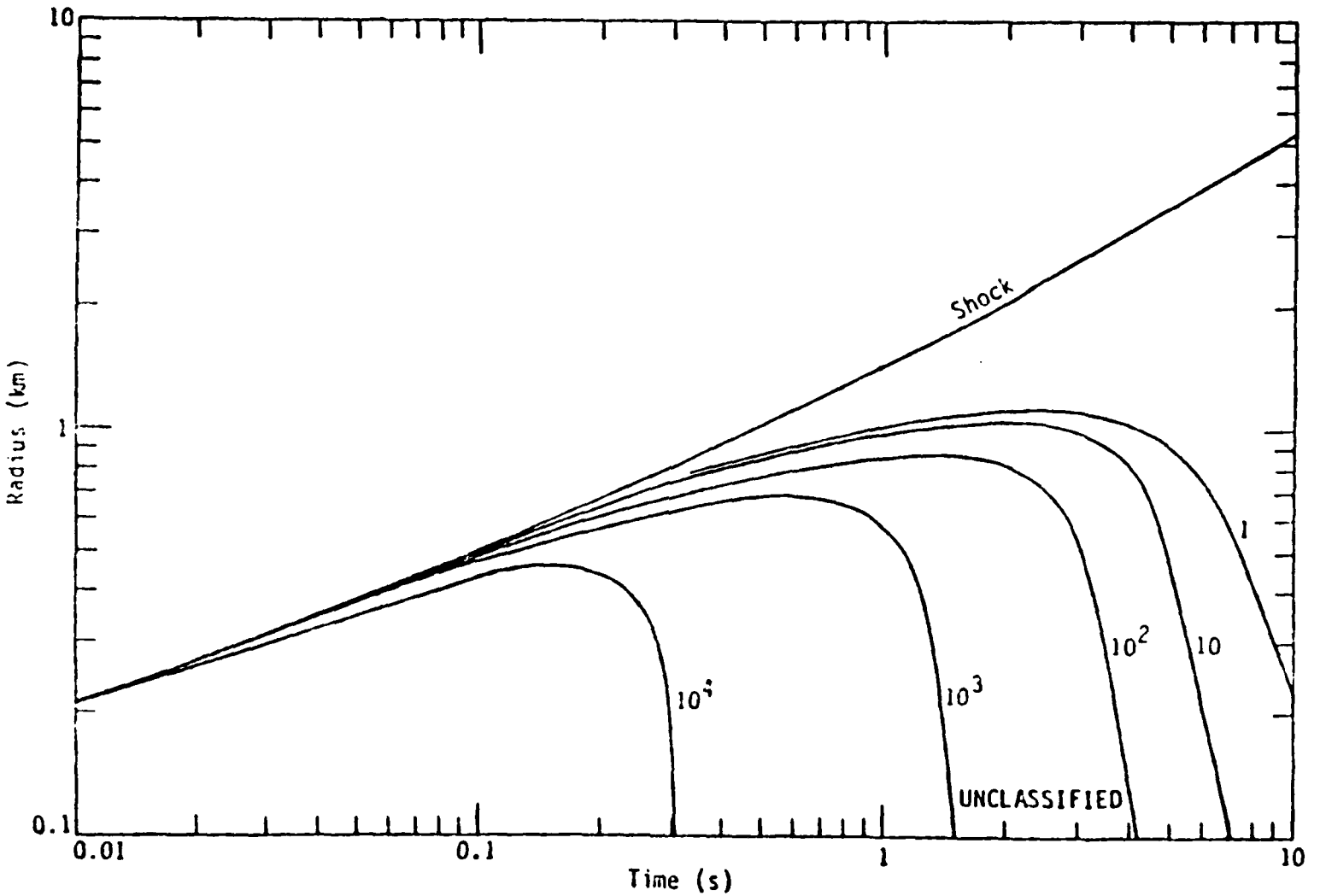


Figure 16. (U) Contours of constant electrical conductivity in radius-time plot for 1-MT surface burst. The numbers near the curves are conductivity in S/m (Ref 5:12).

2) The fireball expansion pushes the magnetic field ahead of itself.

3) And the presence of low density air inside and high density air at the periphery of the shock front modifies the air capture sources of late-time gammas.

An equation for the fireball radius as a function of yield and time is (Ref 5:11):

$$R = 1300\ Y^{1/5}\ t^{2/5} \tag{5-1}$$

where R is the radius (m), Y is the yield (MT), and t is the time in seconds.

For 10 megatons at 60 milliseconds:

$$R = 1300\ (10)^{0.2}\ (.06)^{0.4} \simeq 670m \tag{5-2}$$

For 100 kilotons at 1 millisecond:

$$R = 1300\ (0.1)^{0.2}\ (.001)^{0.4} \simeq 50m \tag{5-3}$$

Fireball effects are, therefore, mainly a concern for large yields and small ranges at very late-times.

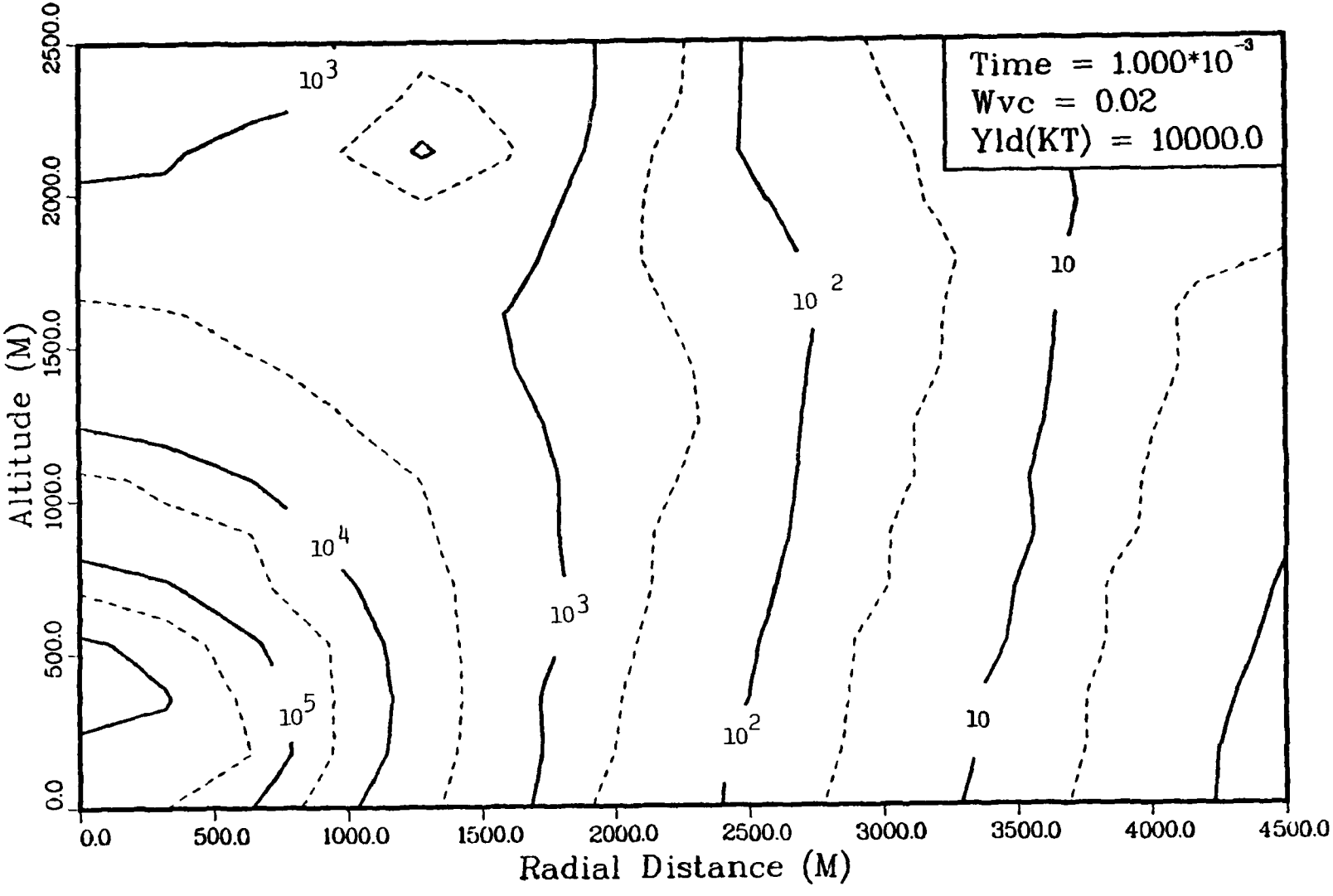


Figure 17. Conduction Current/Displacement Current, Y = 10 Mt

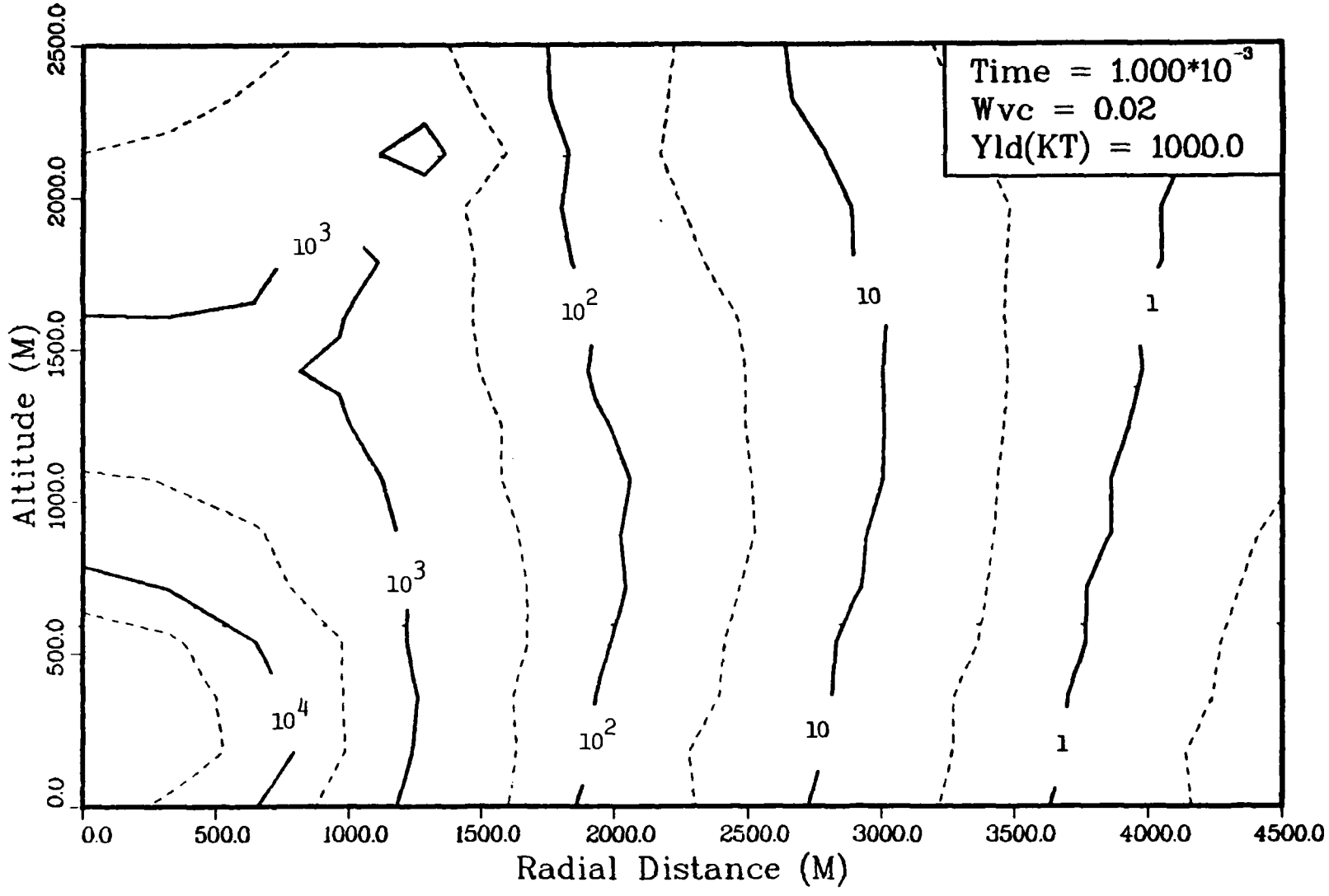


Figure 18. Conduction Current/Displacement Current, Y = 1 Mt

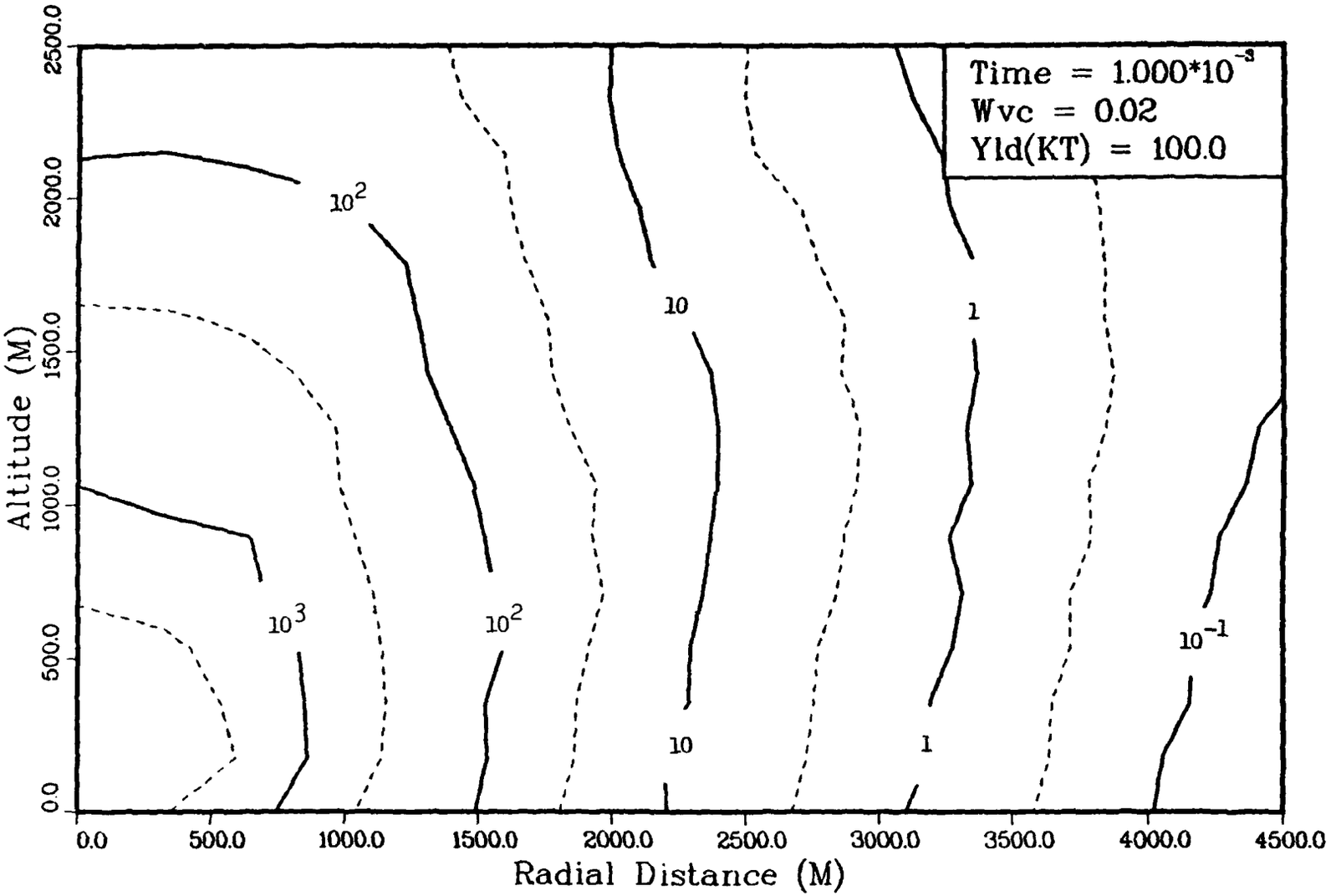


Figure 19. Conduction Current/Displacement Current, Y = 100 Kt

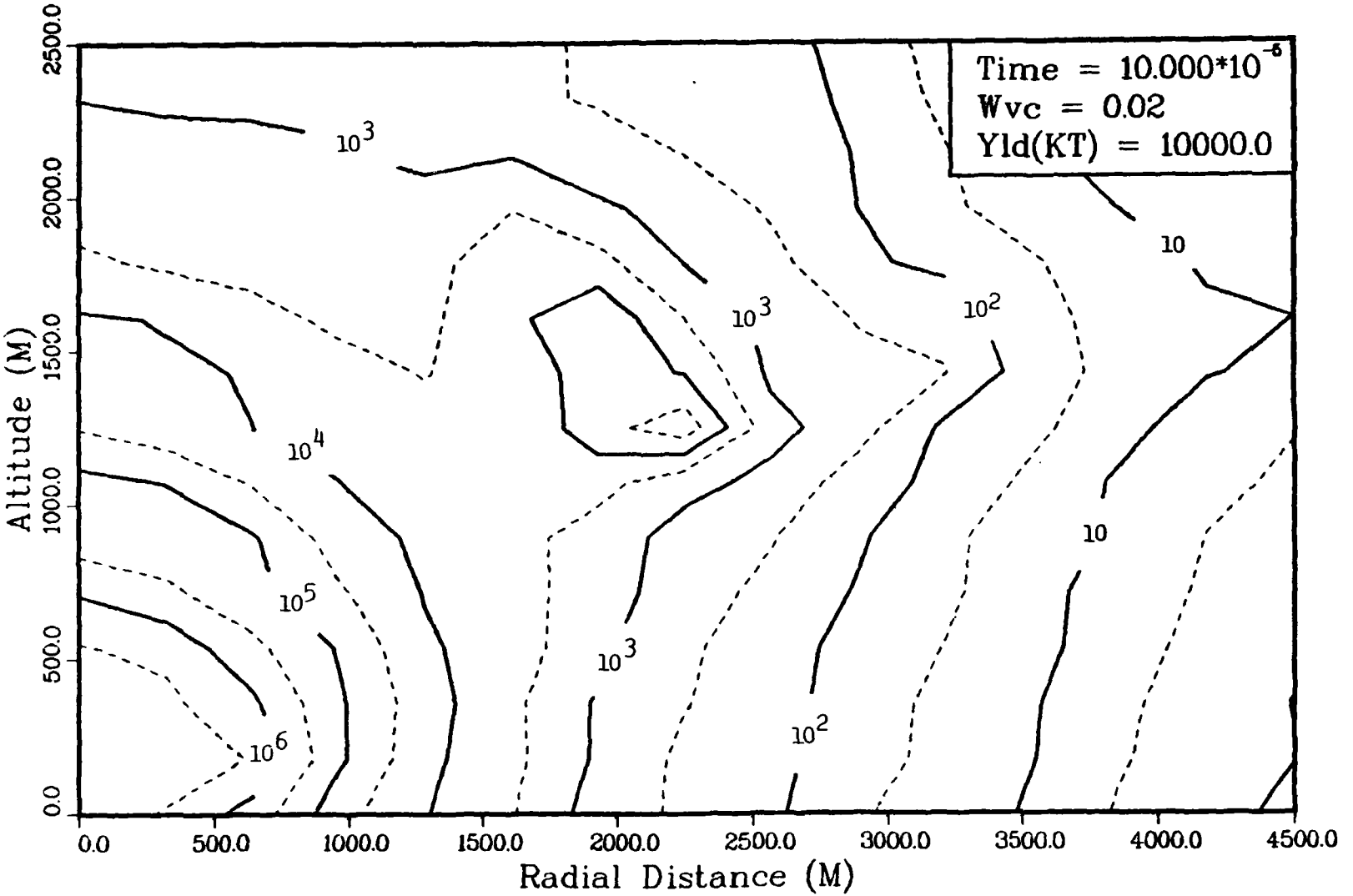


Figure 20. Conduction Current/Displacement Current, T = $10^{-4}$ Sec

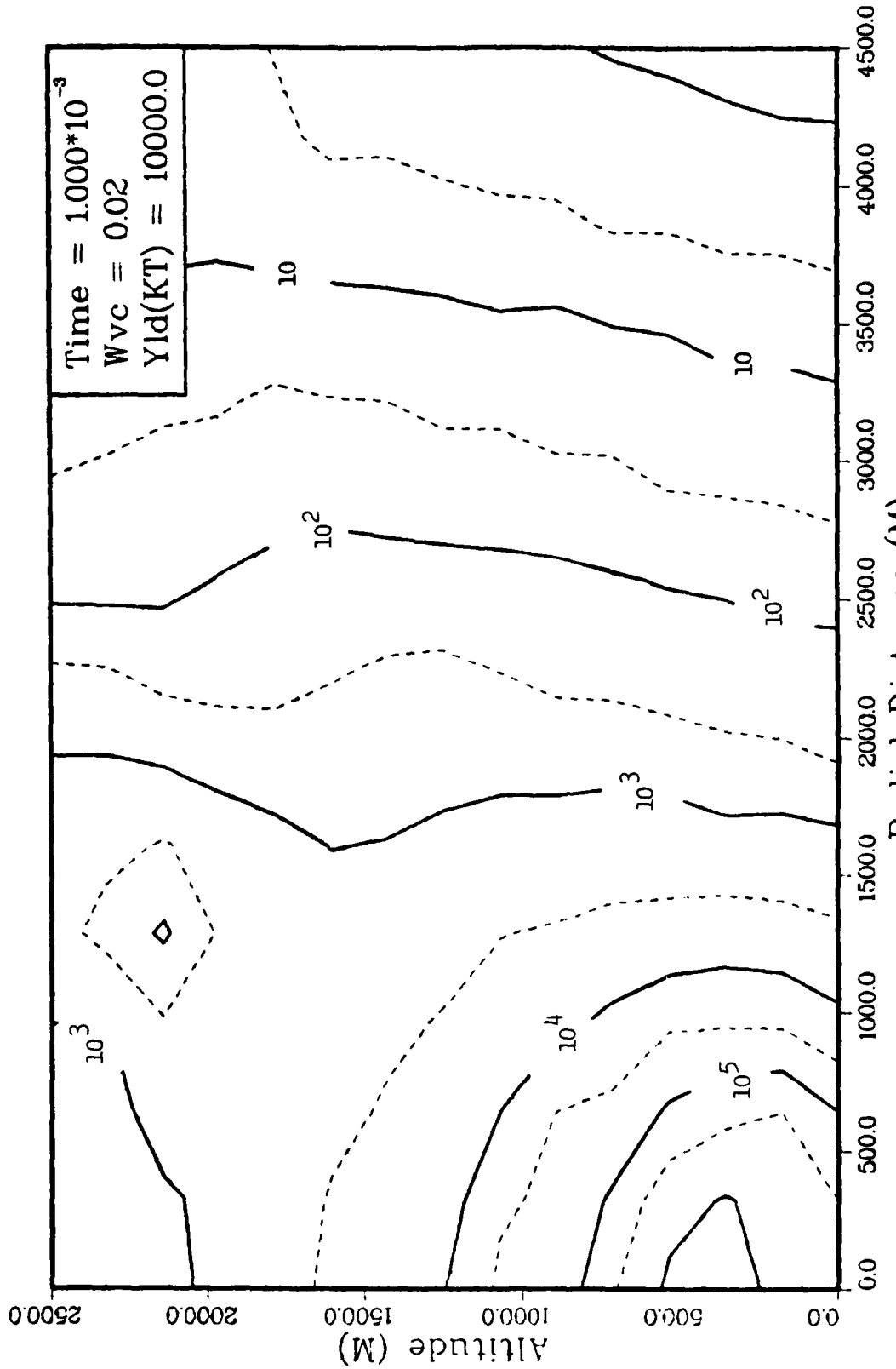


Figure 21. Conduction Current/Displacement Current, T = $10^{-3}$ Sec

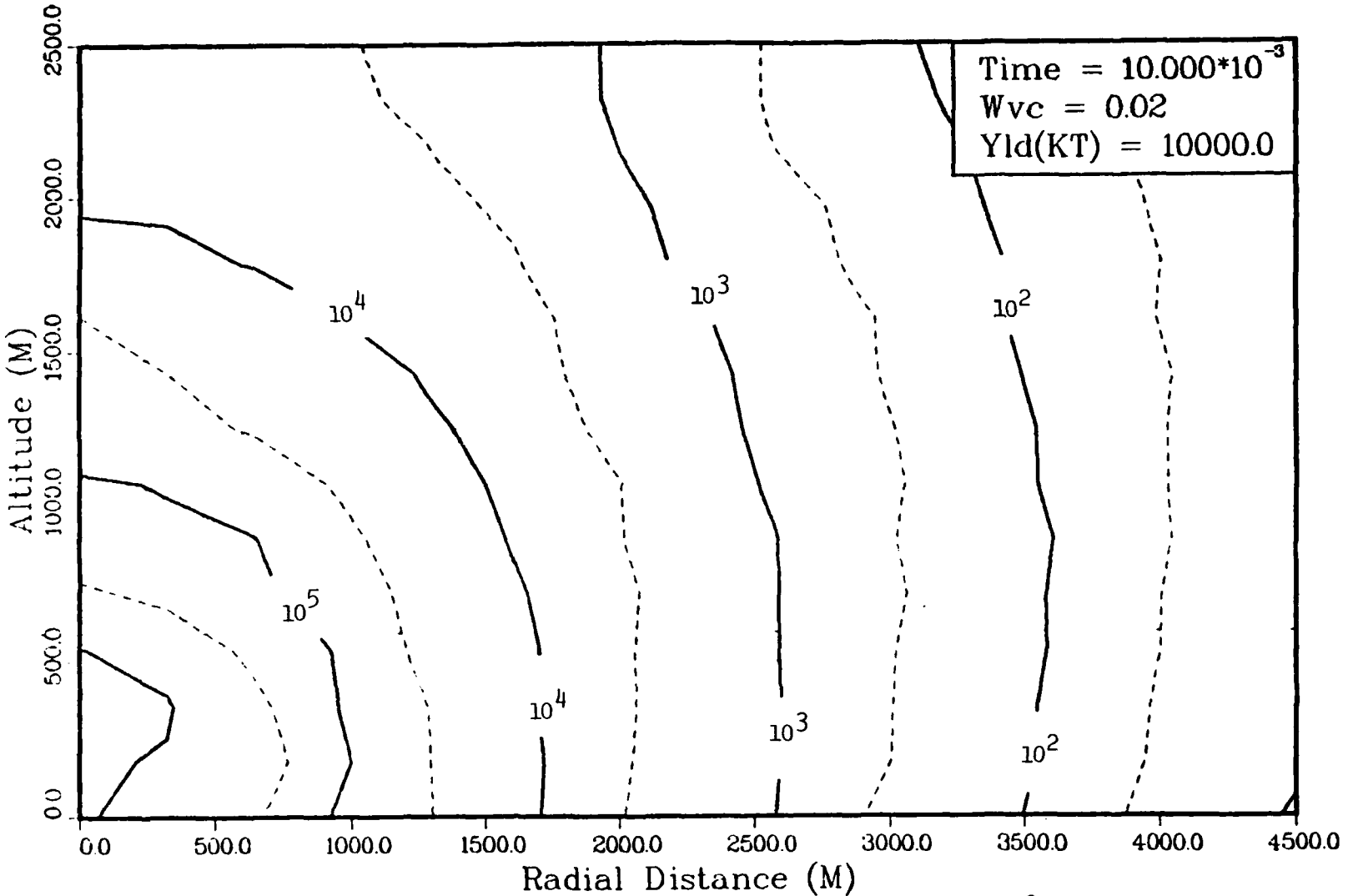


Figure 22. Conduction Current/Displacement Current, T = $10^{-2}$ Sec

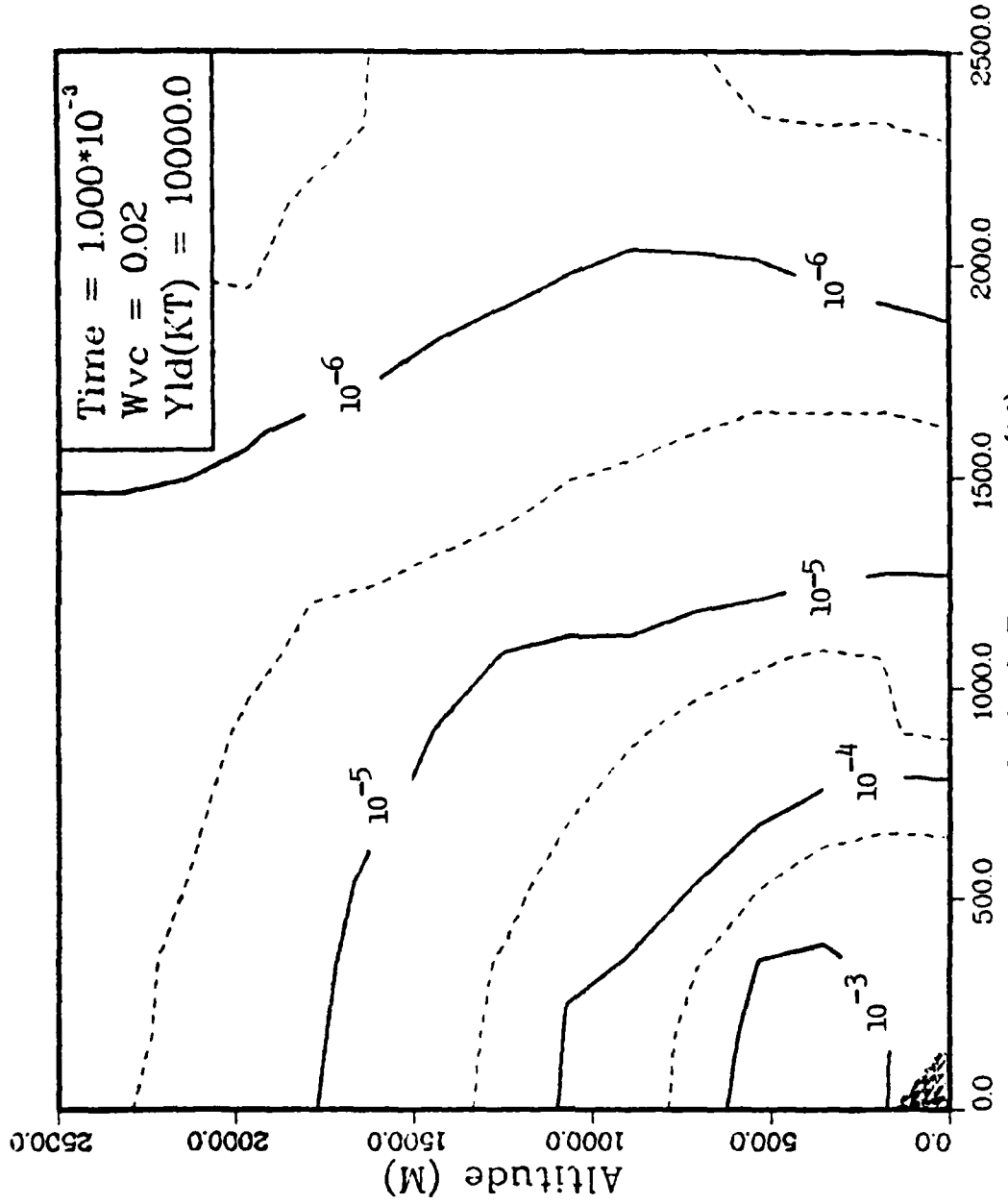


Figure 23. Air Conductivity, Y = 10 Mt

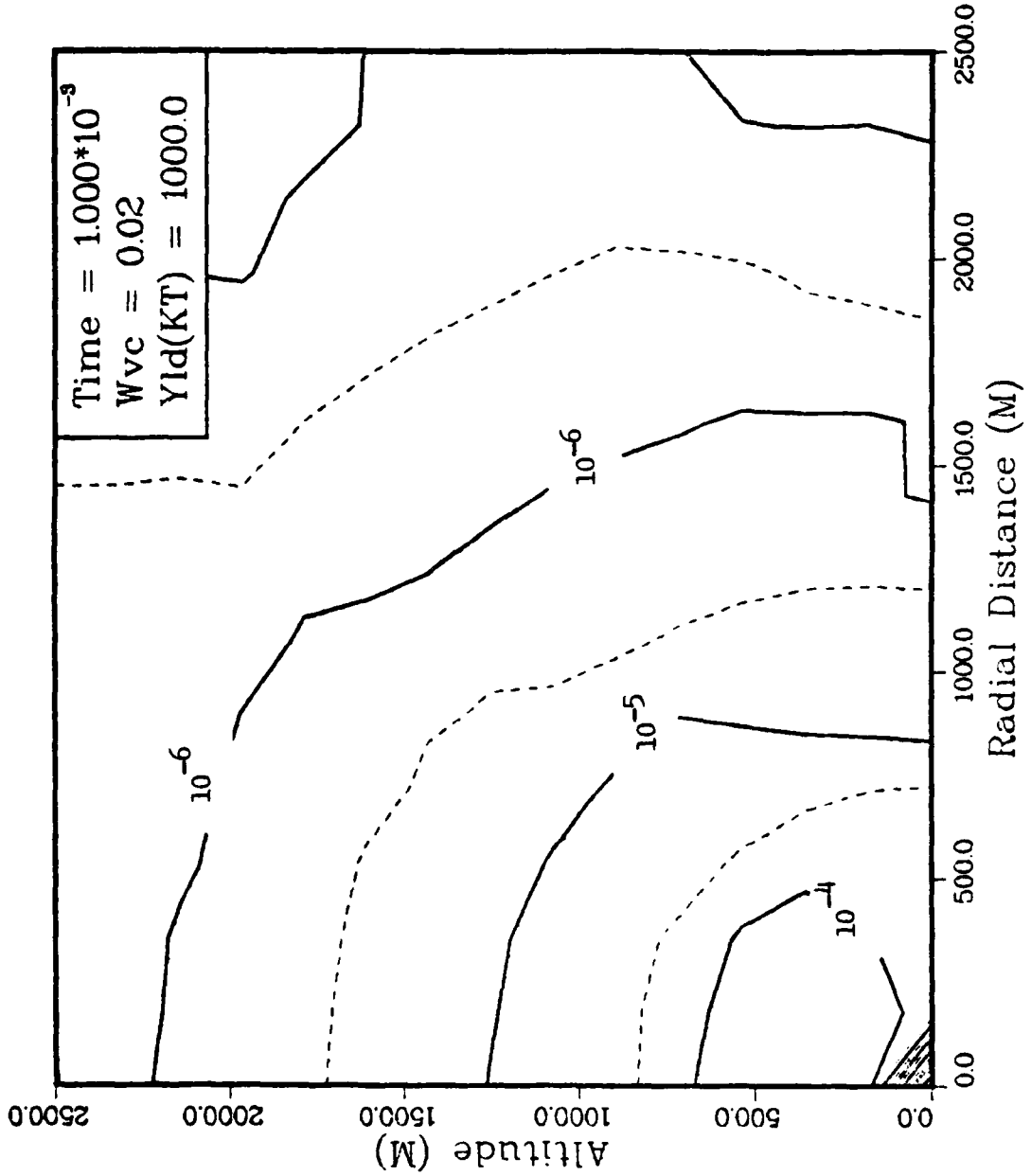


Figure 24. Air Conductivity, Y = 1 Mt

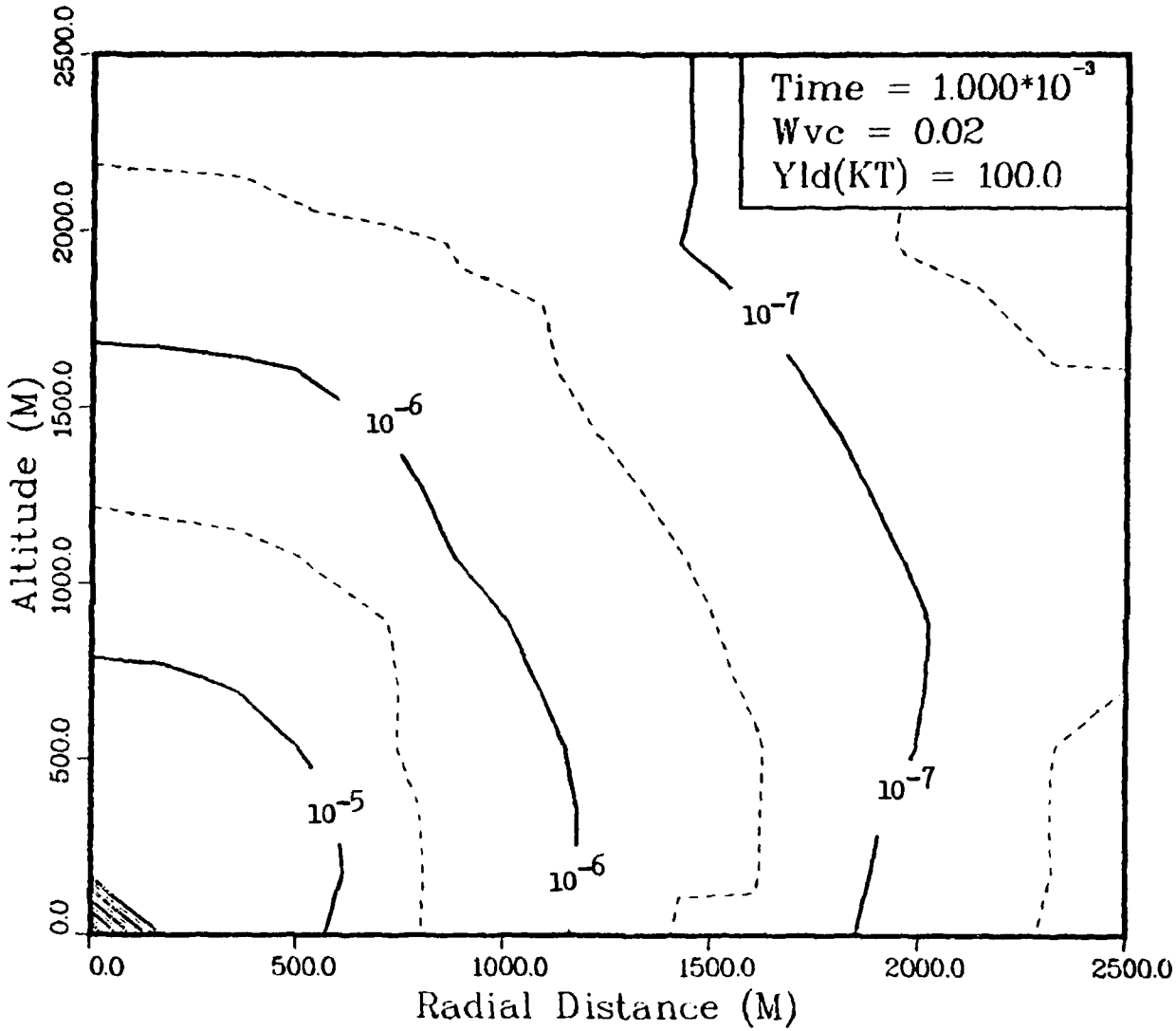


Figure 25. Air Conductivity, Y = 100 Kt

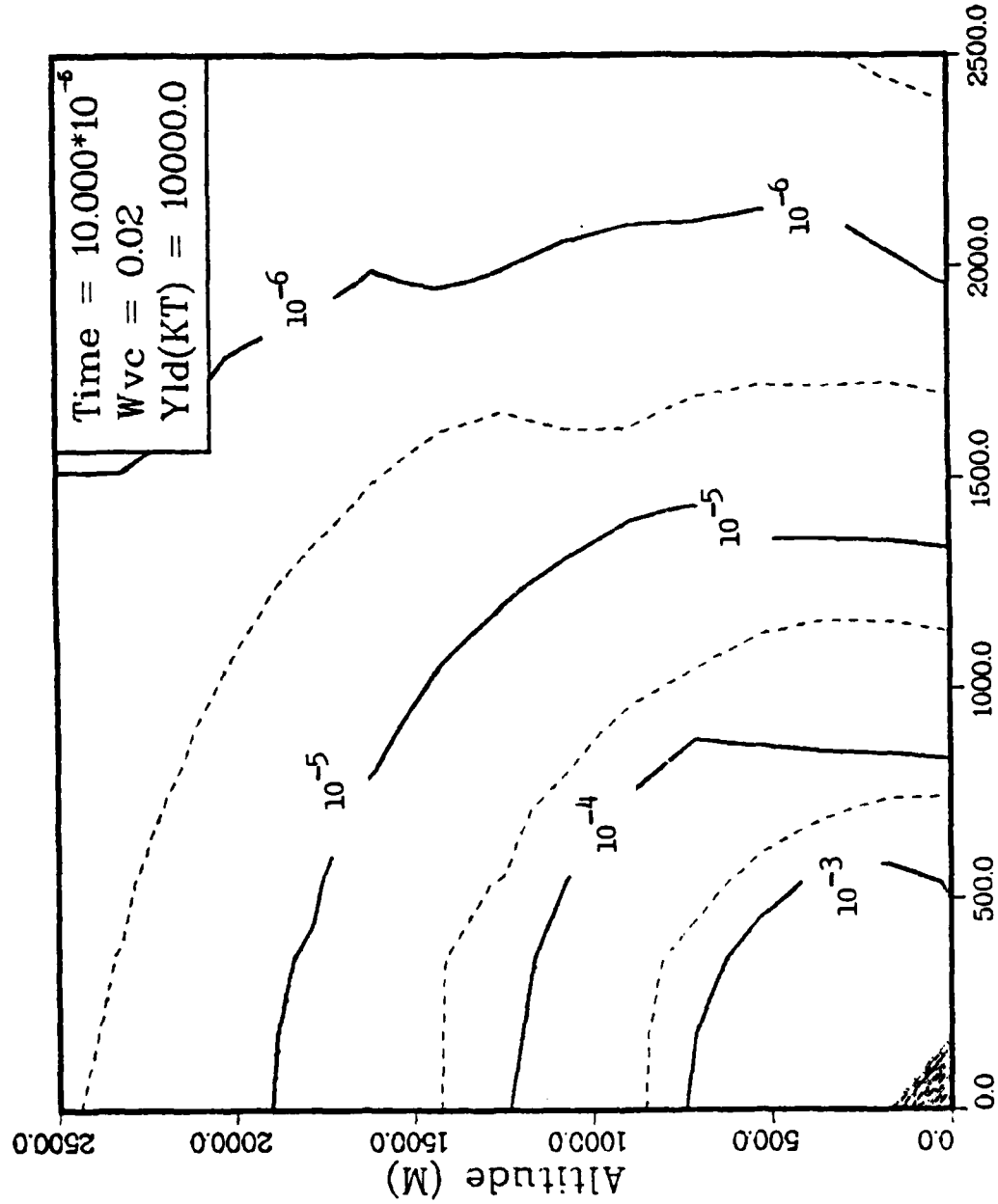


Figure 26. Air Conductivity, T = $10^{-4}$ Sec

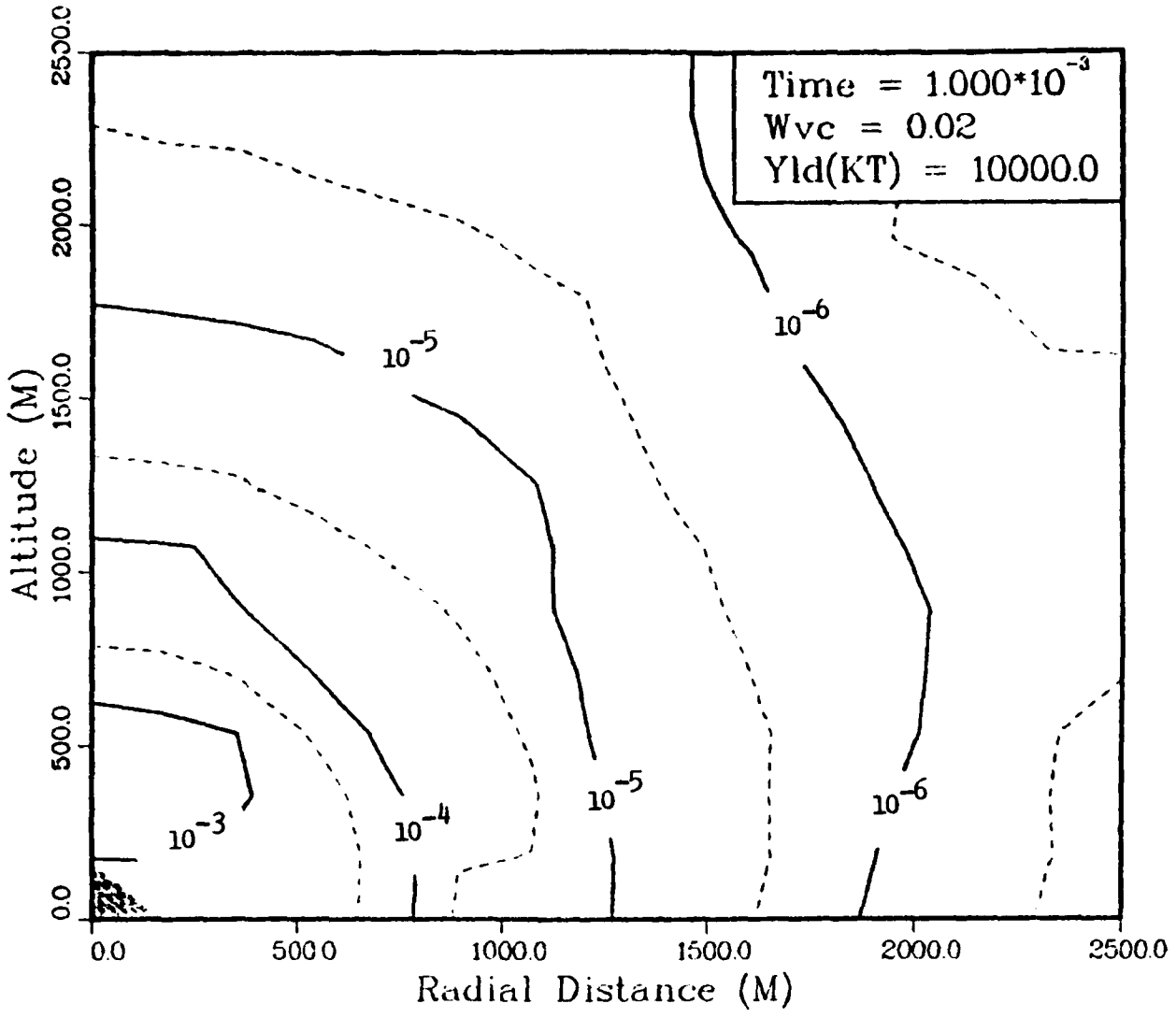


Figure 27. Air Conductivity, T = $10^{-3}$ Sec

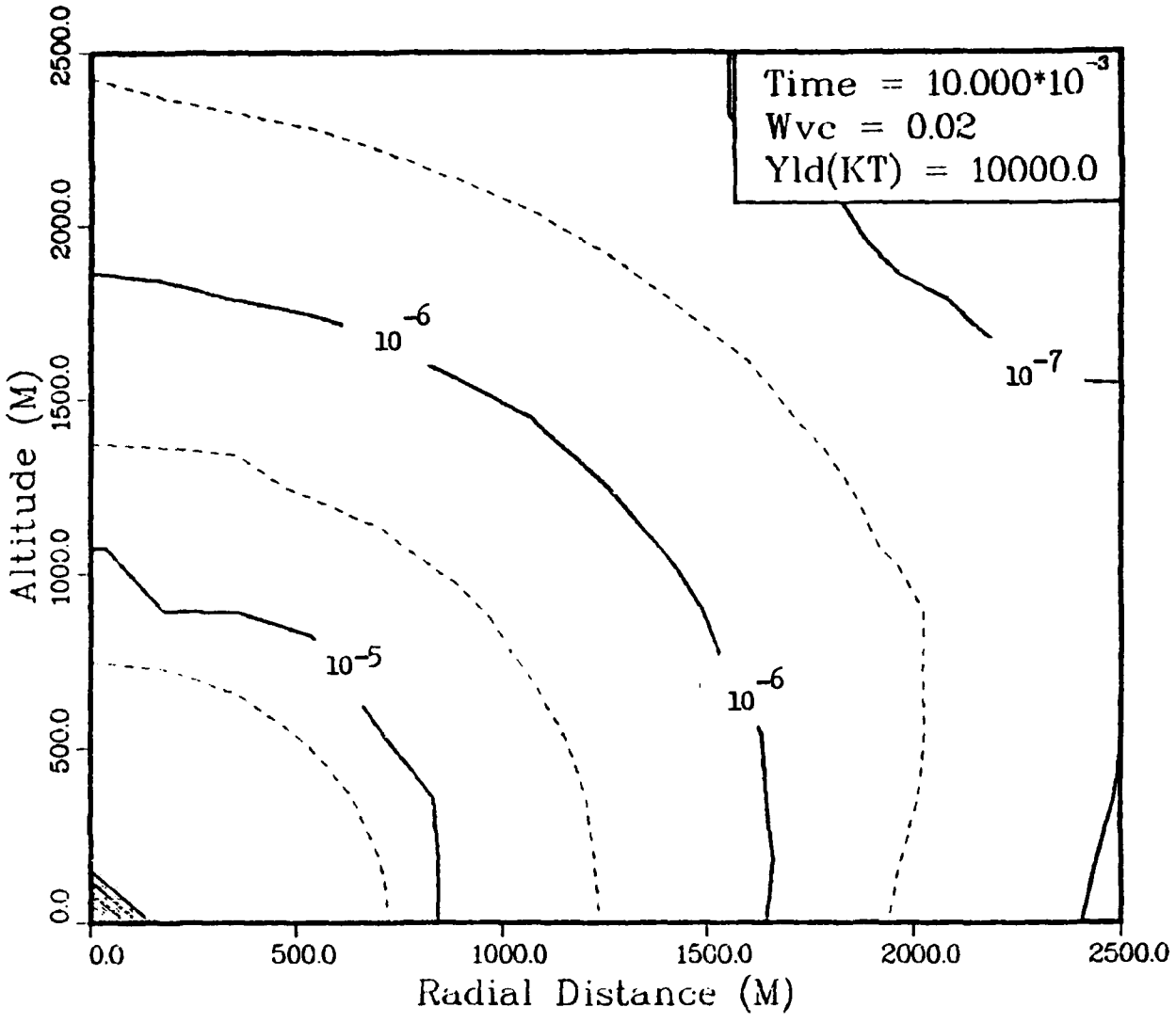


Figure 28. Air Conductivity, T = $10^{-2}$ Sec

## VI. Parametric Studies

This chapter presents the results of the parametric studies of the total electric field values (Ref 4:Ch 8).

### Contour Plots

Figures 29 - 31 show the magnitude of the total electric field as a function of yield. These figures depict the reduction of the importance of the radial electric field with small yields at later-times (see Chapter 2, Figures 3, 4, 5). In addition to the decrease in magnitudes of the total electric field, the figures show the change in the location of the peak electric fields from 45,000 V/m on the ground at 1200 meters for a ten megaton burst to 17,000 V/m on the ground at roughly 500 meters for a 100 kiloton burst.

Figures 29, 32 and 33 show the magnitude of the total electric field as a function of time for a ten megaton burst. As expected, the peak values decrease in time from 50,000 V/m at 100 microseconds to 8500 V/m at 10 milliseconds. However, the location of the peak field is constant in time - it remains at the earth's surface at approximately 1200 meters from the burst.

Finally, Figures 29, 34 and 35 show the magnitude of the total electric field as a function of water vapor fraction for one millisecond (retarded times) after a ten megaton burst. The peak values are a strong function of the water vapor fraction and range from 32,500 V/m at 1200 meters for a water vapor fraction of 0.01 to greater than 80,000 V/m at 700 meters for a water vapor fraction of 0.05.

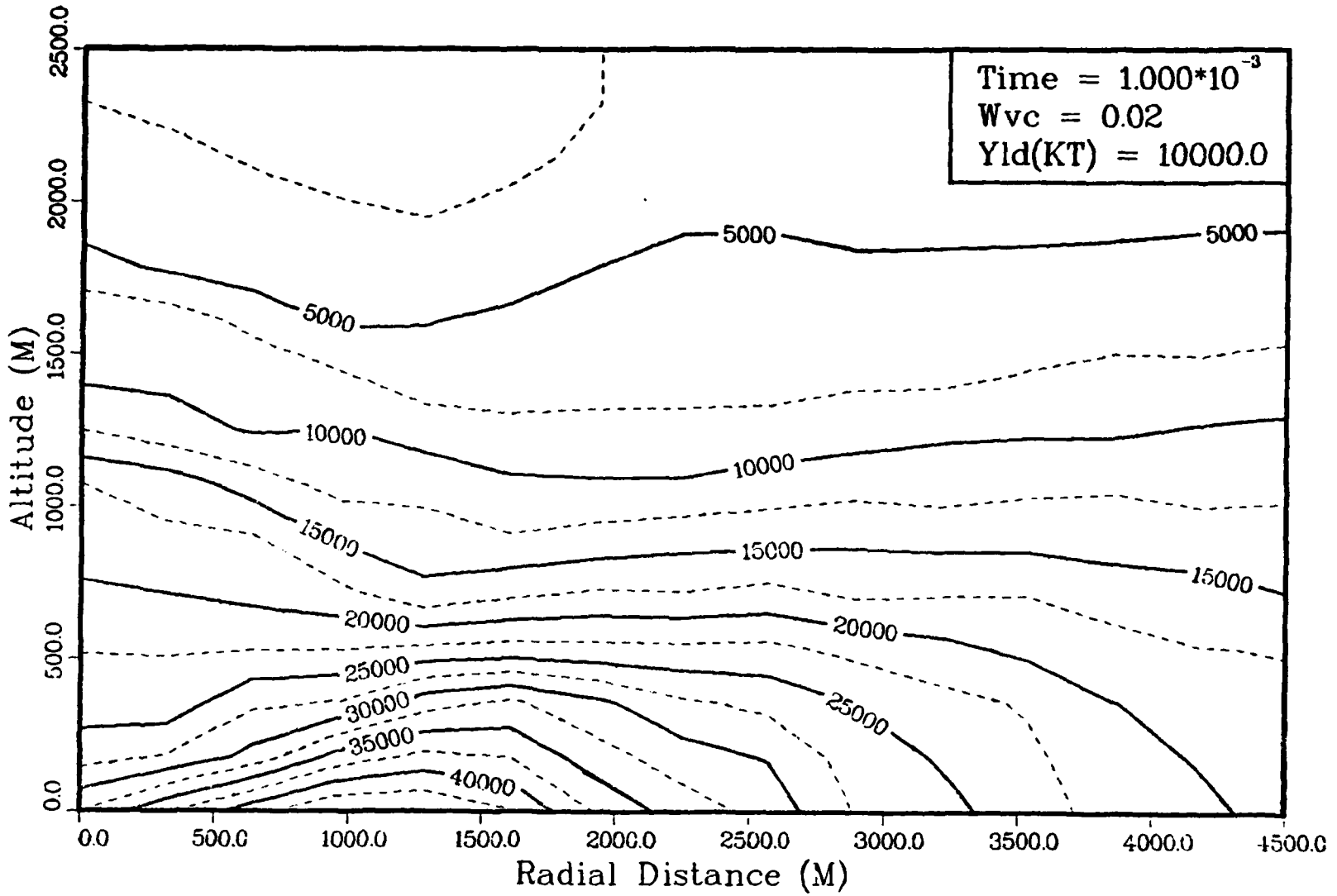


Figure 29. Total Electric Field, Y = 10 Mt

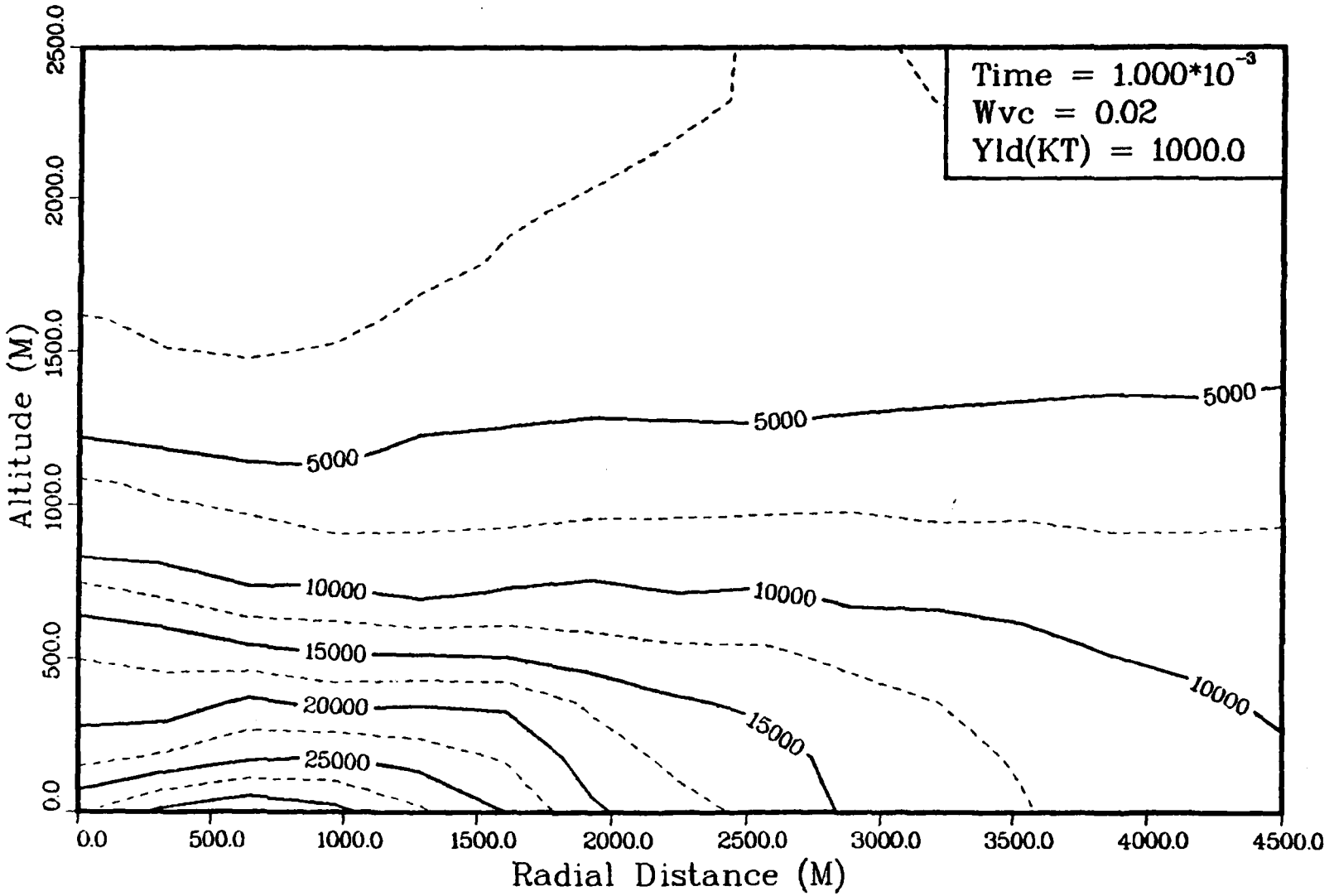


Figure 30. Total Electric Field, Y = 1 Mt

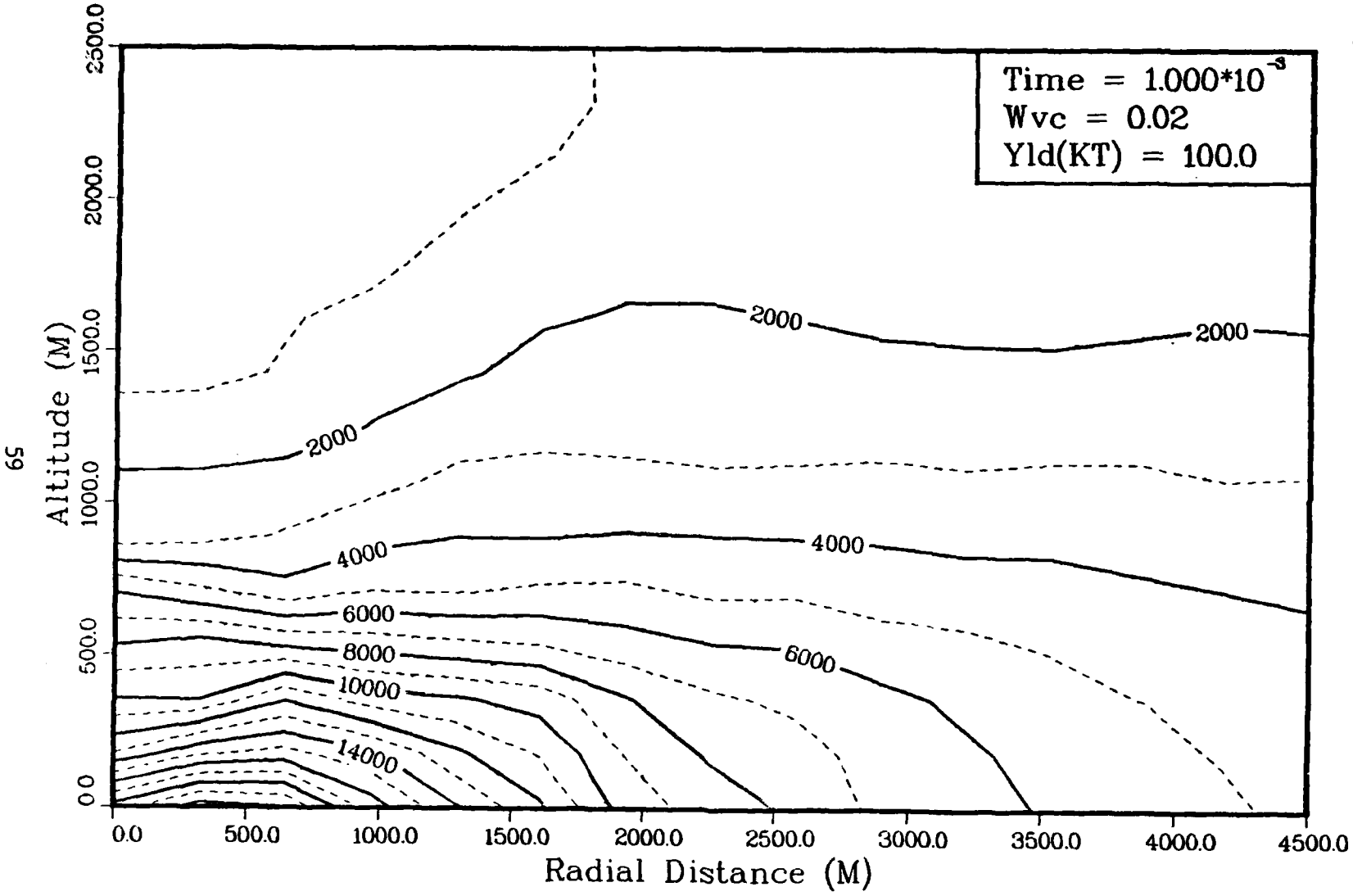


Figure 31. Total Electric Field, Y = 100 Kt

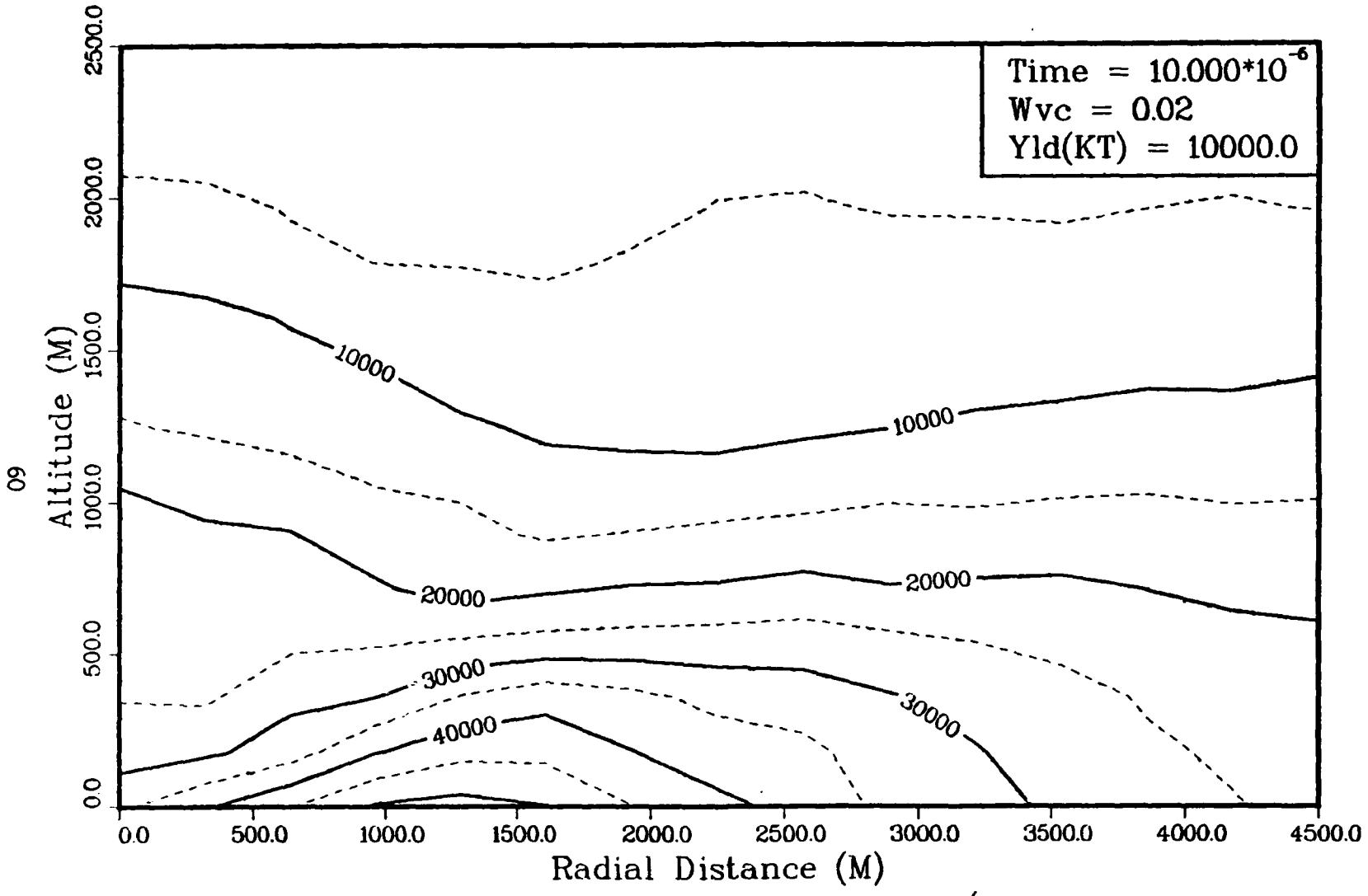


Figure 32. Total Electric Field, T = $10^{-4}$ Sec

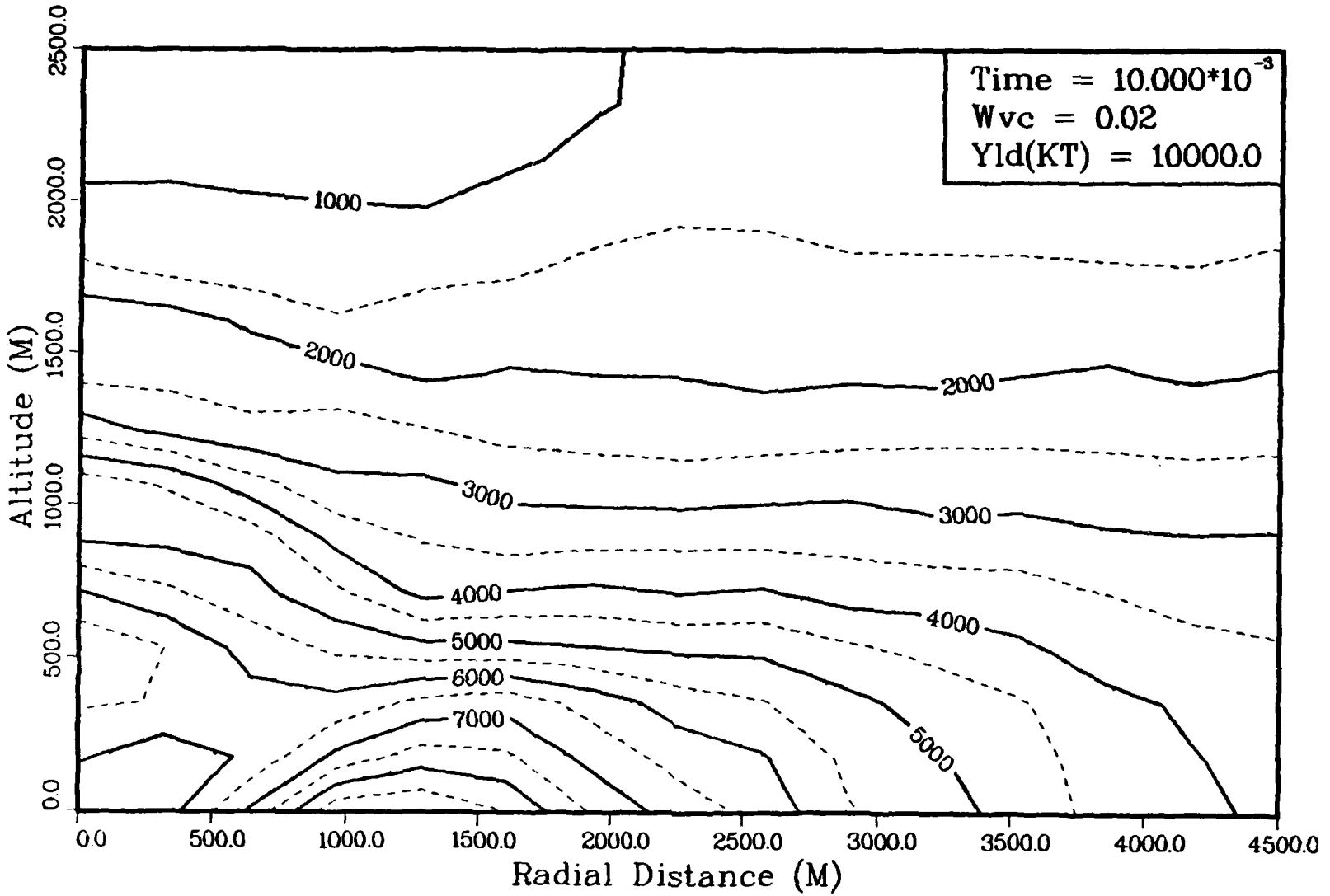


Figure 33. Total Electric Field, T = $10^{-2}$ Sec

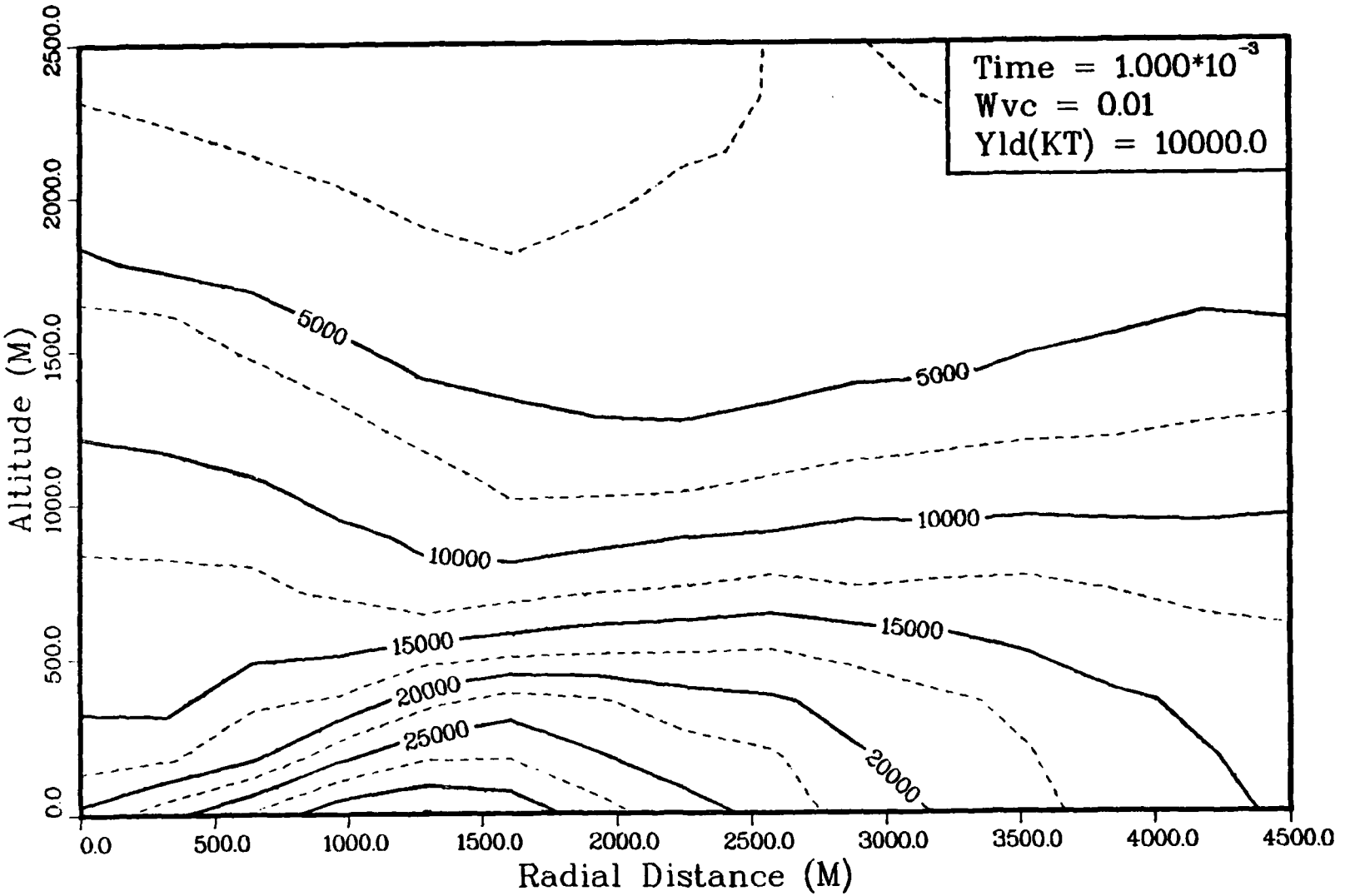


Figure 34. Total Electric Field, WVC = 0.01

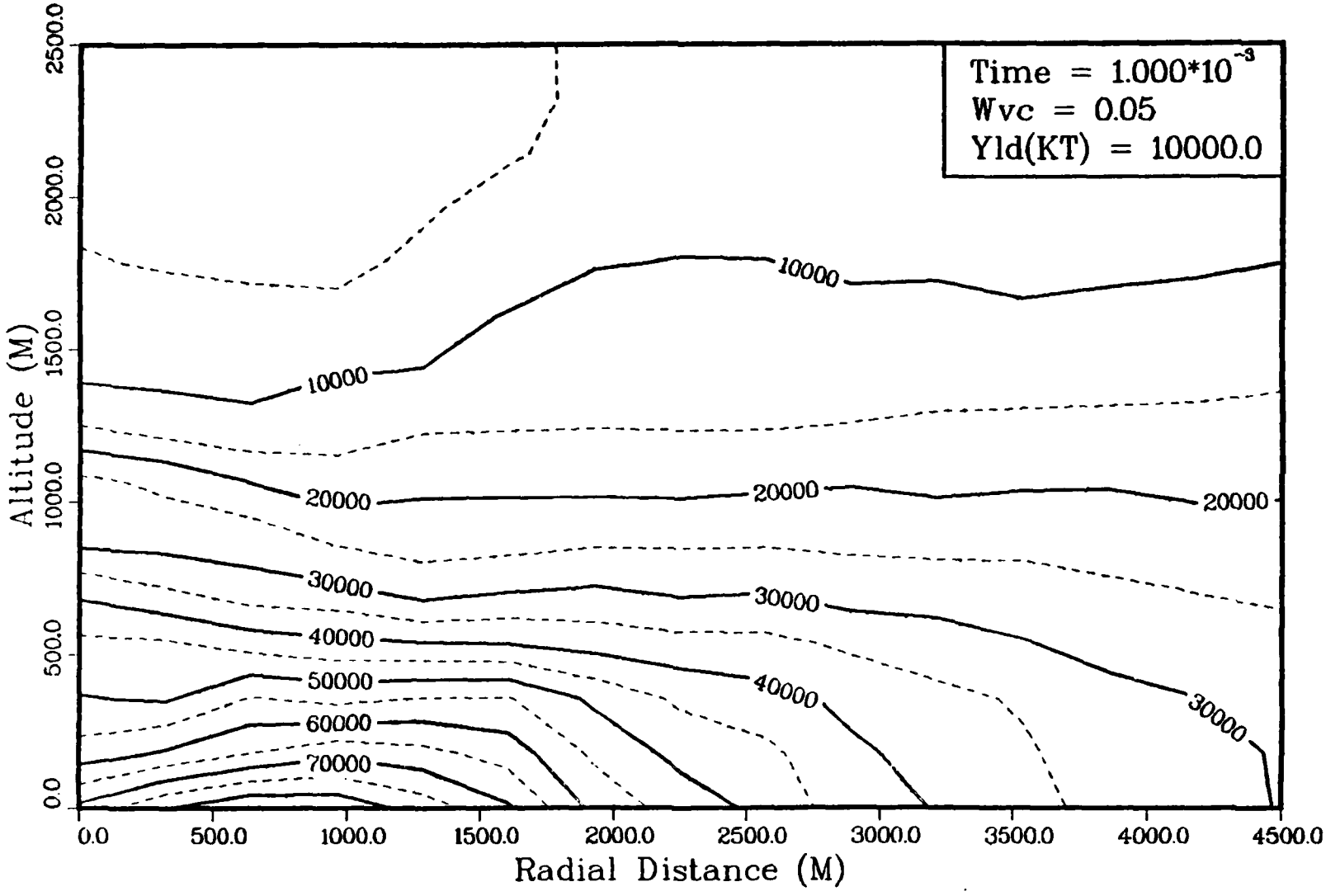


Figure 35. Total Electric Field, WVC = 0.05

# VII. Conclusions and Recommendations

## Conclusions

1. The magnitude of the late-time magnetic fields were calculated, using the time-independent numerical code and were found to agree to within 2 percent of the analytic calculations for ranges less than 2 kilometers. However, using more realistic source terms, peak field values as much as an order of magnitude larger were calculated for ranges greater than 2 kilometers.

2. The quasi-static phase was found to be valid for times greater than 60 microseconds and for ranges between one and three kilometers. The spatial region of validity is a strong function of yield and time and the temporal region of validity is a function of the ground conductivity.

## Recommendations

The following recommendations are suggested:

1. The results from the time-independent calculations should be compared to the results obtained with time-dependent codes (such as LEMP) to determine how well the fields are being predicted (Ref 4:79).

2. The code should be modified to include the new fits (Ref 26) for the electron mobility and attachment rate. A comparison should then be made with the results from the existing code (Ref 4:79).

3. The code should be modified to include the effects of the expanding thermal fireball on the EMP field predictions (Ref 19; 21). These effects become important for large yields and small ranges at later times.

4. The code should be modified to determine the late-time electric and magnetic fields in the ground (Ref 6; 20). Once the below ground fields are calculated, their coupling to and interaction with underground structures can be investigated (Ref 3; 11; 12; 16; 28; and 30).

## Bibliography


1. Burden, Richard L., et al. Numerical Analysis. Boston: Prindle, Weber and Schmidt, 1978.

2. Chervenak, J. G. and V. A. J. van Lint. "Experiments on Air Conductivity Relevant to Source Region EMP," IEEE Transactions on Nuclear Science, NS-29:1880-1886 (December 1982).

3. Curry, J. Regnald, et al. "SREMP Uncertainties with Resistive Power Lines," IEEE Transactions on Nuclear Science, NS-28:4446-44450 (December 1981).

4. Downey, Lt. James R. The Calculation of Late-Time Surface Burst EMP Fields Using a Time-Dependent Numerical Method. MS Thesis GNE/PH/83M-5. School of Engineering, Air Force Institute of Technology (AU), Wright-Patterson AFB OH, March 1983 (AD-A127303).

5. Gilbert, James and M. Arman. Fits to Surface Bursts Environments (U). AFWL-TR-81-174, MRC-R-305, Mission Research Corporation, Santa Barbara, California, April 1982. (AD-C028726L). Classified: Restricted Data, CNWDI.

6. Gilbert, James and Morgan K. Grover. "Analytic Calculation of Late-Time Source-Region EMP Fields Below the Earth's Surface," IEEE Transactions on Nuclear Science, NS-28:4479-4483 (December 1981).

7. Glasstone, Samuel and P. J. Dolan. The Effects of Nuclear Weapons (Third Edition). Washington, D. C.: United States Department of Defense and the Energy Research and Development Administration, 1977.

8. Grover, Morgan K. Some Analytic Models for Quasi-Static Source Region EMP: Application to Nuclear Lightning. RDA-TR-113202-002, (AD-A109 644).

9. Grover, Morgan K. and F. R. Gilmore. A Review of Data for Electron Mobility, Energy, and Attachment Relevant to EMP Air Chemistry. RDA-TR-110002-001, R & D Associates, Marina del Rey, California, March 1980. (AD-A098 874).

10. Hayt, William H. Jr. Engineering Electromagnetics. New York: McGraw-Hill Book Company, 1981.

11. Higgins, D. F. et al. "Source Region EMP Coupling to Long Lines," IEEE Transactions on Nuclear Science, NS-28:4440-4445 (December 1981).

12. Higgins, D. F., D. E. M. O'Dean and K. S. Smith. "SREMP Coupling to Long Buried Lines - A Comparison of Transmission Line and Finite Difference Solutions," IEEE Transactions on Nuclear Science, NS-29:1874-1879 (December 1982).

13. Hill, R. D. "Lightning Induced by Nuclear Burst," Journal of Geophysical Research, 78:6355-6358 (September 1973).

14. Jones, C. W. and W. M. Folkner. Gamma-Ray and Neutron EMP Source Comparisons and Uncertainties for Surface Burst EMP Codes. DC-TN-1298-1, Dikewood Industries, Inc., Albuquerque, New Mexico, June 1980. (AD-B051 0741). Unclassified, Limited.

15. Lam, John. Study of a Source-Region EMP Simulator Concept for MX Missile Basing Components. AFWL-TR-81-119, Dikewood Corporation, Albuquerque, New Mexico, November 1981. (AD B064214). Unclassified, Limited.

16. Lee, K. S. H. (Editor). EMP Interaction Principles, Techniques and Reference Data, EMP Interaction 2-1. DC-EH1289, Dikewood Industries, Inc., Albuquerque, New Mexico, December 1980. (AD-A100 508).

17. Lewis, Kevin N. "The Prompt and Delayed Effects of Nuclear War," Scientific American, 241:35-47 (July 1979).

18. Longley, H. J. and Conrad L. Longmire. Electron Mobility and Attachment Rate in Moist Air. MRC-N-222, Mission Research Corporation, Santa Barbara, California, December 1975.

19. Longmire, Conrad L. and G. D. McCartor. Enhancement of Late-Time EMP Fields by Fireballs from Previous Bursts. MRC-R-556, Mission Research Corporation, Albuquerque, New Mexico, January 1982. (AD-B063546). Unclassified, Limited.

20. Longmire, Conrad L. and James L. Gilbert. The Theory of EMP Coupling in the Source Region. MRC-R-546, Mission Research Corporation, Santa Barbara, California, February 1980. (AD-A108751).

21. Longmire, C. L. and W. E. Hobbs. Fireball Effects in Late-Time EMP from Surface Bursts. MCR-R-249, Mission Research Corporation, Santa Barbara, California, February 1978.

22. Longmire, Conrad L. "On the Electromagnetic Pulse Produced by Nuclear Explosions," IEEE Transactions on Antennas and Propagation, AP-26: 3-13 (January 1978).

23. Merewether, David E. and Robert Fisher. Finite Difference Solutions of Maxwell's Equations for EMP Applications. EMA-79-R4, Electo Magnectic Applications, Inc., Albuquerque, New Mexico, April 1980. (AD B072956). Unclassified, Limited.

24. Messier, Michael A. The Propagation of an Electromagnetic Impulse Through Soil: Influence of Frequency Dependent Parameters. MRC-N-415, Mission Research Corporation, Santa Barbara, California, January 1982. (AD-B064 242). Unclassified, Limited.

25. O'Dell, A. A., C. L. Longmire, and H. J. Longley. The Development of Improved Late-Time Sources for the LEMP Computer Code. MRC-R-104, Mission Research Corporation, Santa Barbara, California, November 1974. (AD-C001 246). Unclassified.

26. Pettus, E. and W. Crevier. Analytic Representation of Electron Mobility and Attachment Data in Dry and Moist Air from Van Lint's HIFX Experiments. MRC-R-576, Mission Research Corporation, Santa Barbara, California, July 1980.

27. Radasky, William A. An Examination of the Adequacy of the Three-Species Air Chemistry Treatment for the Prediction of Surface Burst EMP. MRC-R-244, Mission Research Corporation, Santa Barbara, California, December 1975. (AD-A025 280).

28. Rogers, S. R. and R. A. Perala. "HEMP Field Penetration into an Ideal Shelter Without a Floor Through a Lossy Earth," IEEE Transactions on Nuclear Science, NS-28:4462-4466 (December 1981).

29. Smith, K. S. and W. A. Radasky. An Examination of the Behavior of the Late-Time Electronic and Ionic Conductivities Appropriate for Surface Burst EMP Calculations. DC-TN-1505-2, Dikewood Corporation, Albuquerque, New Mexico, March 1982. (AD-B064 200). Unclassified, Limited.

30. Stettner, R. et al. "Comparison of a One-Dimensional and a Three-Dimensional SREMP Model for an Overhead Line," IEEE Transactions on Nuclear Science, NS-29:1868-1873 (December 1982).

31. Uman, M. A., et al. "Lightning Induced by Thermonuclear Detonations," Journal of Geophysical Research, 77:1591-1596 (March 1972).

32. Wyatt, William T. An Improved Model for EMP-Induced Lightning. HDL-TR-1919, Harry Diamond Laboratories, Adelphi, Maryland, April 1980. (AD-A096 811).

## Appendix A

## Simpson's Composite Rule

In Chapter 3, the numerical solution (Eq 3-17) for the late-time azimuthal magnetic field involved integrals over the polar angle. These integrals were computed, using Simpson's Composite Rule. This method is briefly outlined below.

The general formula for Simpson's Composite Rule over 2m subintervals of [a,b] is

$$\int_a^b F(x)\,dx = \frac{h}{3}\left[F(a) + 2\sum_{j=1}^{m-1} F(x_{2j}) + 4\sum_{j=1}^{m} F(x_{2j-1}) + F(b)\right] + O(h^4)$$

where $a = x_0 < x_1 < \ldots < x_{2m} = b$, $h = (b-a)/2m$, and $x_j = x_0 + jh$ for each $j = 0,1,\ldots,2m$.

The algorithm which was incorporated into the computer code is provided in Figure 36.

To approximate $I = \int_a^b F(x)\,dx$, select an integer $m > 0$.

Step 1 Set $h = (b - a)/2m$.

Step 2 Set $x_i = a + ih$, for each $i = 0,1,\ldots,2m$.

Step 3 Set $i = 0$, and $I_2 = 0$.

Step 4 If $i = 0$, add $F(x_i)$ to $I_2$ and go to Step 5.
If $i = 2m$, add $F(x_i)$ to $I_2$ and go to Step 5.
If $i$ is odd, add $4F(x_i)$ to $I_2$ and go to Step 5.
Add $2F(_i)$ to $I_2$.

Step 5 Add 1 to i.

Step 6 If $i \leq 2m$, go to Step 4.

Step 7 Multiply $I_2$ by 1/3h.

Step 8 The procedure is complete. $I_2$ approximates I with error $O(h^4)$.

Figure 36. Simpson's Composite Algorithm

## Appendix B

## Time-Independent EMP Source Code

The program used to find the late-time EMP was written in Fortran V (Ref 4:114). Every effort was made to include descriptive comments and documentation. Structured programming techniques were applied and many of the calculations are made in various subroutines. The program complies with the 1977 ANSI standard and should, therefore, be transportable.

Other than possible changes in the numerical accuracy of the calculations, the only input to the program is the time, the yield, the water vapor content, and the relative air density. The atmospheric pressure was taken to be one atmosphere (sea level).

```
      PROGRAM SREMP
C
C
C           THIS PROGRAM IS DESIGNED TO FIND THE LATE TIME
C     ELECTRIC AND MAGNETIC FIELDS THAT WOULD RESULT FROM A
C     SURFACE NUCLEAR BURST.  THE PROGRAM USES FITS FOR THE
C     IONIZATION RATE, AND THE RADIAL AND THETA COMPTON CURRENT
C     COMPONENTS THAT WERE DEVELOPED BY O'DELL, LONGMIRE, AND
C     LONGLY FOR USE WITH LEMP-2.
C           THE ELECTRIC FIELD IS SOLVED FOR FIRST BY ASSUMING
C     FIELD INDEPENDENT CONDUCTIVITY. THE TOTAL ELECTRIC FIELD
C     FOUND IS THEN USED AS THE INPUT TO THE FIELD DEPENDENT
C     CALCULATIONS.  NEXT, THE MAGNETIC FIELD IS SOLVED FOR
      USING THE FIELD DEPENDENT SOURCE TERMS, AND FINALLY,
      THE TIME RATE OF CHANGE OF THE MAGNETIC FIELD IS
      DETERMINED FOR THE TIME STEP SPECIFIED.  NOTE ALSO THAT
      THE INITIAL ANSWER USES A SIMPLIFIED APPROXIMATION FOR
      FINDING THE LEGENDRE POLYNOMIAL COEFFICIENTS.
C
C     VARIABLES
        REAL INT1(100,7),INT2(100,7),RAD(100),SIGMAI,SIGMAC
        REAL AL(7,0:102),A,B,C,E(0:100),F(0:100),THTA,JTHTAC
        REAL DR,DIV,CSANG(5),TIME,WVC,TOL,OH,DT,VAL1,VAL2,VAL3
        REAL ETHTA(100,5),ERAD(100,5),ETOT(100,5),ROM1(5,5,7)
        REAL RHS(100,7),ROM2(5,5,7),SUM2(7),LGDRPL,ALGDRP
        REAL YLD,NPKT,RDEN,PRES,LL,UL,H,ANG1,ANG2,ROM3(5,5,7)
        REAL DETOT(100),NETOT(100),CTANG,SUM3(7),LVAL1,LVAL2,LVAL3
        REAL JRADC,HVAL1,HVAL2,HVAL3,ANG,SUM1(7),CANG(90)
        REAL ROM4(5,5,7,7),ROM5(5,5,7,7),SUM4(7,7),SUM5(7,7)
        REAL LGPL(5,8,7),LGPL1(7),LGPL0(7),ALPL0(7),ALPL1(7)
        REAL ALPL(5,8,7),LGPLS0(7),LGPLS1(7),ALPLS0(7)
        REAL ALPLS1(7),ALPLS(5,8,7),LGPLS(5,8,7),U,THETAM
        REAL HFLD(100,20),FA,FB,ODD,EVEN,JCR(100,12),SIGMA(100,12)
```

```
      REAL BDOT(100,20),TIMED,HFLDO(100,20),MHUAIR,COSTHM,SINTHM
      INTEGER I,J,K,NL,M,N,OL,L,COUNT,NR,MAXI,CODE
      INTEGER SL,OSL,T
C
C
C     BEGIN SREMP
C
C
C     SPECIFY THE TIME STEP
C
      DO 650 T=1,2
C
C       INITIALIZE THE NUMBER OF RANGE POINTS, LEGENDRE
C        POLYNOMIALS, TIME, YIELD, AND NEUTRONS/KT.
        N=100
        NL=5
        TIME=1.0E-3*T
        YLD=10000.0
        NPKT=2.0E+23
C
C       ATMOSPHERIC CONDITIONS.
        PRES=1.0
        RDEN=1.0
        WVC=0.02
        MHUAIR=(3.1415926)*4E-7
C
C       INITIALIZE 5 ANGLE VALUES (COSINE OF ANGLE)
        DATA(CSANG(I),I=1,5)/1.0,0.8660254,0.70712,0.5,0.0/
C
C       SOLVE FOR THE ELECTRIC FIELD BY ASSUMING NO FIELD
C        DEPENDENCE AND BY APPROXIMATING THE LEGENDRE
C        COEFFICIENTS.
C
C       FIND THE THETA DEPENDENT INTEGRAL TERMS IN THE
```

```
C         DIFFERENTIAL EQUATION USING ROMBERG INTEGRATION.
          DR=5000.0/N
          DIV=1/DR**2
          NR=5
          LL=0.0
          UL=1.0
          DT=1.0*3.1415926/180.0
          CODE=1
          RAD(1)=DR
          DO 5 M=1,N
            RAD(M)=DR*M
            I=1
            J=1
            H=UL-LL
            THTA=ACOS(0.0)
            ANG1=ABS(COS(THTA+DT))
            ANG2=ABS(COS(THTA-DT))
            SIGMAI=SIGMAC(AL,0.0,DR,NL,M,WVC,TIME,YLD,NPKT,RDEN,CODE)
            LVAL1=1/(SIGMAI*DR*2)*(SIGMAC(AL,0.0,DR,NL,M+1,WVC,TIME,
     +        YLD,NPKT,RDEN,CODE)-SIGMAC(AL,0.0,DR,NL,M-1,WVC,TIME,YLD,
     +        NPKT,RDEN,CODE))
            LVAL2=1/(2*DT*SIGMAI)*(SIGMAC(AL,ANG1,DR,NL,M,WVC,TIME,
     +        YLD,NPKT,RDEN,CODE)-SIGMAC(AL,ANG2,DR,NL,M,WVC,TIME,YLD,
     +        NPKT,RDEN,CODE))
            LVAL3=1/SIGMAI*(2/(DR*M)*JRADC(DR*M,0.0,TIME,YLD,NPKT,RDEN)+
     +        1/(2*DR)*(JRADC(DR*(M+1),0.0,TIME,YLD,NPKT,RDEN)-
     +        JRADC(DR*(M-1),0.0,TIME,YLD,NPKT,RDEN))+
     +        JTHTAC(DR*M,TIME,YLD,NPKT,RDEN)/RAD(M)*((1-COS(THTA))/
     +        TAN(THTA)+SIN(THTA)))
            THTA=ACOS(1.0)
            ANG1=ABS(COS(THTA+DT))
            ANG2=ABS(COS(THTA-DT))
            SIGMAI=SIGMAC(AL,1.0,DR,NL,M,WVC,TIME,YLD,NPKT,RDEN,CODE)
            HVAL1=1/(SIGMAI*DR*2)*(SIGMAC(AL,1.0,DR,NL,M+1,WVC,TIME,
```

```
     +       YLD,NPKT,RDEN,CODE)-SIGMAC(AL,1.0,DR,NL,M-1,WVC,TIME,YLD,
     +       NPKT,RDEN,CODE))
             HVAL2=1/(2*DT*SIGMAI)*(SIGMAC(AL,ANG1,DR,NL,M,WVC,TIME,
     +       YLD,NPKT,RDEN,CODE)-SIGMAC(AL,ANG2,DR,NL,M,WVC,TIME,YLD,
     +       NPKT,RDEN,CODE))
             HVAL3=1/SIGMAI*(2/(DR*M)*JRADC(DR*M,1.0,TIME,YLD,NPKT,RDEN)+
     +       1/(2*DR)*(JRADC(DR*(M+1),1.0,TIME,YLD,NPKT,RDEN)-
     +       JRADC(DR*(M-1),1.0,TIME,YLD,NPKT,RDEN)))
             DO 10 L=1,NL
               IF(M.EQ.1)THEN
                 OL=2*L-1
                 LGPL0(L)=LGDRPL(LL,OL)
                 LGPL1(L)=LGDRPL(UL,OL)
                 ALPL0(L)=ALGDRP(LL,OL)
                 ALPL1(L)=ALGDRP(UL,OL)
               END IF
               ROM1(1,1,L)=H/2*(LVAL1*(LGPL0(L))**2+
     +         HVAL1*(LGPL1(L))**2)
               ROM2(1,1,L)=H/2*(LVAL2*LGPL0(L)*ALPL0(L)+
     +         HVAL2*LGPL1(L)*ALPL1(L))
               ROM3(1,1,L)=H/2*(LVAL3*LGPL0(L)+HVAL3*LGPL1(L))
  10         CONTINUE
C
C            ITERATIVE LOOP FOR INTEGRATION.
  20         CONTINUE
             I=I+1
             IF(I.GT.NR)THEN
               DO 21 L=1,NL
                 INT1(M,L)=ROM1(NR,NR,L)
                 INT2(M,L)=ROM2(NR,NR,L)
                 RHS(M,L)=ROM3(NR,NR,L)*(2*(2*L-1)+1)
  21           CONTINUE
             ELSE
               OH=H
```

```
      H=OH*0.5
      DO 22 L=1,NL
        SUM1(L)=0.0
        SUM2(L)=0.0
        SUM3(L)=0.0
22    CONTINUE
      DO 23 K=1,2**(I-2)
        ANG=LL+(K-0.5)*OH
        THTA=ACOS(ANG)
        ANG1=ABS(COS(THTA+DT))
        ANG2=ABS(COS(THTA-DT))
        SIGMAI=SIGMAC(AL,ANG,DR,NL,M,WVC,TIME,YLD,NPKT,RDEN,CODE)
        VAL1=1/(SIGMAI*DR*2)*(SIGMAC(AL,ANG,DR,NL,M+1,WVC,TIME,
     +    YLD,NPKT,RDEN,CODE)-SIGMAC(AL,ANG,DR,NL,M-1,WVC,TIME,YLD
     +    ,NPKT,RDEN,CODE))*OH
        VAL2=1/(2*DT*SIGMAI)*(SIGMAC(AL,ANG1,DR,NL,M,WVC,TIME,
     +    YLD,NPKT,RDEN,CODE)-SIGMAC(AL,ANG2,DR,NL,M,WVC,TIME,YLD,
     +    NPKT,RDEN,CODE))*OH
        VAL3=1/SIGMAI*(2/(DR*M)*JRADC(DR*M,ANG,TIME,YLD,NPKT,RDEN)
     +    +1/(2*DR)*(JRADC(DR*(M+1),ANG,TIME,YLD,NPKT,RDEN)-
     +    JRADC(DR*(M-1),ANG,TIME,YLD,NPKT,RDEN))+
     +    JTHTAC(DR*M,TIME,YLD,NPKT,RDEN)/RAD(M)*((1-COS(THTA))/
     +    TAN(THTA)+SIN(THTA)))*OH
        DO 24 L=1,NL
          IF(M.EQ.1)THEN
            LGPL(I,K,L)=LGDRPL(ANG,2*L-1)
            ALPL(I,K,L)=ALGDRP(ANG,2*L-1)
          END IF
          SUM1(L)=SUM1(L)+VAL1*(LGPL(I,K,L))**2
          SUM2(L)=SUM2(L)+VAL2*LGPL(I,K,L)*ALPL(I,K,L)
          SUM3(L)=SUM3(L)+VAL3*LGPL(I,K,L)
24      CONTINUE
23    CONTINUE
      DO 25 L=1,NL
```

```
                ROM1(I,1,L)=0.5*(ROM1(I-1,1,L)+SUM1(L))
                ROM2(I,1,L)=0.5*(ROM2(I-1,1,L)+SUM2(L))
                ROM3(I,1,L)=0.5*(ROM3(I-1,1,L)+SUM3(L))
   25         CONTINUE
              DO 26 J=2,I
                DO 27 L=1,NL
                  ROM1(I,J,L)=((2)**(2*(J-1))*ROM1(I,J-1,L)-
     +              ROM1(I-1,J-1,L))/((2)**(2*(J-1))-1)
                  ROM2(I,J,L)=((2)**(2*(J-1))*ROM2(I,J-1,L)-
     +              ROM2(I-1,J-1,L))/((2)**(2*(J-1))-1)
                  ROM3(I,J,L)=((2)**(2*(J-1))*ROM3(I,J-1,L)-
     +              ROM3(I-1,J-1,L))/((2)**(2*(J-1))-1)
   27             CONTINUE
   26           CONTINUE
                GO TO 20
              END IF
    5       CONTINUE
C
C           FIND COEFFICIENTS FOR A GIVEN L
            DO 30 L=1,NL
              OL=2*L-1
              F(N)=0.0
              E(N)=1.0
              DO 40 M=N,1,-1
                A=DIV+1/(DR*RAD(M))+(2*OL+1)/(2*DR)*INT1(M,L)
                B=-(2*DIV+OL*(OL+1)/RAD(M)**2+(2*OL+1)/RAD(M)**2*INT2(M,L))
                C=2*DIV-A
                E(M-1)=-C/(A*E(M)+B)
                F(M-1)=(RHS(M,L)-A*F(M))/(A*E(M)+B)
   40         CONTINUE
              AL(L,0)=0.0
              AL(L,1)=F(0)
              DO 50 I=2,N
                AL(L,I)=AL(L,I-1)*E(I-1)+F(I-1)
```

```
   50       CONTINUE
            AL(L,N+1)=AL(L,N)
            AL(L,N+2)=AL(L,N)
   30     CONTINUE
C
          CODE=0
C
C         NOW SOLVE THE PROBLEM BY INCLUDING THE ELECTRIC FIELD
C           DEPENDENCE OF THE CONDUCTIVITY.  THE LEGENDRE
C           COEFFICIENTS ABOVE SERVE AS THE FIRST GUESS (INPUT)
C           FOR THIS PART OF THE PROBLEM.
C
C         CHOOSE CONVERGENCE TEST ANGLE, MAXIMUM NUMBER OF ITERATIONS,
C          TOLERANCE, AND ROW LIMIT FOR ROMBERG INTEGRATION.
          CTANG=CSANG(5)
          MAXI=15
          TOL=100.0
          NR=4
C
C         FIND THE TOTAL FIELD AT ALL RANGE POINTS AND THE TEST
C          ANGLE USING THE COEFFICIENTS FROM THE THETA INDEPENDENT
C          CALCULATION.
          DO 90 I=1,N
            OETOT(I)=ETOTC(AL,CTANG,DR,NL,I)
   90     CONTINUE
C
C         ITERATIVE LOOP FOR FIELD DEPENDENT CALCULATION.
C
          COUNT=0
  100     CONTINUE
          COUNT=COUNT+1
          PRINT *,'COUNT = ',COUNT
C
C         FIND THE THETA DEPENDENT INTEGRAL TERMS IN THE
```

```
C         DIFFERENTIAL EQUATION USING ROMBERG INTEGRATION.
          DO 110 M=1,N
            I=1
            J=1
            H=UL-LL
            THTA=ACOS(0.0)
            ANG1=ABS(COS(THTA+DT))
            ANG2=ABS(COS(THTA-DT))
            SIGMAI=SIGMAC(AL,0.0,DR,NL,M,WVC,TIME,YLD,NPKT,RDEN,CODE)
            LVAL1=1/(SIGMAI*DR*2)*(SIGMAC(AL,0.0,DR,NL,M+1,WVC,TIME,
     +        YLD,NPKT,RDEN,CODE)-SIGMAC(AL,0.0,DR,NL,M-1,WVC,TIME,YLD,
     +        NPKT,RDEN,CODE))
            LVAL2=1/(2*DT*SIGMAI)*(SIGMAC(AL,ANG1,DR,NL,M,WVC,TIME,
     +        YLD,NPKT,RDEN,CODE)-SIGMAC(AL,ANG2,DR,NL,M,WVC,TIME,YLD,
     +        NPKT,RDEN,CODE))
            LVAL3=1/SIGMAI*(2/(DR*M)*JRADC(DR*M,0.0,TIME,YLD,NPKT,RDEN)+
     +        1/(2*DR)*(JRADC(DR*(M+1),0.0,TIME,YLD,NPKT,RDEN)-
     +        JRADC(DR*(M-1),0.0,TIME,YLD,NPKT,RDEN))+
     +        JTHTAC(DR*M,TIME,YLD,NPKT,RDEN)/RAD(M)*((1-COS(THTA))/
     +        TAN(THTA)+SIN(THTA)))
            THTA=ACOS(1.0)
            ANG1=ABS(COS(THTA+DT))
            ANG2=ABS(COS(THTA-DT))
            SIGMAI=SIGMAC(AL,1.0,DR,NL,M,WVC,TIME,YLD,NPKT,RDEN,CODE)
            HVAL1=1/(SIGMAI*DR*2)*(SIGMAC(AL,1.0,DR,NL,M+1,WVC,TIME,
     +        YLD,NPKT,RDEN,CODE)-SIGMAC(AL,1.0,DR,NL,M-1,WVC,TIME,YLD,
     +        NPKT,RDEN,CODE))
            HVAL2=1/(2*DT*SIGMAI)*(SIGMAC(AL,ANG1,DR,NL,M,WVC,TIME,
     +        YLD,NPKT,RDEN,CODE)-SIGMAC(AL,ANG2,DR,NL,M,WVC,TIME,YLD,
     +        NPKT,RDEN,CODE))
            HVAL3=1/SIGMAI*(2/(DR*M)*JRADC(DR*M,1.0,TIME,YLD,NPKT,RDEN)+
     +        1/(2*DR)*(JRADC(DR*(M+1),1.0,TIME,YLD,NPKT,RDEN)-
     +        JRADC(DR*(M-1),1.0,TIME,YLD,NPKT,RDEN)))
            DO 120 L=1,NL
```

```
                ROM1(1,1,L)=H/2*(LVAL1*(LGPL0(L))**2+
     +            HVAL1*(LGPL1(L))**2)
                ROM1(1,1,L)=H/2*(LVAL1*(LGPL0(L))**2+
     +            HVAL1*(LGPL1(L))**2)
                ROM2(1,1,L)=H/2*(LVAL2*LGPL0(L)*ALPL0(L)+
     +            HVAL2*LGPL1(L)*ALPL1(L))
                ROM3(1,1,L)=H/2*(LVAL3*LGPL0(L)+HVAL3*LGPL1(L))
                DO 121 SL=1,NL
                  IF(M.EQ.1.AND.COUNT.EQ.1)THEN
                    OSL=2*SL-1
                    LGPLS0(SL)=LGDRPL(LL,OSL)
                    LGPLS1(SL)=LGDRPL(UL,OSL)
                    ALPLS0(SL)=ALGDRP(LL,OSL)
                    ALPLS1(SL)=ALGDRP(UL,OSL)
                  END IF
                  IF(SL.EQ.L)THEN
                    ROM4(1,1,L,SL)=0.0
                    ROM5(1,1,L,SL)=0.0
                  ELSE
                    ROM4(1,1,L,SL)=H/2*(LVAL1*LGPL0(L)*LGPLS0(SL)+
     +                HVAL1*LGPL1(L)*LGPLS1(SL))
                    ROM5(1,1,L,SL)=H/2*(LVAL2*ALPLS0(SL)*LGPL0(L)+
     +                HVAL2*ALPLS1(SL)*LGPL1(L))
                  END IF
  121           CONTINUE
  120         CONTINUE
C
C             ITERATIVE LOOP FOR INTEGRATION.
  130         CONTINUE
              I=I+1
              IF(I.GT.NR)THEN
                DO 140 L=1,NL
                  INT1(M,L)=ROM1(NR,NR,L)
                  INT2(M,L)=ROM2(NR,NR,L)
```

```
                RHS(M,L)=ROM3(NR,NR,L)
                DO 141 SL=1,NL
                  RHS(M,L)=RHS(M,L)-1/(2*DR)*(AL(SL,M+1)-AL(SL,M-1))*
     +              ROM4(NR,NR,L,SL)+1/RAD(M)**2*AL(SL,M)*ROM5(NR,NR,L,SL)
  141           CONTINUE
  140         CONTINUE
            ELSE
              OH=H
              H=OH*0.5
              DO 150 L=1,NL
                SUM1(L)=0.0
                SUM2(L)=0.0
                SUM3(L)=0.0
                DO 151 SL=1,NL
                  SUM4(L,SL)=0.0
                  SUM5(L,SL)=0.0
  151           CONTINUE
  150         CONTINUE
              DO 160 K=1,2**(I-2)
                ANG=LL+(K-0.5)*OH
                THTA=ACOS(ANG)
                ANG1=ABS(COS(THTA+DT))
                ANG2=ABS(COS(THTA-DT))
                SIGMAI=SIGMAC(AL,ANG,DR,NL,M,WVC,TIME,YLD,NPKT,RDEN,CODE)
                VAL1=1/(SIGMAI*DR*2)*(SIGMAC(AL,ANG,DR,NL,M+1,WVC,TIME,
     +            YLD,NPKT,RDEN,CODE)-SIGMAC(AL,ANG,DR,NL,M-1,WVC,TIME,YLD
     +            ,NPKT,RDEN,CODE))*OH
                VAL2=1/(2*DT*SIGMAI)*(SIGMAC(AL,ANG1,DR,NL,M,WVC,TIME,
     +            YLD,NPKT,RDEN,CODE)-SIGMAC(AL,ANG2,DR,NL,M,WVC,TIME,YLD,
     +            NPKT,RDEN,CODE))*OH
                VAL3=1/SIGMAI*(2/(DR*M)*JRADC(DR*M,ANG,TIME,YLD,NPKT,RDEN)
     +            +1/(2*DR)*(JRADC(DR*(M+1),ANG,TIME,YLD,NPKT,RDEN)-
     +            JRADC(DR*(M-1),ANG,TIME,YLD,NPKT,RDEN))+
     +            JTHTAC(DR*M,TIME,YLD,NPKT,RDEN)/RAD(M)*((1-COS(THTA))/
```

```
     +           TAN(THTA)+SIN(THTA)))*OH
                 DO 170 L=1,NL
                   SUM1(L)=SUM1(L)+VAL1*(LGPL(I,K,L))**2
                   SUM2(L)=SUM2(L)+VAL2*LGPL(I,K,L)*ALPL(I,K,L)
                   SUM3(L)=SUM3(L)+VAL3*LGPL(I,K,L)
                   DO 171 SL=1,NL
                     IF(M.EQ.1.AND.COUNT.EQ.1)THEN
                       LGPLS(I,K,SL)=LGDRPL(ANG,2*SL-1)
                       ALPLS(I,K,SL)=ALGDRP(ANG,2*SL-1)
                     END IF
                     SUM4(L,SL)=SUM4(L,SL)+VAL1*LGPL(I,K,L)*
     +                 LGPLS(I,K,SL)
                     SUM5(L,SL)=SUM5(L,SL)+VAL2*LGPL(I,K,L)*
     +                 ALPLS(I,K,SL)
   171             CONTINUE
   170           CONTINUE
   160         CONTINUE
               DO 180 L=1,NL
                 ROM1(I,1,L)=0.5*(ROM1(I-1,1,L)+SUM1(L))
                 ROM2(I,1,L)=0.5*(ROM2(I-1,1,L)+SUM2(L))
                 ROM3(I,1,L)=0.5*(ROM3(I-1,1,L)+SUM3(L))
                 DO 181 SL=1,NL
                   IF(SL.EQ.L)THEN
                     ROM4(I,1,L,SL)=0.0
                     ROM5(I,1,L,SL)=0.0
                   ELSE
                     ROM4(I,1,L,SL)=0.5*(ROM4(I-1,1,L,SL)+SUM4(L,SL))
                     ROM5(I,1,L,SL)=0.5*(ROM5(I-1,1,L,SL)+SUM5(L,SL))
                   END IF
   181             CONTINUE
   180         CONTINUE
               DO 190 J=2,I
                 DO 200 L=1,NL
                   ROM1(I,J,L)=((2)**(2*(J-1))*ROM1(I,J-1,L)-
```

```
     +            ROM1(I-1,J-1,L))/((2)**(2*(J-1))-1)
                ROM2(I,J,L)=((2)**(2*(J-1))*ROM2(I,J-1,L)-
     +            ROM2(I-1,J-1,L))/((2)**(2*(J-1))-1)
                ROM3(I,J,L)=((2)**(2*(J-1))*ROM3(I,J-1,L)-
     +            ROM3(I-1,J-1,L))/((2)**(2*(J-1))-1)
                DO 201 SL=1,NL
                  ROM4(I,J,L,SL)=((2)**(2*(J-1))*ROM4(I,J-1,L,SL)-
     +              ROM4(I-1,J-1,L,SL))/((2)**(2*(J-1))-1)
                  ROM5(I,J,L,SL)=((2)**(2*(J-1))*ROM5(I,J-1,L,SL)-
     +              ROM5(I-1,J-1,L,SL))/((2)**(2*(J-1))-1)
  201           CONTINUE
  200         CONTINUE
  190       CONTINUE
            GO TO 130
          END IF
  110   CONTINUE
C
C       FIND COEFFICIENTS FOR A GIVEN L
        DO 210 L=1,NL
          OL=2*L-1
          F(N)=0.0
          E(N)=1.0
          DO 220 M=N,1,-1
            A=DIV+1/(DR*RAD(M))+(2*OL+1)/(2*DR)*INT1(M,L)
            B=-(2*DIV+OL*(OL+1)/RAD(M)**2+(2*OL+1)/RAD(M)**2*INT2(M,L))
            C=2*DIV-A
            E(M-1)=-C/(A*E(M)+B)
            F(M-1)=((2*OL+1)*RHS(M,L)-A*F(M))/(A*E(M)+B)
  220     CONTINUE
          AL(L,0)=0.0
          AL(L,1)=F(0)
          DO 230 I=2,N
            AL(L,I)=AL(L,I-1)*E(I-1)+F(I-1)
  230     CONTINUE
```

```
            AL(L,N+1)=AL(L,N)
            AL(L,N+2)=AL(L,N)
  210     CONTINUE
C
C         FIND THE VALUE OF THE TOTAL ELECTRIC FIELD AT ALL RANGE
C          POINTS AND THE SPECIFIED ANGLE AND CHECK FOR GOODNESS OF
C          FIT.
C
          DO 240 I=1,N
            NETOT(I)=ETOTC(AL,CTANG,DR,NL,I)
  240     CONTINUE
          DO 250 I=5,N
            IF(ABS(NETOT(I)-OETOT(I)).LE.TOL)THEN
            ELSE
              DO 260 J=1,N
                OETOT(J)=NETOT(J)
  260         CONTINUE
              IF(COUNT.LT.MAXI)THEN
                GO TO 100
              END IF
            END IF
  250     CONTINUE
C
C         FIND THE ELECTRIC FIELD COMPONENTS AND THE MAGNITUDE
C          OF THE TOTAL ELECTRIC FIELD (AT 5 DIFFERENT RADII).
          DO 270 I=1,90
            CANG(I)=COS(I*3.1415926/180.0)
            DO 280 J=1,5
              IJ=J*10
              ERAD(I,J)=0.0
              ETHTA(I,J)=0.0
              SIGMA(I,J)=SIGMAC(AL,CANG(I),DR,NL,IJ,WVC,TIME,YLD,
     +         NPKT,RDEN,CODE)
              JCR(I,J)=JRADC(DR*IJ,CANG(I),TIME,YLD,NPKT,RDEN)
```

```
            DO 290 K=1,NL
              ERAD(I,J)=ERAD(I,J)-(AL(K,IJ+1)-AL(K,IJ-1))/
     +          (2*DR)*LGDRPL(CANG(I),2*K-1)
              ETHTA(I,J)=ETHTA(I,J)+1/RAD(IJ)*AL(K,IJ)*
     +          ALGDRP(CANG(I),2*K-1)
  290       CONTINUE
            ETOT(I,J)=SQRT(ETHTA(I,J)**2+ERAD(I,J)**2)
  280     CONTINUE
  270   CONTINUE
C
C
C  FIND THE AZIMUTHAL MAGNETIC FIELD AT 20 RADIALS AND AT 18 ANGLES.
C  USE SIMPSON'S COMPOSITE RULE FOR THE POLAR ANGLE INTEGRATION.
C
C
      DO 293 I=5,90,5
        THETAM = I*3.1415926/180.0
        COSTHM = COS(THETAM)
        SINTHM = SIN(THETAM)
        DT = THETAM/90.0
        DO 292 M=1,20
          IJ=M*5
          EVEN = 0.0
          ODD = 0.0
          RAD(M)=DR*IJ
          FA=U(AL,1.0,DR,NL,IJ,WVC,TIME,YLD,NPKT,RDEN,CODE,DR*IJ)
          FB=U(AL,COSTHM,DR,NL,IJ,WVC,TIME,YLD,NPKT,RDEN,CODE,DR*IJ)
          DO 291 J=1,44
            CANG(J)=COS(2*J*DT)
            EVEN=EVEN+2.0*U(AL,CANG(J),DR,NL,IJ,WVC,TIME,YLD,NPKT,
     +           RDEN,CODE,DR*IJ)
            CANG(J)=COS((2*J-1)*DT)
            ODD=ODD+4.0*U(AL,CANG(J),DR,NL,IJ,WVC,TIME,YLD,NPKT,RDEN,
     +         CODE,DR*IJ)
```

```
  291         CONTINUE
              CANG(45)=COS(89*DT)
              ODD=ODD+4.0*U(AL,CANG(45),DR,NL,IJ,WVC,TIME,YLD,NPKT,RDEN,
     +            CODE,DR*IJ)
              HFLD(I,M)=RAD(M)*(FA+EVEN+ODD+FB)*DT/(3.0*SINTHM)
  292       CONTINUE
  293     CONTINUE
C
C  FIND THE TIME RATE OF CHANGE IN THE MAGNETIC FIELD FOR THE
C  TIME STEP SPECIFIED.
C
          IF(T.GT.1)THEN
          DO 294 I=5,90,5
            DO 295 J=1,20
               BDOT(I,J)=MHUAIR*((HFLD(I,J)-HFLDO(I,J))/(TIME-TIMEO))
  295       CONTINUE
  294     CONTINUE
          WRITE(7,'(//)')
          DO 296 I=5,90,5
            WRITE(7,297) (BDOT(I,J),J=2,20,2)
  296     CONTINUE
          I=90
          WRITE(7,297) (BDOT(90,J),J=3,5,2)
          WRITE(7,'(//)')
  297     FORMAT(1P10E13.4)
          END IF
          TIMEO=TIME
          DO 298 I=5,90,5
            DO 299 J=1,20
              HFLDO(I,J)=HFLD(I,J)
  299       CONTINUE
  298     CONTINUE
C         PRINT OUT RESULTS
          PRINT 300,TIME
```

```
300   FORMAT(///,28X,'TIME =',1X,1P1E13.4,/)
      PRINT 310,WVC
310   FORMAT(28X,'WVC =',1X,F5.2,/)
      PRINT 320,YLD
320   FORMAT(28X,'YIELD(KT) =',1X,F9.2,/)
      PRINT 330,COUNT
330   FORMAT(28X,'NO. ITERATIONS =',1X,I3,//)
      IF(NL.EQ.5)THEN
        PRINT 340
340     FORMAT(26X,'POLYNOMIAL  COEFFICIENTS',/)
        PRINT 350
350     FORMAT(4X,'RP',7X,'A1',11X,'A3',11X,'A5',11X,'A7',11X,'A9',/)
        DO 360 I=0,N,5
          PRINT 370,I,(AL(J,I),J=1,NL)
370       FORMAT(3X,I3,2X,1P5E13.4)
360     CONTINUE
      END IF
      PRINT 380
380   FORMAT(/,32X,'RADIAL FIELD',/)
      PRINT 390
390   FORMAT(4X,'TH',7X,'10',11X,'20',11X,'30',11X,'40',11X,'50',/)
      DO 400 I=5,90,5
        PRINT 410,I,(ERAD(I,J),J=1,5)
410     FORMAT(3X,I3,2X,1P5E13.4)
400   CONTINUE
      PRINT 420
420   FORMAT(/,32X,'THETA  FIELD',/)
      PRINT 430
430   FORMAT(4X,'TH',7X,'10',11X,'20',11X,'30',11X,'40',11X,'50',/)
      DO 440 I=5,90,5
        PRINT 450,I,(ETHTA(I,J),J=1,5)
450     FORMAT(3X,I3,2X,1P5E13.4)
440   CONTINUE
      PRINT 460
```

AD-A144 598 AN INVESTIGATION INTO THE QUASI-SSATIC PHASE OF THE SURFACE BURST SOURCE..(U) AIR FORCE INST OF TECH WRIGHT-PATTERSON AFB OH SCHOOL OF ENGI.. K M HODGDON 2/2

UNCLASSIFIED MAR 84 AFIT/GNE/ENP/84M-7 F/G 20/14 NL

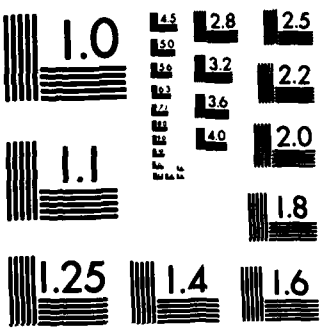

```
460   FORMAT(/,32X,'TOTAL  FIELD',/)
      PRINT 470
470   FORMAT(4X,'TH',7X,'10',11X,'20',11X,'30',11X,'40',11X,'50',/)
      DO 480 I=5,90,5
        PRINT 490,I,(ETOT(I,J),J=1,5)
490     FORMAT(3X,I3,2X,1P5E13.4)
480   CONTINUE
      PRINT 500
500   FORMAT(/,32X,'   SIGMA    ',/)
      PRINT 510
510   FORMAT(4X,'TH',7X,'10',11X,'20',11X,'30',11X,'40',11X,'50',/)
      DO 520 I=5,90,5
        PRINT 530,I,(SIGMA(I,J),J=1,5)
530     FORMAT(3X,I3,2X,1P5E13.4)
520   CONTINUE
      PRINT 540
540   FORMAT(/,32X,'JCOMPTON RAD',/)
      PRINT 550
550   FORMAT(4X,'TH',7X,'10',11X,'20',11X,'30',11X,'40',11X,'50',/)
      DO 560 I=5,90,5
        PRINT 570,I,(JCR(I,J),J=1,5)
570     FORMAT(3X,I3,2X,1P5E13.4)
560   CONTINUE
      PRINT 580
580   FORMAT(/,32X,'  H FIELD   ',/)
      PRINT 585
585   FORMAT(4X,'TH',7X,'10',11X,'20',11X,'30',11X,'40',11X,'50',/)
      DO 590 I=5,90,5
        PRINT 600,I,(HFLD(I,J),J=4,20,4)
        WRITE(7,610) (HFLD(I,J),J=2,20,2)
590   CONTINUE
      I=90
      WRITE(7,610) (HFLD(90,J),J=3,5,2)
600   FORMAT(3X,I3,2X,1P5E13.4)
```

```
  610   FORMAT(1P10E13.4)
        PRINT 620
  620   FORMAT(///)
  650 CONTINUE
      END
      REAL FUNCTION INZRTC(RAD,CSANG,TIME,YLD,NPKT,RDEN)
C
C            THIS FUNCTION GIVES THE IONIZATION RATE FOR
C       ANY RADIUS, ANGLE, TIME, YIELD, NO. OF NEUTRONS/KT,
C       AND RELATIVE AIR DENSITY.
C
C     VARIABLES
        REAL RAD,RADC,CSANG,TIME,YLD,NPKT
        REAL RDEN,RHO,GCS,ACS
C
C     BEGIN INZRTC
C
        IF(ABS(RAD-0.001).LE.0.001)THEN
          RAD=0.001
        END IF
        RHO=RDEN*1.225
        RADC=RAD*100
        GCS=35.0*RHO*YLD*NPKT/(RADC)**2*(1+1.3*CSANG)*
     +    (1-EXP(-3.88E-5*RHO*RADC))*EXP(-3.71E-5*(1-0.33*
     +    CSANG)*RHO*RADC-8.33E+2*TIME)
        ACS=2.2*RHO*YLD*NPKT/(RADC)**2*(1-0.3*CSANG)*
     +    (1-EXP(-3.88E-5*RHO*RADC))*EXP(-3.43E-5*(1-0.25*
     +    CSANG)*RHO*RADC-16.7*TIME)
        INZRTC=(GCS+ACS)*1.0E+6
      END
      REAL FUNCTION JRADC(RAD,CSANG,TIME,YLD,NPKT,RDEN)
C
C            THIS FUNCTION GIVES THE RADIAL CURRENT FOR
C       ANY RADIUS, ANGLE, TIME, YIELD, NO. OF NEUTRONS/KT,
```

```
C       AND RELATIVE AIR DENSITY.
C
C      VARIABLES
         REAL RAD,RADC,CSANG,TIME,YLD,NPKT
         REAL RDEN,RHO,GCS,ACS
C
C      BEGIN JRADC
C
           IF(ABS(RAD-0.001).LE.0.001)THEN
             RAD=0.001
           END IF
           RHO=RDEN*1.225
           RADC=RAD*100.0
           GCS=3.9E-22*YLD*NPKT/(RADC)**2*(1+16*CSANG)*
     +       (1-EXP(-7.75E-5*RHO*RADC))*EXP(-2.65E-5*RHO*RADC-
     +       8.33E+2*TIME)
           ACS=2.8E-23*YLD*NPKT/(RADC)**2*(1+1.3*CSANG)*
     +       (1-EXP(-2.58E-5*RHO*RADC))*EXP(-2.2E-5*RHO*RADC-
     +       16.7*TIME)
           JRADC=-(GCS+ACS)*1.0E+5
         END
         REAL FUNCTION JTHTAC(RAD,TIME,YLD,NPKT,RDEN)
C
C              THIS FUNCTION GIVES THE THETA COMPTON CURRENT FOR
C       ANY RADIUS, TIME, YIELD, NO. OF NEUTRONS/KT, AND RELATIVE
C       AIR DENSITY. THE ANGULAR DEPENDENCE DOES NOT APPEAR HERE
C       BECAUSE IT IS INCLUDED IN THE CALCULATION IN THE MAIN PROGRAM.
C
C      VARIABLES
         REAL RAD,RADC,TIME,YLD,NPKT,RDEN,RHO,GCS
C
C      BEGIN JTHTAC
C
           RHO=RDEN*1.225
```

```
      RADC=RAD*100.0
      GCS=8.2E-22*YLD*NPKT/(RADC)**2*EXP(-4.61E-5*RHO*RADC-
     +    8.33E+2*TIME)
      JTHTAC=GCS*1.0E+5
      END
      REAL FUNCTION ERADC(AL,CSANG,DR,NL,I)
C
C           THIS FUNCTION GIVES THE RADIAL ELECTRIC FIELD
C     COMPONENT FOR ANY ANGLE AND RADIUS.
C
C     VARIABLES
        REAL  AL(7,0:102),CSANG,LGDRPL,DR
        INTEGER I,L,NL
C
C     BEGIN ERADC
C
        IF(I.EQ.0)THEN
          ERADC=0.0
        ELSE
          ERADC=0.0
          DO 10 L=1,NL
            ERADC=ERADC-(AL(L,I+1)-AL(L,I-1))/(2*DR)*LGDRPL(CSANG,2*L-1)
 10       CONTINUE
        END IF
      END
      REAL FUNCTION ETHTAC(AL,CSANG,DR,NL,I)
C
C           THIS FUNCTION GIVES THE THETA COMPONENT OF
C     THE ELECTRIC FIELD FOR ANY ANGLE AND RADIUS
C
C     VARIABLES
        REAL AL(7,0:102),CSANG,ALGDRP,DR
        INTEGER I,L,NL
C
```

```
C      BEGIN ETHTAC
C
         IF(I.EQ.0)THEN
           ETHTAC=0.0
         ELSE
           ETHTAC=0.0
           DO 10 L=1,NL
             ETHTAC=ETHTAC+1/(DR*I)*AL(L,I)*ALGDRP(CSANG,2*L-1)
   10      CONTINUE
         END IF
       END
       REAL FUNCTION ETOTC(AL,CSANG,DR,NL,I)
C
C            THIS FUNCTION GIVES THE ABSOLUTE VALUE OF
C      THE TOTAL ELECTRIC FIELD AT ANY ANGLE AND RADIUS
C
C      VARIABLES
         REAL ERADC,ETHTAC,AL(7,0:102),CSANG,DR
         INTEGER I,NL
C
C      BEGIN ETOTC
C
         ETOTC=SQRT((ERADC(AL,CSANG,DR,NL,I))**2+
     +     (ETHTAC(AL,CSANG,DR,NL,I))**2)
       END
       REAL FUNCTION SIGMAC(AL,CSANG,DR,NL,I,WVC,TIME,YLD,NPKT,
     +  RDEN,CODE)
C
C            THIS FUNCTION GIVES THE CONDUCTIVITY AT ANY RADIUS AND
C      ANGLE VALUE. THE WATER VAPOR CONTENT AND TOTAL FIELD EFFECTS
C      ARE INCLUDED
C
C      VARIABLES
         REAL AL(7,0:102),CSANG,DR,WVC,TIME,YLD,NPKT
```

```
      REAL RDEN,MUI,MUE,MUA,KA,KN,ARGE,AC,BC,CC,KC
      REAL PWVC,EPS0,ESU,EPS1,EPS2,PRES,KA3,KA2,R
      REAL MUEMAX,INZRT,INZRTC,ETOTC
      INTEGER I,NL,CODE
C
C     BEGIN SIGMAC
C
      IF(CODE.EQ.1)THEN
C       FIELD INDEPENDENT CONDUCTIVITY
        MUE=0.25
        MUI=2.5E-4
        KA=1.5E+8
        KN=2.0E-12
        INZRT=INZRTC(I*DR,CSANG,TIME,YLD,NPKT,RDEN)
        SIGMAC=1.6E-19*(INZRT/KA*MUE+2*MUI*SQRT(INZRT/KN))
      ELSE
C       FIELD DEPENDENT CONDUCTIVITY
C       DATA FOR LONGMIRE FITS (MUE + KA)
        DATA AC,BC,CC/2.457,0.6884,1.195/
        KN=2.0E-12
        MUI=2.5E-4
        PWVC=100.0*WVC
        KC=PWVC**(0.834)
        EPS1=0.07853*(1+AC*KC)
        EPS2=3.015+CC*KC
        MUEMAX=1.5/(1.0+96.97*(WVC)**(0.787))
        ESU=ETOTC(AL,CSANG,DR,NL,I)/30020.0
        IF(ESU.LE.EPS1)THEN
          EPS0=ESU/(1+AC*KC)
        ELSE IF(ESU.GT.EPS1.AND.ESU.LE.EPS2)THEN
          EPS0=(SQRT((BC*KC/2)**2+ESU)-BC*KC/2)**2
        ELSE
          EPS0=ESU-CC*KC
        END IF
```

```
            MUA=1.0E+6/RDEN*((16.8+EPS0)/(0.63+26.7*EPS0))**(0.60)
            R=1.55+210/(1+11.8*EPS0+7.2*EPS0**2)
            MUE=MUA/(1-WVC+WVC*R)/3.002E+6
            IF(MUE.GE.MUEMAX)THEN
              MUE=MUEMAX
            END IF
            KA3=1.0E+8*RDEN**2*((0.62+800*EPS0**2)/(1+1.0E+3*EPS0**2*
     +        (EPS0*(1+0.03*EPS0**2))**(0.33333333)))
            IF(EPS0.LT.1.1)THEN
              ARGE=25.0
            ELSE
              ARGE=-21.15/EPS0
            END IF
            IF(ABS(ARGE).GT.20.0)THEN
              KA2=0.0
            ELSE
              KA2=1.22E+8*RDEN*EXP(-21.15/EPS0)
            END IF
            KA=(1-WVC)*((1+34.4*WVC)*KA3+KA2)
            INZRT=INZRTC(I*DR,CSANG,TIME,YLD,NPKT,RDEN)
            SIGMAC=1.6E-19*(INZRT/KA*MUE+2*MUI*SQRT(INZRT/KN))
          END IF
        END
        REAL FUNCTION LGDRPL(CSANG,L)
C
C           THIS FUNCTION GIVES THE VALUE OF A LEGENDRE
C       POLYNOMIAL FOR ANY ANGLE AND ANY POLYNOMIAL.
C
C       VARIABLES
          REAL CSANG,P(0:20)
          INTEGER L
C
C       BEGIN LGDRPL
C
```

```
      IF(L.EQ.0)THEN
        LGDRPL=1.0
      ELSE IF(L.EQ.1)THEN
        LGDRPL=CSANG
      ELSE
        P(0)=1.0
        P(1)=CSANG
        DO 10 I=2,L
          P(I)=(2.0*I-1.0)/I*CSANG*P(I-1)+(1.0-I)/I*P(I-2)
10      CONTINUE
        LGDRPL=P(L)
      END IF
    END
    REAL FUNCTION ALGDRP(CSANG,L)
C
C           THIS FUNCTION GIVES THE VALUE OF THE ASSOCIATED
C     LEGENDRE POLYNOMIAL FOR ANY ANGLE AND POLYNOMIAL.
C
C     VARIABLES
      REAL CSANG,AP(0:20)
      INTEGER L
C
C     BEGIN ALGDRP
C
      IF(L.EQ.0)THEN
        ALGDRP=0.0
      ELSE IF(L.EQ.1)THEN
        ALGDRP=SQRT(ABS(1-CSANG**2))
      ELSE
        AP(0)=0.0
        AP(1)=SQRT(ABS(1-CSANG**2))
        DO 10 I=2,L
          AP(I)=(2.0*I-1.0)/(I-1.0)*CSANG*AP(I-1)+I/(1.0-I)*AP(I-2)
10      CONTINUE
```

```
          ALGDRP=AP(L)
        END IF
      END
      REAL FUNCTION U(AL,CSANG,DR,NL,I,WVC,TIME,YLD,NPKT,RDEN,CODE,RAD)
C
C          THIS FUNCTION CALCULATES THE FUNCTION OF THETA FOR THE
C     SIMPSON'S RULE INTEGRATION FOR ANY ANGLE AND ANY RADIUS.
C
C     VARIABLES
        REAL AL(7,0:102),CSANG,DR,WVC,TIME,YLD,NPKT,RDEN,RAD,THTA
        REAL P,T,A,SIGMAC,ERADC,JRADC
        INTEGER I,NL,CODE
C
C     BEGIN U
C
        P=SIGMAC(AL,CSANG,DR,NL,I,WVC,TIME,YLD,NPKT,RDEN,CODE)
        T=ERADC(AL,CSANG,DR,NL,I)
        A=JRADC(RAD,CSANG,TIME,YLD,NPKT,RDEN)
        THTA=ACOS(CSANG)
        U=(P*T+A)*SIN(THTA)
      END
```

## VITA

1Lt Kenneth M. Hodgdon was born on 19 October 1958 in Aquadilla, Puerto Rico. He graduated from High School in Tucson, Arizona, in 1976 and attended the United States Air Force Academy in Colorado Springs, Colorado from which he received the degree of Bachelor of Science in Basic Sciences in May 1980. Upon graduation, he received a commission in the USAF and began active duty service as a Nuclear Hardness and Survivability Technical Applications Program Manager on the Minuteman and Peacekeeper Missile Systems at the Ballistic Missile Office, Norton Air Force Base, California. While stationed at Norton Air Force Base, he attended the University of Southern California from which he received the degree of Master of Science in Systems Management in August 1982. Lt Hodgdon entered the School of Engineering, Air Force Institute of Technology, in August 1982.

Permanent address: #3 Elm Street
Sanford, Maine 04073

UNCLASSIFIED

SECURITY CLASSIFICATION OF THIS PAGE

## REPORT DOCUMENTATION PAGE

| | |
|---|---|
| 1a. REPORT SECURITY CLASSIFICATION: UNCLASSIFIED | 1b. RESTRICTIVE MARKINGS |
| 2a. SECURITY CLASSIFICATION AUTHORITY | 3. DISTRIBUTION/AVAILABILITY OF REPORT: Approved for public release; distribution unlimited. |
| 2b. DECLASSIFICATION/DOWNGRADING SCHEDULE | |
| 4. PERFORMING ORGANIZATION REPORT NUMBER(S): AFIT/GNE/ENP/84M-7 | 5. MONITORING ORGANIZATION REPORT NUMBER(S) |
| 6a. NAME OF PERFORMING ORGANIZATION: School of Engineering; 6b. OFFICE SYMBOL (If applicable): AFIT/EN | 7a. NAME OF MONITORING ORGANIZATION |
| 6c. ADDRESS (City, State and ZIP Code): Air Force Institute of Technology, Wright-Patterson AFB, Ohio 45433 | 7b. ADDRESS (City, State and ZIP Code) |
| 8a. NAME OF FUNDING/SPONSORING ORGANIZATION; 8b. OFFICE SYMBOL (If applicable) | 9. PROCUREMENT INSTRUMENT IDENTIFICATION NUMBER |
| 8c. ADDRESS (City, State and ZIP Code) | 10. SOURCE OF FUNDING NOS. — PROGRAM ELEMENT NO. / PROJECT NO. / TAS NO / WORK UNIT NO. |
| 11. TITLE (Include Security Classification): See Box 19 | |
| 12. PERSONAL AUTHOR(S): Kenneth M. Hodgdon, M. S., 1st Lt., USAF | |
| 13a. TYPE OF REPORT: MS Thesis; 13b. TIME COVERED FROM _____ TO _____; 14. DATE OF REPORT (Yr., Mo., Day): 1984 March; 15. PAGE COUNT: 105 | |
| 16. SUPPLEMENTARY NOTATION | |

| 17. COSATI CODES | | | 18. SUBJECT TERMS (Continue on reverse if necessary and identify by block number) |
|---|---|---|---|
| FIELD | GROUP | SUB. GR. | EMP, Late-Time, Source Region, Surface Burst, Quasi-Static |
| 20 | 14 | | |
| 15 | 06 | | |

19. ABSTRACT (Continue on reverse if necessary and identify by block number)

Title: AN INVESTIGATION INTO THE QUASI-STATIC PHASE OF THE SURFACE BURST SOURCE REGION EMP.

Thesis Advisor: John H. Erkkila, Lt. Colonel, USAF

Approved for public release: IAW AFR 190-17.
LYNN E. WOLAVER
Dean for Research and Professional Development
Air Force Institute of Technology (AFIT)
Wright-Patterson AFB OH 45433

| | |
|---|---|
| 20. DISTRIBUTION/AVAILABILITY OF ABSTRACT: UNCLASSIFIED/UNLIMITED ☒ SAME AS RPT. ☐ DTIC USERS ☐ | 21. ABSTRACT SECURITY CLASSIFICATION: UNCLASSIFIED |
| 22a. NAME OF RESPONSIBLE INDIVIDUAL: John H. Erkkila, Lt. Colonel, USAF | 22b. TELEPHONE NUMBER (Include Area Code): 513-255-2012; 22c. OFFICE SYMBOL: AFIT/ENP |

DD FORM 1473, 83 APR EDITION OF 1 JAN 73 IS OBSOLETE.

UNCLASSIFIED

SECURITY CLASSIFICATION OF THIS PAGE

A numerical solution was developed to find the aboveground late-time magnetic fields resulting from a surface nuclear burst. The time derivative in Maxwell's magnetic curl equation was ignored and the result was expressed in integral form using Stokes' law. This expression is expanded in spherical coordinates, the radial Compton current and the radial conduction current source terms were calculated, using the time-independent code, developed by Downey (Ref 4), and the polar integrals were calculated, using Simpson's Composite Rule. Magnetic field values were calculated and compared with Longmire's (Ref 20) analytic expression. For $r < 2$ Km, the results differed by less than 2.7. However, for $r > 2$ Km, the numerical values were an order of magnitude larger.

The electric and magnetic field calculations were then used to test the spatial and temporal regions of validity of the simplified boundary condition and the quasi-static approximations. The assumption that the ground conductivity greatly exceeds the air conductivity leads to a simplified boundary condition at the earth's surface ($E_r = 0$), and, in turn, to an inner radial limit to the validity of the results. The quasi-static approximation that the conduction current greatly exceeds the displacement current leads to an outer radial limit, and, finally, the quasi-static approximation that the electric fields be derivable from a scalar potential determines the time regime over which the results are valid. The quasi-static phase was found to be valid for $t > 60$ microseconds and for 1 Km $< r <$ 3 Km. The spatial region of validity is a strong function of yield and time, and the temporal region is a function of air and ground conductivities.

The computer program included in this report is useful for late-time EMP calculations because of the short execution time and its wide range of applicability. In addition, these results are a useful starting point for calculating the below ground fields.

END

FILMED

DTIC